Design and characterisation of a parallel miniaturised bioreactor system for mammalian cell culture

A thesis submitted to University College London for the degree of Doctor of Engineering

By

Omar Al-Ramadhani MEng

The Advanced Centre
for Biochemical Engineering
Department of Biochemical Engineering
University College London
Torrington Place
London
WC1E 7JE
UK

HEL Group
9-10 Capital Business Park
Manor Way
Borehamwood
Hertfordshire
WD6 1GW
UK

ABSTRACT

Optimisation of a mammalian cell culture process requires the testing of many process parameters. High yielding processes can result in reduced batches, hence bringing the product to market quicker and increasing manufacturing capacity. To reduce the cost and duration of process optimisation a novel miniaturised stirred bioreactor system (MBR), the BioXplorer™, a prototype of a commercial MBR system initially developed for microbial fermentations is described here. The system enables the operation of 4-16, 500 mL, independently controlled bioreactors in parallel. Each bioreactor is a scale down model of a lab-scale stirred tank bioreactor (STR) and constructed from the same materials. Agitation of the bioreactor can be via a magnetically driven 4 blade marine impeller or a directly driven 3 blade marine impeller. Aeration can be achieved through a variety of sparger designs directly into the culture or via the headspace at a maximum flow rate of 200 mL/min. A detailed characterisation of the key engineering parameters has been conducted focusing on power input and the power to volume ratio (P/V), mixing time and the overall volumetric mass transfer coefficient (k_La). Successful scale comparison studies were conducted to 5L scale using constant P/V and mixing time, employing an industrially relevant GS-CHO cell line producing an IgG antibody. The growth kinetics and product titres compared favourably in both systems when conducting fed-batch operations. μ_{max} in the MBR was 0.024 h^{-1} and the maximum viable cell concentration was 10.4 x 10^6 cells/mL while in the 5L STR μ_{max} was 0.029 h^{-1} and the maximum viable cell concentration was 9.8 x10^6 viable cells/mL. The product titres were also very similar in both the MBR (1.07 g/L) and the 5L STR (1.05 g/L). It has also been shown that the MBR can conduct continuous feeding using built-in peristaltic pumps, maintaining the glucose concentration in the culture at approximately 2.0 g/L after initiation of feeding. The MBR described here potentially provides a valuable and effective tool for process optimisation and is capable of performing complex feeding strategies.

ACKNOWLEDGMENT

The All Mighty Allah gave me the strength and ability to complete this work and nothing occurs without His will. I will be eternally grateful for everything Allah the Greatest has given me and for everything he has not given me.

I would like to thank my parents, Saad and Nahla, who have supported and encouraged me to achieve since I can remember. They have offered me material and emotional support throughout this EngD programme that has surpassed all reasonable expectation. Wanting to make them proud has spurred me on through the most difficult moments.

The patience afforded to me by my beautiful wife, Ayesha, and adorable children Hajer and Sa'ad kept me sane and focused, particularly when writing up. I hope this thesis will go some way to compensating for all the lost weekends and annual leave that were invested in writing it.

I would also like to thank my twin sister Selma who always provided a touch of sibling rivalry that also played a part in motivating me through the programme.

I would like to make clear my respect and thanks to my supervisors Dr Frank Baganz and Dr Mark Appleton and my adviser Professor Gary Lye who trusted me with this project and offered me a great deal of support and guidance. I would also like to thank Roy Eggleston who trained me to use the system and my sponsoring company HEL for all the financial and technical support.

I was grateful for the opportunity to work with Dr Andrew Tait who always seemed to have the answers whenever I hit a brick wall.

I must thank the mammalian cell culture team and in particular Nick Silk and Tomas Paoli, who not only put up with me for four years, but also supported and helped me with my practical work.

I would like to thank Miguel Pardo, Naqash Raja, Hani El-Sabbahy, Wasim Domah and Shaukat Ali for all their support and encouragement.

Finally, I would like to thank the Operations team in the Direct Clinical Care Division at the Royal National Orthopaedic Hospital and particularly the Deputy Director of Operations and Transformation, Patsy Spence, for their kind support during my placement with the organisation.

DECLARATION

I, Omar Al-Ramadhani, confirm that the work presented in this thesis is my own. Where information has been derived from other sources, I confirm that this has been indicated in the thesis.

Signed……..

Date……

TABLE OF CONTENTS

LIST OF FIGURES

LIST OF TABLES

List of symbols, abbreviations and dimensionless numbers

Symbols

Δp	Excess Laplace pressure (N m^{-2})
μ_{max}	Maximum specific growth rate (h^{-1})
a	Gas-liquid interfacial area
C*	Saturated dissolved oxygen concentration (mg/L)
C_L	Actual dissolved oxygen concentration (mg/L)
Di	Impeller diameter (m)
D_p	Bubble size (m)
D_T	Tank diameter (m)
ε_T	Energy dissipation rate (W/kg)
$\overline{\varepsilon}_T$	Mean energy dissipation rate (W/kg)
ε'_T	Maximum energy dissipation rate (W/kg)
k_La	Overall volumetric mass transfer coefficient (h^{-1})
M	Molar concentration (mol L^{-1})
N	Impeller rotational speed (rps)
N_p	Power number
P/V	Power per unit volume (W/m^3)
Pg	Gassed power (W)
Pug	Ungassed power (W)
Q_p	Cell specific productivity (pg/cell/day)
Q_{glc}	Specific glucose consumption rate (pg/cell/day)
Re	Reynolds number
T_m	Mixing time (secs)
V	Volume (m^3)

v	Kinematic viscosity (m^2/s)
λ	Kolmogorov length scale (μm)
$\overline{\lambda}_K$	Mean Kolmogorov length scale (μm)
λ'_K	Kolmogorov length scale in the impeller region
ρ_L	Liquid density (kg/m^3)
σ	Surface tension ($N\ m^{-1}$)
ω	Angular velocity (radians s^{-1})

Abbreviations

CD-CHO	A type of chemically defined animal component free media for CHO cell culture
cGMP	Current good manufacturing practice
CHO	Chinese Hamster Ovary
CIP	Clean in place
CMO	Contract manufacturing organisation
DCO_2	Dissolved carbon dioxide %
DHFR	Dihydrofolate reductase
DOT	Dissolved oxygen tension %
FDA	Food and Drug Administration
GS	Glutamine synthetase
HPLC	High performance liquid chromatography
IVCC	Integral of viable cell concentration (cells/mL/day)
LS	Lab-scale
LSB	Large-scale bioreactor
MABs	Monoclonal Antibodies
MBR	Miniature bioreactor
MSX	Methionine sulfoximine

MTP	Microtiter plates
MWP	Microwell plates
RO	Reverse osmosis
rpm	Revolutions per minute
SOP	Standard operating procedures
STR	Stirred tank bioreactor
TCA	Tricarboxylic acid cycle
VCC	Viable cell concentration (x 10^6 cells/mL)
VVM	Volume per volume per minute

Chapter 1: Introduction

1.1 The growing demand for mammalian cell culture products

Mammalian cell bioprocesses predominantly produce proteins that are defined as recombinant proteins, monoclonal antibodies (MABs) and nucleic acid-based products, with MABs assuming the majority of the market share (Butler 2005). These drugs are often used to treat cancer and other major illnesses like rheumatoid arthritis and crohns disease, but have a low potency (Farid, 2006) and hence require a relatively high dosage (>100 mg).

MABs attracted excitement when they were first developed in the late 1970's because companies could produce MABs against any antigen by fusing together murine lymphocytes and immortal myeloma cells to form hybridomas (Yoshinari et al, 1995). The first MAB, OKT3 (Muromonab) an immunosuppressant for reduction of acute rejection in heart and liver transplants, was approved by the FDA in 1986 (Hooks et al, 1991). MABs had many early uses particularly in diagnostic assays and medical diagnosis. Unfortunately, their early use as therapeutics was disappointing because of their immunogenicity. Recently, however, more humanlike MABs have been developed with many humanized MABs coming onto the market (Butler, 2005) and over a 100 now in clinical trials, indicating that there is a renewed excitement about MABs potential therapeutic uses (Kretzmer, 2002).

1.1.1 Bright future for MABs

In 2006, the global sales of MABs hit $20.6 billion and it was predicted that the market would grow by around 20% a year (Pavlou and Belsey, 2005) and was predicted to over double by 2010 (Browne and Al-Rubeai, 2007). This prediction has been well justified with the global MAB market estimated to be worth $43 billion in 2010 (online reference 1). These encouraging statistics have resulted partly from the commercialisation of many humanized MABs but also because of

the efficiency in the biomanufacture of these products (Butler, 2005). Therapeutic antibodies also enjoy an above average approval success rate of 29% for chimeric antibodies and 25% for humanized antibodies once they reach clinical testing, compared to only 11% for small molecules (Carter, 2006). The future looks bright for the MAB market because of the almost endless applications and functions MABs can fulfil.

1.1.2 Generics – biosimilars

An advantage that MABs offer is that they will face less competition from generics manufacturers. This is mainly due to the complexity of the biological product and also because of the time consuming and difficult nature of process development and optimisation. The costs of process development in themselves, will prove inhibitory as it is estimated that it will cost around $100 million to manufacture follow-on MABs. It is also likely that gaining FDA approval will be far from straight forward and will be more bespoke for the product. The EU Directive 2001/83/EC, as amended, stated that 'where a biological medicinal product which is similar to a reference biological product, does not meet the conditions in the definition of generic medicinal products, the results of appropriate pre-clinical tests or clinical trials relating to these conditions must be provided' (Zuniga and Calvo, 2010). This all makes the development of novel MABs more attractive as there is added regulatory protection from generics producers, which could extend the commercial life of the product beyond that provided by the patent.

1.1.3 Global manufacturing capacity

With so many products in the pipeline there has been a growing concern regarding the available large scale capacity to produce them. Figure 1.1 shows the number of products and their Kg capacity demand over the last twenty years. Since the year 2000, there has been a sudden increase in the demand for extra Kg capacity mainly due to the higher clinical doses required of humanized MAB products. This sudden increase in demand has resulted in a worldwide shortage of bioreactor capacity and hence contract manufacturing organisations (CMOs) have been enjoying an upsurge in business (Butler, 2005). There has been

significant investment in increasing capacity, especially by CMOs, however any increases in capacity requirement can be offset by increasing cell line productivity (Butler, 2005). In order to do this, a close examination of the current methods of cell screening and process optimisation are required, as well as highlighting areas that can be improved to deliver more efficient and consequently more cost effective processes.

Figure 1.1: **A graph showing the demand for manufacturing capacity of MABs and the cumulative product approvals from 1986-2006.** The arrow represents the time when a substantial increase in biomanufacturing capacity came on-line to meet demand (taken from Butler, 2005).

1.2 The current method of process development

1.2.1 Cell line selection

Effective cell line selection is an essential part of bioprocess development with a high performing cell line being key to an efficient process (Butler, 2005). Ideally, the cell line should exhibit good growth kinetics and productivity, produce a product of high quality and maintain stability over many generations (70-100).

Currently, cell line selection is a long and labour intensive process (Betts and Baganz, 2006) (refer to Fig. 1.2 and 1.3). One of the main reasons for this is that upon transfection many clones are produced and the majority of them are low producing. Hence, to isolate the few high producing cell lines, a large number of cell lines have to be screened (Van Blokland et al, 2006).

After the cell suspension has been transfected with the gene vector, the cells are grown in microwell plates (MWPs), where initial cell growth and productivity is assessed. MWPs are used initially as they are a high throughput system, which facilitates the culture and evaluation of 1000s of transfectants. Unfortunately, because of the MWP's basic design, only very limited data can be generated about a cell line's growth kinetics and productivity. This is primarily because conventional MWPs lack the operational and analytical instrumentation required to control and monitor cell cultures in a similar way to large-scale bioreactors (LSBs). Currently, there is no sophisticated high throughput system that can act as an accurate predictive model for LSBs.

After the microwell stage, cell lines exhibiting the best growth and productivity progress to the following stage, where they are assessed in slightly larger and more sophisticated bioreactors. As the scale of bioreactor increases, the number of cell lines that can be evaluated diminishes, which results in an elimination process of sub-optimal cell lines. This process of increasing scale and reducing cell lines continues until the lab-scale bioreactor stage where only several cell lines are evaluated.

The early stages of cell line screening can also prove to be inaccurate predictions of a cell line's performance in LSBs. This is because small scale, high throughput bioreactors, are mechanically very different and lack the levels of control and monitoring capabilities found in LSBs. Hence, cell lines that are eliminated early on, may in fact prove to be very good performers in LSBs and will be lost from the screening process. It has been reported by Birch et al (2005), that the final product concentration or cell specific productivity obtained in lab-scale bioreactors are often 0.8 – 1.2 fold the values obtained in shake flask assessment, however there are exceptions. In this case where seven cell lines

were evaluated, for six of them the shake flask evaluation was a good predictive model, however for one cell line it was a poor predictive model. For this cell line, the lab-scale bioreactor value for antibody concentration was almost 2 fold that found in the shake flask model. If many cell lines are to be evaluated (100's), then a more reliable, predictive model is required, otherwise a situation can arise where a significant number of sub-optimal cell lines are being evaluated in the final lab-scale bioreactor stage and potentially optimal cell lines are eliminated early in the selection process. The use of a more accurate, parallel, high throughput system will ensure that optimal cell lines are not eliminated during early stage evaluation and hence will provide a wider variety of good performers to select from.

Figure 1.2: **A typical process for developing a mammalian cell line** (taken from Lai et al, 2013)

Figure 1.3: **Typical stages and times involved in cell line selection** (taken from Birch et al, 2005).

1.2.2 Process optimisation

When developing a fermentation process, the media and feed optimisation along with defining critical process parameters such as dissolved oxygen tension (DOT), temperature, CO_2 and pH, represent a challenging and time consuming process (Ge et al, 2006). Media and feed compositions are extremely complex, and hence optimising these along with the critical process parameters requires hundreds and possibly thousands of experiments. This, however, is not currently feasible due to practical and economic limitations. These factors have led to CMOs developing generic processes that are suitable for the majority of cell lines, but being optimal for very few.

Initial process optimisation is often carried out in shake flasks where tens of experimental parameters can be tested. These experiments are then transferred to lab-scale bioreactors which are scale down models of LSBs. Unfortunately, because of the cost and labour intensity of running bioreactor experiments there

is almost always a compromise made on the number of experiments and subsequent quantity of data.

1. This limits the combinations of process parameters that can be tested and as a result can lead to sub-optimal processes being developed (Ge et al, 2006).
2. Due to the limitation in the number of bioreactors, there can be a compromise on the number of replicates used for each combination of experimental parameters. Without an adequate number of replicates there can be doubts about the reproducibility and accuracy of the experimental results.

Companies often find themselves in a dilemma when deciding on how much time and resource to invest in process optimisation. Any improvements to the process will generally reduce the cost of manufacturing, however in today's fiercely competitive markets, companies want to deliver their products to market as quickly as possible to maximise the length of their patents.

1.3 Current high throughput systems

As mentioned before a high throughput system is required to screen and evaluate a large number of early transfectants and to conduct process optimisation. The two most predominant bioreactor systems that are currently employed are microtitre plates (MTPs) or MWPs and shake flasks. Due to their small scales and ease of handling, they have an inherent high throughput capability.

1.3.1 Shake flasks

Shake flasks represent the most basic and widely used bioreactors in research and development and one of their principal advantages is ease of handling. They have been in use for the last fifty years and are a cheap and easy to use option (Betts and Baganz, 2006). As the name suggests, they are merely flasks, often made of glass (hydrophilic or hydrophobic) or plastic with a plug to seal the vessel. The plug can be merely cotton wool or sealed screw caps, depending on the level of

sterility required. Conventional shake flasks have no monitoring and control capabilities and are mechanically very different to stirred tank bioreactor (STR) systems. They lack a direct agitation mechanism, like an impeller for example, which alters the dynamics of mass transfer and mixing.

They are housed in incubators that control temperature, can provide agitation in the case of shaken incubators (orbital or linear) and if necessary, can provide some gaseous exchange. Culture aeration has been one of the main limitations of this technology as there is no sparger to provide gas into the culture. There are two main strategies of gassing the culture. In the case of a closed cap, the culture has to be manually gassed. If a vented cap is used and the incubator has the ability to control gas content, then gaseous exchange can take place. The main limiting factor however, lies in the surface area to volume ratio of the culture and so to increase gas exchange a larger surface area to volume ratio is often used. There has been work in developing more sophisticated shake flask systems. Baffles have been utilised to improve mass transfer, especially if there is a need for high oxygen transfer (Buchs et al, 2000). The use of a sterile online device to measure oxygen transfer rate has also been reported (Anderlei and Buchs, 2001) along with a respiration activity monitoring system (RAMOS) (Anderlei et al, 2004). This instrumentation requires dedicated hardware, which makes handling more difficult and hence reduces the system's high throughput capability.

1.3.2 Microtitre/Microwell plates

MTPs and MWPs have been used as useful tools in bioprocess development mainly due to their inherent high throughput capability. When handling adherent cell lines the plates are merely housed in a static incubator, but when handling suspension adapted cell lines, the plates are most often housed on rotating, heated blocks capable of controlling temperature. Traditionally, there has been little to no instrumentation to monitor and control conditions in the wells, but recently significant progress has been made. They do, however, suffer from several disadvantages:

1. Reproducibility can be difficult with inconsistencies between wells in different positions on the same plate.
2. Small culture volumes limit the size and number of samples that can be taken. This can be overcome by using sacrificial wells, but again the problem with reproducibility remains.
3. Evaporation of fluid from the culture can significantly increase culture osmolality. There have been attempts to limit this, by using breathable membranes, but this can have negative effects on oxygen transfer.
4. Relatively low oxygen transfer mainly because they are shaken systems and rely on surface aeration.
5. The volumetric mass transfer coefficient obtained in shaken MWPs is often 10 fold lower than that seen in conventional scale fermenters (Reis et al, 2006 and Betts and Baganz, 2006)

Recently there has been progress in developing instrumentation that can monitor and control certain processing parameters, as well as introducing magnetic stirrers to improve mixing. Plate readers have been developed although they can often only measure 1 or 2 parameters (Reis et al, 2006). Elmahdi et al (2003) reported the use of a pH probe in a 7 mL microwell system. Kensy et al (2009), reported the use of a MTP reader capable of monitoring pH and dissolved oxygen based on the use of immobilised fluorophores at the bottom of standard 24-well MTP's. This technology allowed for continuous measurement even during shaking, rather than having to stop shaking to take a reading. Microbial growth can be monitored in MTPs using a spectrometer using turbidimetric analysis but only up to cell densities of 0.2-0.3 g/L (Weuster-Botz et al, 2005).

Silk et al (2009), reported the use of feeding strategies in 24 standard round well plates, using a commercially available 'sandwich lid' to allow gas exchange and minimise evaporation. To counteract the evaporation that did occur, appropriate dilution of the bolus feeds was carried out to maintain culture volume.

Wen et al (2012), reported the use of a 24-MWP with a variety of different static mixer configurations that improved agitation and aeration and gas permeable lids that reduced evaporation. They also evaluated the effects of using square and

round well plates. Cell proliferation was measured by using the TECAN GENiosPro™ microplate reader. They reported that, by optimising the static mixer, more consistent cell culture could be achieved with little well to well variation and reduced cell aggregation. Finally, scale comparison cultivations were carried out using CHO cells that showed good similarity to cultures grown in 100 mL shake flasks but no data was presented comparing performance to lab-scale bioreactors.

Chen et al (2008) conducted an extensive study on the microbioreactor system (Micro 24), a 24 microwell system, which provides non-invasive online monitoring and control for DOT, pH and temperature. Fed-batch scale comparison studies were carried out that showed fairly good reproducibility with a 2 L bioreactor; however, foaming was a major issue. To combat the excessive foaming, surface aeration was used, antifoam was added and DOT control was disabled. Due to the excessive foaming the researchers were not able to demonstrate simultaneous control of both DOT and pH over the whole course of a 12-day fed-batch culture. Foaming did still take place after these measures were taken and resulted in some variation amongst the wells.

1.4 Disposable bioreactors

The wavebag type disposable bioreactor was introduced in 1999 by Vijay Singh and provided a fairly versatile platform technology, as it has been used for media storage, seed inocula and cell culture. The bags come pre-sterilised and can be mounted on to a platform that rocks the bag producing waves in the culture, which provides mixing. They have been shown to support high cell density cultures ($> 10^6$ cells/mL) and have been utilised in process optimisation in the research and development setting at volumes as low as 0.1 L and in large scale manufacturing (500 L) (online reference two).

Single use cell bag bioreactors have also been developed to fit into stainless steel containers that resemble the shape of conventional stainless steel vessels. They can be fitted with pitched blade impellers or magnetically stirred impellers to

provide similar agitation conditions to conventional bioreactors (Agrawal and Bal, 2012). Although these systems are not currently high throughput, they do offer a disposable alternative to conventional stainless steel reactors and have the potential to be developed further.

1.5 Miniature stirred tank bioreactors

Miniature stirred tank bioreactors (MBRs) are simply scale down models of larger STRs at volumes anywhere between around 10-300 ml (Betts and Baganz, 2006). They have similar monitoring and control capabilities as they can control pH, DOT and temperature and have a direct mechanical stirrer and gas sparger. Like lab-scale bioreactors they are made of borosilicate glass or polycarbonate with a top head-plate made of stainless steal, polycarbonate or polyetheretherketone. The head-plate is often big enough to allow for the insertion of temperature, pH and DOT probes (Kumar et al, 2004). They have the potential ability to accommodate fed-batch regimes, which are an important process optimisation strategy (Betts and Baganz, 2006). They can also be designed to the same aspect ratios as LSBs, which aids in process scale-up.

1.5.1 Mechanical similarities

MBRs are mechanically similar to conventional bioreactors and employ very similar forms of agitation and aeration and hence can allow for accurate reproducibility of the fundamental engineering parameters found within conventional bioreactors (Kumar et al, 2004), volumetric mass transfer rates and mixing times for example (Betts and Baganz, 2006).

1.5.2 Volumes

The culture volumes supported by MBRs provide a good compromise between those volumes used in microtitre plates (MTPs) and in lab/large scale bioreactors. MTPs utilise small culture volumes and thus benefit from cost savings and small foot prints. Unfortunately they also present many operating challenges, such as, evaporation, which has an amplified effect for slow growing cultures. Small

volumes restrict the number and volume of samples that can be taken for analysis and hence are only suitable for micro-analytical methods (Kumar et al, 2004). MBRs can process culture volumes which are small enough to allow for high throughput parallel operation whilst providing enough culture volume for frequent sampling.

1.5.3 Instrumentation

One of the limitations of small scale reactor systems is the lack of instrumentation to conduct on-line monitoring. There has been considerable progress in developing this technology and MBRs can now continuously monitor and control temperature, pH and dissolved oxygen (Kumar et al, 2004). Lamping et al (2003) reported the use of an incorporated fibre-optic probe able to monitor dissolved oxygen (DO) and pH. Optical sensors have gained popularity due to their low cost, non-intrusive manner and their ease in adapting to miniaturised systems (Ge et al, 2006). The use of a novel optical density probe which allows for on-line estimation of biomass growth kinetics has also been reported (Gill et al, 2008). This is of great benefit as it reduces the need for daily sampling for off-line estimation of biomass, which helps to maintain culture volume. It also reduces the amount of labour required to conduct manual or automated off- line cell counts.

1.5.4 Examples of miniature bioreactor systems

Soley et al (2012), reported the development and use of a disposable 6 minibioreactor system (refer to Fig. 1.4). The system is comprised of a fixed platform that contains the instrumentation, sensors and actuators and a disposable part which is a set of 6 single use minibioreactor vessels with a working volume of 10-15 mL each. The vessels are agitated by a magnetically induced stirring pendulum and are aerated via surface aeration. The other interesting feature of the system was the use of two optical probes, one that could measure total cell density and pH and the other that could measure DOT. The group were able to grow hybridoma cells in parallel, at different conditions, but did not provide any scale comparison data.

Figure 1.4: **Photo of a minibioreactor plate housing 6 minibioreactors** (taken from Soley et al, 2012).

TAP Biosystems have developed a high throughput advanced microscale bioreactor system (ambr^{TM}) for cell line development using either 24 or 48 bioreactors with a working volume of 10-15 mL. The bioreactors are mechanically similar to conventional STRs and have a pitched blade impeller to provide agitation and direct sparging capability. They also have the ability to monitor and control pH and DOT by using sensors and a fluorescence reader in the base. The ambr^{TM} also comes with an automated workstation that is capable of 'closed loop' control of pH and DOT with independent control of O_2 and CO_2 for each vessel. It provides automated liquid handling for reactor set-up, feed and base addition as well as automated sampling. It can be installed in laminar flow hoods allowing aseptic operation and optional integrated cell viability analysis (online reference three). Recent scale comparison studies have been reported by Hsu et al (2012), which show fairly good similarity between the ambr^{TM} and a 2L STR, however the ambr^{TM} was only sampled once in the first 7 days (on day 3) and at this point the viable cell concentration (VCC) was consistently far below that produced in the 2L STR.

Table 1.1 summarises the technical specifications of the HEL BioXplorer™ system along with 4 other high throughput, parallel bioreactor systems. The table includes a mini-bioreactor system produced by DASGIP, the Micro 24 produced by Pall, the Multifors 2 system produced by INFORS HT, the ambr 250™ - a larger version of the ambr™ and the HEL BioXplorer™ system. All information in the table has been taken from technical specification documents for the respective systems from the companies' websites.

Table 1.1: A comparison of 5 commercial miniature bioreactor systems. All information has been taken from technical specification documents from the respective companies' websites

	DASGIP Mini Bioreactor	**Micro-24 MicroReactor System (Pall)**	**INFORS HT Multifors 2**	**ambr 250™ (TAP Biosystems)**	**BioXplorer™ (HEL)**
Total volume (mL)	300	-	700 or 1000	-	500
Working volume (mL)	60-250	3-7	500 or 750	100-250	100-400
Number of vessels	4-32	24 wells	6	12-24	4-16
Vessel type	Re-useable standard vessels and headplate (can also support single use vessels)	Single or re-useable cassette	Re-useable standard vessels and headplate	Single use	Re-useable standard vessels and headplate
Agitation	Direct driven pitched blade	Orbiting base plate	Magnetically stirred pitched blade	Magnetically stirred pitched blade	Magnetically or directly driven marine
Process control	Temperature, pH and DOT	Temperature, pH and DOT for each well	Temperature, pH and DOT	Temperature, pH and DOT	Temperature, pH and DOT
Advanced monitoring	-	-	Viable cell density CO_2 evolution rate O_2 uptake rate Respiratory quotient	-	-
Gas delivery	Gas mixing with individual gas mixture from air, O_2, CO_2 and N_2 - Direct or surface aeration	1 gas injector per well - flow through a vent tube into the headspace - Gas mixing available	Air/O_2/N_2/ CO_2 gas mixing capability through a ring sparger or headspace aeration	Not specified	Separate air, O_2, N_2 and CO_2 gas sparging or surface aeration
Advanced operation	Fed-batch and continuous feeding - pump rates as low as 0.3 mL/hr	-	Fed-batch and continuous feeding 0.18 - 200 mL/hr - use of respiratory quotient for substrate feed control	Liquid-handling automation for culture setup and inoculation, addition of feeds and alkali, and culture sampling	Fed-batch and continuous feeding - feed flow rates as low as 0.1 mL/hr

1.5.5 The ideal MBR system

The ideal solution would be a system capable of high throughput, parallel operation that could monitor and control a range of physical variables (temperature, pH and DOT etc…) and allow the operator to test a wide range of process factors like medium and feed composition. The system would have to be designed with scaleability in mind and allow for accurate scale-up to lab and possibly pilot and manufacturing scale. If this is not the case, then any work done in the high throughput system is unreliable, as there is no guarantee that the growth kinetics and productivity will be reproduced at large scale. Historically, there has often been a compromise between throughput and the size and variety of information obtainable from each experiment (Gill et al, 2008). These limitations have been due to either small culture volumes or reduced monitoring capabilities due to a lack of appropriate sensing equipment (Maharbiz et al, 2004).

1.6 Cell line process characteristics

The cell line employed in a process plays a central role in bioreactor design and subsequent process development and optimisation. Mammalian cell lines are particularly difficult to culture because of many reasons. Table 1.2 lists some of the main characteristics of a modern Chinese Hamster Ovary (CHO) cell line process.

Table 1.2**:** A summary of the major process considerations for current CHO cell line processes.

Mammalian cell culture characteristics	
Shear sensitivity	Particularly shear sensitive (due to a lack of an outer cell wall), but not as sensitive as originally thought
Media	The industry standard is to use complex chemically defined animal component free media
Growth kinetics	Fed-batch cultures often last over 15 days. Maximum viable cell concentrations often reach above 10^7 cell/ml
Productivity	Some companies claim their processes can consistently produce 5 g/L - 10 g/L (Lim et al, 2010)
Selectable gene markers	The two most common are the GS system and DHFR
Sterility	Mammalian cell culture processes are particularly prone to contamination and hence good aseptic technique is required when culturing
Product quality	Very human like due to accurate post translational glycosylation

Although mammalian cells are notoriously difficult to culture they remain the cell line of choice for the production of MABs and recombinant proteins, even though they are less productive than other cell lines. This is mainly due to their ability to add glycans to synthesised proteins (glycosylation) in a human like manner (Butler, 2005). Their ability to closely mimic the glycosylation patterns of human proteins ensures that the proteins they produce have the required levels of efficacy.

Mammalian cells are particularly shear sensitive as they lack an outer cell wall, which poses many engineering limitations. Excessive shear stresses, which result from agitation and aeration can cause cell membrane rupturing and cell death. The cell's shear sensitivity limits the intensity of agitation and aeration that can be operated, which makes achieving high mass transfer more difficult (Motobu et al. 1998).

1.6.1 CHO cells

CHO cells were one of the first hosts to be used for stable gene transfer because of the availability of metabolic CHO mutants deficient in dihydrofolate reductase (DHFR) activity (De Jesus and Wurm, 2011). Two critical developments in genetic engineering facilitated the wide use of these cells; these developments were the molecular cloning of genes into plasmid DNA and the chemically mediated delivery of those plasmids into cultured mammalian cells. The first CHO derived cell lines included those that produced recombinant interferons and tissue type plasminogen activator (tPA) (Hacker et al 2009). In 1986, tPA produced in CHO cells became the first FDA approved recombinant therapeutic protein. Genentech produced tPA by large scale mammalian cell culture in LSBs, a technology that was adapted from those reactors used for bacterial culture. There has not been a major shift in the principle bioreactor technology used for mammalian cell culture over the last 25 years, with large scale STRs still the most common technology. However, culture performance has increased dramatically over the same period, mainly due to improved media compositions and the introduction of sophisticated feeding strategies (refer to Fig. 1.5).

Figure 1.5: **Final fed-batch process titres as a function of the year in which the process was developed** (taken from Markusen and Robinson, 2010).

Table 1.3: Process performance from early processes in the 80's and 90's to more modern processes.

	Early processes	Modern processes
Culture duration (days)	7	Over 15
Maximum viable cell concentration (x 10^6 cells/ml)	1-2	0ver 15
Cell specific productivity (pg/cell/day)	10-20	50-100
Product yields (g/L)	0.05-0.1	Over 5 is now common (Li et al 2010)

1.6.2 GS-CHO

GS-CHO cell lines benefit from having a gene expression system that makes use of selection via glutamine metabolism and powerful viral promoters. Glutamine is an essential amino acid for CHO cell culture and is important for the synthesis of purine, pyrimidine and amino sugars and also provides a carbon source for the

tricarboxylic acid cycle (Lim et al, 2010). Glutamine is synthesised from glutamate and ammonia by the enzyme glutamine synthetase (GS). Mouse myeloma cell lines do not produce enough endogenous GS and hence must be supplied with glutamine in the external environment in order to survive. Wild type CHO cells do produce enough endogenous GS to survive and hence do not require additional glutamine in the media. A GS inhibitor can be used, namely methionine sulphoximine (MSX) to inhibit the endogenous GS so that only the cells that have been successfully transfected with the product vector, which also has the GS enzyme gene will survive. The cells that are successfully transfected can grow in glutamine free media with MSX because they produce enough GS to synthesise glutamine (Vernon, 2004).

1.7 Scale-up

1.7.1 Introduction

The large demand for therapeutic proteins from mammalian cells has resulted in many manufacturers utilising very large bioreactors (up to 20,000 L has been reported). With process optimisation taking place at lab-scale this makes accurate scale-up a critically important step. If scale-up is not successful the repercussions can be very serious, with adverse effects on the economic performance of the process and on operational stability. Scaling-up biochemical processes can be complicated due to the presence of innately complex biological entities.

As mentioned before the growth kinetics, productivity and product quality obtained with scale-down experiments have to be mimicked in large-scale, otherwise there is no guarantee that optimised process conditions will be maintained.

The aim of scale-up is to maintain certain critical conditions so that the performance of the cells are not greatly affected - these include:

1. DOT
2. Dissolved carbon dioxide
3. pH
4. Temperature
5. Shear forces
6. Nutrient concentrations

The above can be affected by any one of these factors:

1. Mixing
2. Oxygen transfer
3. Shear forces

1.7.2 Mixing

Mixing can be defined as achieving homogeneity and mixing time as the time taken to achieve homogeneity. Mixing time can be determined by measuring the response to the introduction of a measurable entity (example, acid or base addition) (Varley and Birch, 1999) and 95% of mixing time equates to the time taken for the concentration to reach 95% of its final value. Mixing has a direct effect on mass and heat transfer, which are two key thermodynamic parameters.

Poor mixing can result in:

1. pH gradients
2. Temperature gradients
3. Compartmentalisation
4. Nutrient gradients
5. Poor parameter control

Mixing should be optimised so that a homogenous environment is produced within the reactor. Otherwise the cells will travel through a variety of environments within the reactor, which can have adverse effects on the cell's growth kinetics and productivity. Mixing times should also be minimised so that

responses to any changes in operating conditions like temperature and pH can be as fast as possible.

Transfer properties depend highly on agitator design and operation as this is what creates the majority of mixing. So, when scaling-up it is important to highlight the transfer property that is most critical to the performance of the bioprocess. This task is made harder by the fact that mammalian cells are particularly fragile and have very complex nutritional requirements. Mixing has become an increasingly crucial parameter in designing a mammalian cell process. Due to improved cell growth kinetics and more complex media and feed additions there is a potential for increased concentration gradients of gasses, nutrients and pH.

Gasses must be well dispersed as a build-up in concentration of toxic gasses (like CO_2) can harm cells and this is particularly important if CO_2 is used to control pH. The deprivation of oxygen can also harm the cells especially when high cell numbers are reached in the late exponential to stationary growth phase (Varley and Birch, 1999).

1.7.3 Oxygen transfer

The equation for oxygen transfer is:

$$OTR = K_La\ (C^* - C_L) \qquad 1.1$$

K_La = overall mass transfer coefficient (h^{-1} or sec^{-1})
C^* = equilibrium oxygen concentration (mg/L)
C_L = concentration of dissolved gas in liquid (mg/L)

Oxygen transfer can be effected by;

1. The headspace pressure in the vessel
2. The hydrostatic pressure
3. Media coalescence
4. Bubble size

The constant volumetric oxygen mass transfer coefficient can often be the magnitude that is kept constant in scale-up and involves oxygen transfer from gas bubbles to the cells. This is because in aerobic processes oxygen transfer to the cells is often a limiting factor high cell density growth.

1.7.4 Shear

Shear stress is a force that acts on and parallel to a surface or body. Excessive shear stress can have adverse effects on cells and can cause damage to the cell's membrane and hence result in cell death. Shear can have many other effects however on; fluid mixing, cell suspension, mass transfer, product formation and cell growth (Varley and Birch, 1999). Shear is an important factor in mammalian cell culture processes as mammalian cells are particularly shear sensitive as they do not have a protective outer cell wall.

The main causes of shear are due to aeration and agitation:

1. Agitation

Impellers in a stirred tank reactor provide the majority of agitation and hence mixing. In order to achieve a good level of mixing the culture must be adequately agitated to provide turbulent flow regimes. The theory is that cell death in cell suspension can occur when Kolmogorov eddy sizes approach the size of the cells. However, it has been found that cells grown in the absence of sparging were able to withstand much higher levels of agitation than those grown in the presence of sparging. This would suggest that the method of aeration plays an important role in shear damage (Nienow, 2006).

2. Aeration

Aeration is a very important factor and plays a key role on determining the levels of shear. Shear forces can be caused by bubble rising, bubble generation and bubble bursting, with the latter two being the most important. It was found in

work done by Chalmers (1994) that hybridoma cells could withstand agitation speeds of up to 450 rpm with no cell damage when no air sparging was present, but with air sparging present, cell damage did occur. It has also been found that the size of bubbles has an effect with smaller bubbles causing greater cell damage (Nienow, 2006). This can also be understood from the following equation:

$$\Delta p = 4\sigma/D_p \qquad 1.2$$

Δp = excess Laplace pressure (N m^{-2})
σ = surface tension (N m^{-1})
D_p = bubble size (m)

If the bubble size decreases the excess pressure increases, which increases the speed of recoil of the bubble lip and hence increases the shear force on the cell. There have been ways to protect the cells to a certain degree. The use of a non-ionic surfactant, Pluronic F-68 has been shown to be effective in reducing cell damage. One theory behind this is that Pluronic F-68 prevents cells from attaching to bubbles and hence protects them from the bursting effect. Another way of protecting cells is to ensure that there is as little foaming as possible. This is because the bursting of bubbles is the most likely cause of cell damage and with a high build-up of foam there will inevitably be a large number of bursting bubbles. Foaming can be reduced by making antifoam additions to the culture, however antifoam can diminish mass transfer, make downstream processing more complicated and have an adverse effect on some medium components (Varley and Birch, 1999, Nienow, 2006). In conclusion, the shear effects on the cells appear to be a combination of both aeration and agitation.

1.7.5 Scale-up methods

There are many methods that can be used to perform scale-up:

1. Rules of thumb

Generally, when using rules of thumb a constant value of a particular operating variable is used and geometric similarity is implicitly assumed. The variable that is chosen to base scale-up on differs and depends on the process and is usually the one that is the rate determining regime at lab and production scale. So for example, for an aerobic, fed-batch process the most critical variable would be mass transfer.

Table 1.4: The effects on other parameters when one parameter is kept constant on scale-up.

Scale up criterion	**P**	**P/V**	**N**	**D_i**	**Re**
Equal P/V	10^3	1	0.22	2.15	21.5
Equal N	10^5	10^2	1	10^2	10^2
Equal tip speed	10^2	0.1	0.1	1	10
Equal Re	0.1	10^{-4}	0.01	0.1	1

P = Power, V = Volume, N = Impeller speed, D_i = Impeller diameter, Re = Stirrer Reynolds number.
(Adapted from Jenkins et al, 1992)

2. Dimensional analysis

This method is commonly used in scale-up of chemical processes. Dimensionless groups of parameters for example Froude number (Fr) and Reynolds number (Re) can be obtained from the dimensionless momentum, mass and heat balances, as well as their boundary and initial conditions in the dimensionless form.

This technique is driven by the need for dimensionless consistency and the constraints this places on the functional relationship between variables. It allows for the grouping of a number of variables in a problem to form dimensionless

groups. Dimensionless numbers are quotients between two fundamental properties for example:

$$\mathrm{Re} = \frac{\text{inertia forces}}{\text{viscous forces}} \qquad 1.3$$

3. Regime analysis

This method is used in first scaling down a large scale bioreactor in order to design a lab-scale bioreactor. After this the process can then be optimised at lab-scale and then transferred to large-scale. The approach consists of determining if there is a rate-controlling mechanism, what it is and if it will change on scale-up. If the rate is controlled by more than one process, then there exists a mixed rate-controlling mechanism (refer to Fig. 1.6).

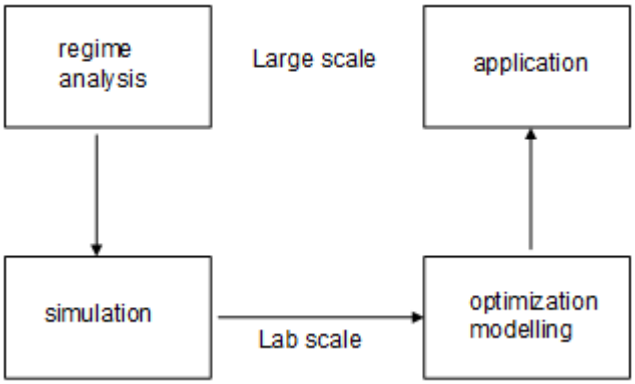

Figure 1.6: **An illustration of the stages involved in regime analysis** (Adapted from Asenjo and Merchuk, 1994).

1.7.6 Potential problems on scale-up

1.7.6.1 Shear

As scale increases the impeller tip speed has to increase to maintain a similar level of mixing, thus increasing the impeller shear forces on the cells. This is because there is an increase in both macro and micro turbulence (Varley and Birch, 1999).

1.7.6.2 Mixing

Generally, in larger scale bioreactors it is more difficult to achieve homogeneity (mixing) (Nienow, 2006) and to maintain the same level of mixing on scale-up, the agitation rate has to increase. Bioreactor developers have been reluctant to increase agitation rate because of the perceived shear damage this will have on the cells. However, it has been found that mammalian cells are not as shear sensitive as originally thought and can withstand higher agitation rates. With this in mind, the use of higher agitation rates may be utilised to reduce the difference in mixing.

1.7.6.3 Mass transfer

Mass transfer is generally reduced by up to half on scale-up from pilot to production scale reactors. To overcome this, the use of oxygen enrichment, better mixing and increased sparge flow are all options. Better mixing and increased sparge flow would often involve increased agitation and aeration, which can increase the shear effects on cells (Marks, 2003). It has been found in most LSBs that the shear force released by bursting bubbles is at least an order of magnitude greater than mixing induced shear forces. Hence, a minimum aeration rate should be adopted with increased mass transfer delivered by an increase in agitation rate.

1.8 Project aims

This study aims to evaluate the potential of the HEL BioXplorer™ MBR system to carry out rapid process development/optimisation of advanced mammalian cell culture processes. The study was underpinned by a detailed engineering characterisation of the MBR system and that of a 5L STR. The engineering characterisation involved the determination of core engineering parameters such as power input, mixing time and the volumetric mass transfer coefficient as well as the hydrodynamic conditions in the MBR system.

This data was compared with that of a 5L STR and was used as basis to evaluate the scale-up potential of the MBR system. This work involved comparison of cell growth kinetics and antibody production of an industrially relevant GS-CHO cell line grown in fed-batch culture in the MBR system and 5L STR using equal power per unit volume as a scale-up criterion. The cell culture performance in the MBR system was subsequently optimised through a series of batch cultivations which focused on optimising gas delivery to the system. This work centred on evaluating different sparger designs and the impact of direct gas sparging vs surface aeration.

Finally, the MBR's ability to conduct industry standard advanced feeding regimes was evaluated with the operation of continuous feeding using the system's in-built peristaltic pumps.

Chapter 2: Materials and Methods

2.1 Chemicals

The chemicals used in this work were obtained from BDH (Dorset, UK) and the cell culture media, a chemically defined animal component free media (CD-CHO) was obtained from Gibco, Invitrogen (Paisley, UK). All the water used in the evaluation was RO water. All the filters used were re-usable, 0.2 μm Sartorius Midisart 2000 PTFE filters (Epsom, UK).

2.2 Lab-scale bioreactor design and construction

The bioreactor used was a 5L STR Biostat BDCU (Sartorius Stedim Biotech, New York, USA). It had a working volume aspect ratio of 1:1 and consisted of a borosilicate glass vessel supported by a stainless steel scaffold and was sealed with a stainless steel head plate. Mixing was achieved by a single 3 bladed marine impeller rotated by a rotor shaft in the head plate. The motor used was a 0.34 kW Kollmorgen Seidel motor, (GmbH and co, Dusseldorf, Germany). There was a distance of 6 cm from the centre line of the impeller to the base of the vessel. The impeller was screwed on to a rotating, stainless steel impeller shaft that was connected to the motor on the head plate. Aeration of the vessel was achieved via the use of a horseshoe shaped sparger. A sintered sparger was not used as the large quantity and small size of bubbles caused excessive foaming. The airflow rate was manually regulated using a standard laboratory rotameter in the range of 0 - 666 mL/min; during operation the gas flow was capped at 100 mL/min.

The head plate accommodated on-line probes for dissolved oxygen, temperature and pH. The O_2 probe used was an InPro® 6000 series O_2 12mm Sensor (Mettler Toledo, Leicester). There was also a single multi-port with 4 openings, two of which allowed for the addition of antifoam and base. For the third port a silicon tube was attached going from the interior of the port to the bottom of the vessel

and this was used as an inoculation/harvest line. The remaining port can be used for feed additions in fed-batch cultures but this was not needed so was closed off using a gate clamp. The exhaust gas port was connected to a capped, empty sterile glass bottle, with the cap having two openings. One opening was closed with an air filter and the other was connected to the exhaust port by silicone tubing. The inlet gas was filtered through a re-usable 0.2 μm Midisart 2000 PTFE filter (Sartorius, Epsom, UK).

2.3 Miniaturised bioreactor design and construction

The MBR vessels were modelled based on the lab-scale vessel with a working volume 1:1 aspect ratio and also made of borosilicate glass. These vessels were sealed with a stainless steel head plate which was attached to the vessel by a stainless steel tightening collar. Mixing was achieved either by a 3 bladed directly driven overhead impeller or a 4 bladed magnetic bottom driven impeller. The direct driven impeller was screwed on to a rotating, stainless steel impeller shaft that was connected to the motor on the head plate. The vessel was housed in a polyblock which also controls the temperature of the vessels. Aeration was achieved by a number of different sparger designs; these are described in Section 2.17. The rotameters have a maximum controlled flowrate of 200 mL/min (Cache Quality Instrumentation, Wakefield, UK). The airflow rate was manually regulated using a standard laboratory rotameter in the range of 0-200 ml/min. The head plate could accommodate on-line probes for dissolved oxygen, temperature and pH. The DOT probe used was the oxyferm 120 FDA (Hamilton, Bonaduz, Switzerland). The pH probe used was the easyferm 120 (Hamilton, Bonaduz, Switzerland). The head plate has a port for antifoam and base additions, a gas out port and a port to attach a dip tube for the sampling port. The head plate also accommodates a septum port and 2 ports for antifoam detectors that set off an alarm when both sensors come in contact with antifoam. The inlet gas was filtered through a re-usable 0.2 μm Midisart 2000 PTFE filter (Sartorius, Epsom, UK).

Table 2.1: Summary of the important bioreactor vessel and impeller dimensions.

	Unit	MBR	5L
Total volume	L	0.5	7
Working volume	L	0.30	3.5
Total height	m	0.14	0.32
Diameter	m	0.08	0.16
Aspect ratio (working volume)	H/L	1:1	1:1
Number of impellers	-	1	1
Type of impeller	-	Direct or magnetic driven marine	Elephant ear marine
Impeller diameter	m	Direct – 0.034 Magnetic – 0.032	0.062
Impeller depth	m	Direct – 0.0070	0.045
Impeller blade angle	°	30	45
Impeller diameter:vessel diameter	-	Direct – 0.41 Magnetic – 0.42	0.41
Shaft diameter	m	Direct – 0.0080 Magnetic – 0.0030	0.015
Number of impeller blades	-	Direct – 3 Magnetic – 4	3

2.4 Cell line and culture conditions

The cell line used in this work was a GS-CHO cell line, CY01, obtained from Lonza Biologics, Slough. The growth medium was chemically defined animal component free (CD-CHO) supplemented with 1 mL/L of 25 mmol/L Methionine Sulfoximine (MSX) (Sigma-Aldrich Company Ltd, Dorset, England) (refer to Section 2.16). The cells were routinely passaged every 3/4 days in 250 ml Erlenmyer (E250) shake flasks with vented caps in shaken CO_2 incubators with culture volumes of 100 ml. Passages were conducted by inoculating an appropriate volume of pre-warmed (~37°C) CD-CHO medium to achieve a seeding density of 0.2 x 10^6 cells /ml.

2.5 Lab scale bioreactor fermentation

Before sterilising the bioreactor the pH probe was calibrated. The bioreactor was sterilised in an autoclave at 121°C for 40 minutes along with 100 ml antifoam and 1 L base. The antifoam solution was made by adding 3 ml of C emulsion antifoam (Sigma Aldrich, Dorset, UK) to 97 ml of RO water to make a 3 % solution. The 0.1 M base solution was made of two powders, hydrogen bicarbonate and hydrogen carbonate. Before sterilisation the reactor was filled with enough water to cover the probes to ensure the probes did not dry up during and after the autoclave run. As soon as the bioreactor was taken out of the autoclave and returned to the bench the probes were connected to the controller and this was particularly important for the DOT probe, as it requires 6 hours to fully polarise. After the DOT probe was polarised the RO water was drained from the reactor and then the reactor was filled with 3 L of CD-CHO media. The heating jacket was then turned on and once the temperature of the media reached 37°C the DOT probe could be calibrated along with recalibrating the pH probe.

Once the calibrations were complete the bioreactor was inoculated with enough cell culture to achieve a seeding density of 2.0 x 10^5 cells/ml. The operating process parameters are listed in table 2.2.

Table 2.2: 5L STR operating parameters.

Process Parameter	Setpoint
DOT (%)	30
pH	7.1
Temp (°C)	37
Stirrer Speed (rpm)	260

2.6 Miniaturised bioreactor fermentation

2.6.1 Preparation and sterilisation

Before sterilising the bioreactor the pH probe was calibrated. This was done by first immersing the pH probe in pH buffer solution at pH 7 and waiting for a stable reading at room temperature. The pH recorded by the probe was inputted into the control software at the recorded temperature. This procedure was repeated while immersing the pH probe in pH buffer at pH 4.

The bioreactor was sterilised in an autoclave at 121°C for 40 minutes along with 50 ml antifoam and 50 ml base in separate bottles. The antifoam solution was made by adding 1.5 ml of C emulsion antifoam (Sigma Aldrich, Dorset, UK) to 48.5 ml of RO water to make a 3 % solution. The 0.1M base solution was made of two powders, hydrogen bicarbonate and hydrogen carbonate. Before sterilisation the reactor was filled with enough water to cover the probes to ensure the probes did not dry up during and after the autoclave run. As soon as the bioreactor was taken out of the autoclave and returned to the polyblock the probes were connected to the controller and this was particularly important for the DOT probe, as it requires 6 hours to fully polarise. After the DOT probe was

polarised the RO water was drained from the reactor and then the reactor was filled with CD-CHO media. Once the temperature of the media reached 37°C the DOT probe could be calibrated along with recalibrating the pH probe.

Once the calibrations were complete the bioreactor was inoculated with enough cell culture to achieve a seeding density of 0.2×10^6 cells /ml. Both the media fill and inoculation was carried out in a vertical laminar flow hood. The operating process parameters for the MBR system are listed in table 2.3.

Table 2.3: Direct and magnetically stirred MBR operating parameters.

Process Parameter	**Setpoint**
DOT (%)	30
pH	7.1
Temp (°C)	37
Stirrer Speed (rpm)	410 (direct driven) 350 (magnetically driven)

2.7 Determination of viable cell concentration

The miniature and lab-scale bioreactor samples were counted daily by automated trypan blue dye cell exclusion method using the Vi-CELL Automated Cell Viability Analyser (Beckman Coulter, UK). 1 ml samples were spun down at 4000 RPM for 5 minutes and the supernatant retained for future metabolite analysis and stored at -20°C. The Vi-CELL also measured the average cell size.

2.8 Metabolite analysis

Metabolite analysis was conducted using the Nova Bioprofile 400 (Nova Biomedical, Cheshire, UK). Before running any samples the analyser was

calibrated to measure the concentrations of glucose, lactate, glutamine and ammonia. Analysis was conducted by thawing the retained supernatant samples and running them through the analyser at appropriate dilutions. The specific glucose consumption rate was calculated by dividing the glucose consumed by the integral viable cell concentration (IVCC) per day.

2.9 Bolus feeding

The feed used in the fed-batch cultivations was a 10 x concentration of CD-CHO media. The glucose concentration in the feed was increased from 65 g/L (the amount in 10 x CD-CHO) to 150 g/L by adding 85 g/L glucose (Sigma-Aldrich Company Ltd, Dorset, England). The feed was administered once daily to the MBRs when the glucose concentration fell below 2 g/L in order to bring the glucose level back to 2 g/L. The feed was delivered by injecting through a septum using a 2 mL syringe in the MBR and a 50 mL syringe in the 5L STR. The feed was filtered using a 0.22 μm Stericup filter (Millipore Express^{TM} Plus, Oxford, UK).

2.10 Continuous feeding

The feed was made in the same way as described for bolus feeding. The feed was administered to the MBR in order to maintain the glucose level at 2 g/L and fed continuously throughout the day at calculated flow rates. Flow rates were calculated based on historical data on glucose consumption rates and predicted viable cell concentration. Based on these figures the amount of glucose added to the MBR system over a 24 hour period was calculated.

The feed was delivered via the inbuilt feed pumps (RS, Watford, UK). Checks were made to ensure that the flow rates recorded by the pump were accurate. These checks were conducted for 3 flow rates, including the pump's slowest flow rate of 0.1 ml/h, 0.2 ml/h and 0.4 ml/h. Flow rates were consistently maintained at very low flow rates (0.1-0.4 ml/h) during feeding which necessitated the use of tubing with an internal bore size of 0.08 cm.

2.11 Characterization of bioreactor power input

The ungassed power (Pug) requirement of the MBR system was measured using a small scale air bearing dynamometer; the setup of which was similar to that described by Nienow and Miles (1969) with a force transducer (refer to Fig. 2.1). The glass vessel from the MBR system (D_T = 0.08 m) was filled with the culture working volume of RO water (300 ml) and mounted onto the top plate of the air bearing. To facilitate stirring, the impeller was connected to an overhead electric motor. The setup for the magnetically driven impeller was slightly different to that of the directly driven impeller. The directly driven impeller was screwed onto its impeller shaft as per standard operation, however the magnetically driven impeller was attached to the bottom of its impeller shaft with a waterproof adhesive. The MBR impeller was placed vertically and through the centre of the vessel in the same position as it would be had the headplate of the bioreactor been present. The clearance level of the impellers was the same as that used in the fermentations.

Changes in the force exerted on the sensor by the air bearing's arm were logged on a PC using WinIso software (HEL Ltd, Borehamwood, Hertfordshire, UK). Power input generated from impeller stirring manifested in changes in the force applied on the sensor and these measurements were used to calculate power input. The torque generated was measured using a pre-calibrated force transducer (FS Series, Honeywell, Lanarkshire, UK). From the torque measurements the power draw can be calculated using:

$$P = FR\omega \qquad 2.1$$

P = power requirement (W)
F = force applied on the sensor (N)
R = length of the arm pressing against the force sensor (m)

ω is the angular velocity, given by

$$\omega = 2\pi N \qquad 2.2$$

N = impeller rotational speed (rps)

The power input into the bioreactor is calculated using:

$$P = N_p \rho_L N^3 Di^5 \qquad 2.3$$

N_p = power number a dimensionless number

ρ_L = liquid density (kg/m^3)

N = impeller rotational speed (rps)

Di = impeller diameter (m)

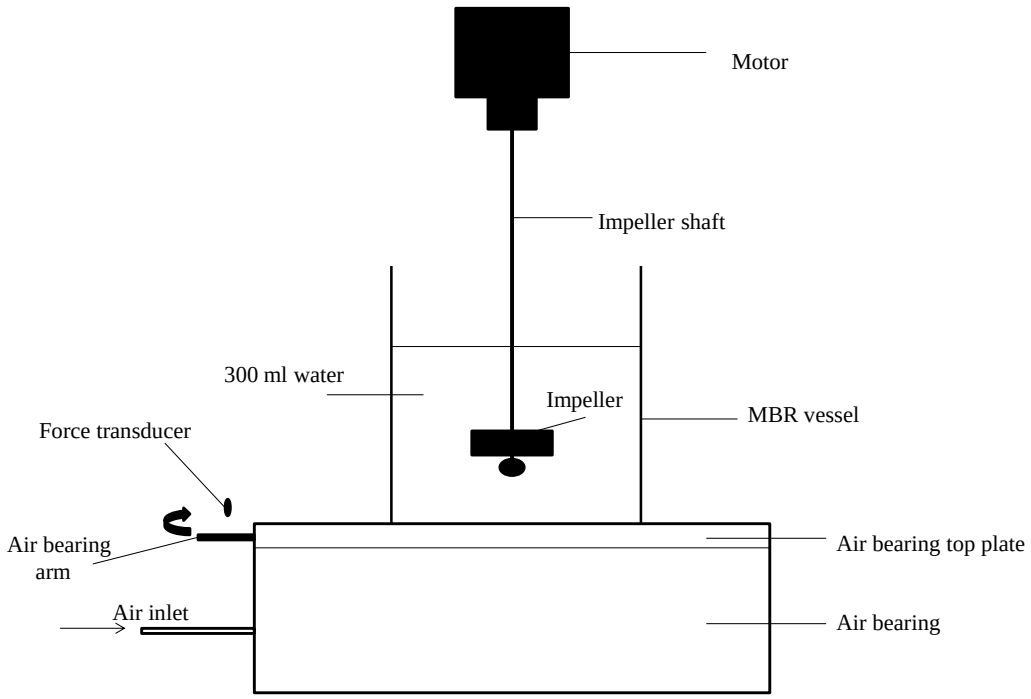

Figure 2.1: Schematic diagram of the experimental setup to measure power input into the MBR.

2.12 Characterisation of k_La

k_La measurements were determined using the static gassing out method. One trial was carried out in RO water with 63 gL^{-1} NaCl to investigate the method with

non-coalescing liquids. The second trial was carried out in CD-CHO media, the same media used in the fermentations. This is because the level of foaming in CD-CHO media was very significant and hence could affect the k_La measurements.

The DOT probe used in the trials was the same one used in the fermentations (Oxyferm FDA 120). The trials examined three different variables; the impeller design, the sparger design and the agitation rate. Before the trials, the probe response time was measured. This was done by placing the probe in a syringe with 0% oxygen achieved by sparging 100% nitrogen. Then quickly placing the DOT probe in fully oxygenated media at the appropriate agitation speed.

Once the bioreactor was setup with the appropriate impeller and sparger the agitation rate was set and the liquid totally de-oxygenated by sparging nitrogen gas. At this point the gas sparged was air (21% oxygen) and the rate of re-oxygenation was measured. The rate of re-oxygenation was measured from 20-80% oxygen to avoid imprecise start times and minor calibration issues.

k_La was calculated by calculating the slope of the graph of $\ln(C^*-C_L)$ vs time which has a gradient of k_La.

The equation for oxygen transfer is:

$$OTR = K_La\ (C^* - C_L) \qquad 2.4$$

K_La = overall mass transfer coefficient (h^{-1} or sec^{-1})
C^* = equilibrium oxygen concentration (mg/L)
C_L = concentration of dissolved gas in liquid (mg/L)

2.13 Characterisation of mixing time

2.13.1 Decolourisation method

Mixing time was measured using the iodine and sodium thiosulphate decolourisation method (Bujalski et al, 1999 and Hirati et al, 2007). 1.8 M sodium thiosulphate solution was added to 0.5 M iodine solution at a ratio of 1:99 (v/v) for both the MBR and 5L STR trials. After a minute of mixing, 0.99 M sodium thiosulphate was added via a pipette just above the surface of the liquid and projected into the impeller region. The mixing time was determined to be the period between the point at which the thiosulphate solution had been completely added to the iodine, and the point when the iodine solution became completely colourless. Time measurement was done by visual inspection and by using a stopwatch.

2.13.2 pH tracer method

The vessel was filled to working volume with RO water (300 ml). This was followed by addition of KOH to increase the pH. Once the pH reading had steadied HCL was added to lower the pH. The time taken for the pH reading to drop over 95% of the pH difference was measured as the mixing time. The quantities of acid and base used for the MBR and the 5L STR provided proportional molarity of each addition so that the starting pH, final pH and pH drop were consistent.

2.14 High speed camera imaging

The camera used was a DVR Fastcam (Photron, California, USA). The resolution used was 640 x 480 pixels, recording at 125 frames per second with a shutter speed of 1/frame rate.

2.15 HPLC

Product titre was quantified using High Pressure Liquid Chromatography (Agilent technologies, series 1200, Stockport, UK). A 1 ml protein A column was used (HiTrap^{TM}, GE Healthcare, Buckinghamshire, UK).

The analysis required the use of 2 buffers.

Equilibration buffer = 20 mM sodium phosphate @ pH 7 (~6.5)

For 1L – 1.084g NaH_2PO_4

– 3.273g $Na_2HPO_4.7H_2O$

Elution buffer = 20 mM glycine @ pH 2.8 (~5/6)

For 1L – 1.5g Glycine

The pH of the buffers was adjusted to the required pH by using 2M HCL. In order to reduce the build-up of contaminants on the column the buffers were filtered before use through a Stericup 0.22 µm filter (Millipore Express^{TM} Plus, Oxford, UK).

- 200 µl of the samples were aliquoted on to a 96 well plate and analysed by the plate reader with 100 µl of the sample injected on to the column.
- Analysis was performed at a flow rate of 1 ml/min.
- Detection was carried out at 220 nm and 280 nm.
- The approximate pressure during running of the HPLC was between 26 – 40 bar with a maximum limit of 80 bar.

2.15.1 Data analysis

The product titre was derived by calculating the area under the peak (PA) at 280 nm which corresponded to a retention time of 5.7 min and then multiplying by the dilution factor (DF). This figure should then be divided by 2,100 as this is the peak area that corresponds to 1 g/L.

Determination of IgG titre (g/L) = [DF x PA @ 280nm]/2100

Cell specific productivity was calculated by dividing the antibody concentration by the integral of viable cell concentration.

2.16 Methionine sulfoximine preparation

Methionine sulfoximine (MSX) (Sigma Aldrich, Dorset, UK) solution was made up to a concentration of 25 mM in Dulbecco's PBS (DPBS) solution. 250 mg of MSX powder was added to and left to dissolve in 55.49 ml DPBS at room temperature. This solution was then filtered through a 0.22 µm Stericup filter in a laminar flow hood and then aliquoted into 1.5 ml Nunc cryotubes and stored at -20°C. MSX was used by thawing in a 37°C water bath and then added to cell culture media at 1ml/L.

2.17 Design modifications

The MBR system that was built for this project was a basic protocol that lacked some features that were required for effective mammalian cell culture. Fundamentally, the sparger provided with the system, a vertical 0.31 cm diameter tube with a 15 µm filter attached was not suitable for mammalian cell culture (refer to Section 3.4.4). The system did not come equipped with a sampling mechanism which meant that sampling would have to be conducted in an aseptic vertical laminar flow hood. This would have required disconnecting the system from the polyblock and the main controller unit at least once a day. Sampling could be carried out by unscrewing the headplate and pipetting a sample. If this was carried out every day, it would have posed a significant risk of contaminating the vessel due to opening the system. Also there would be no process control for this period of time (roughly 5 minutes), which could effect culture performance.

Daily sampling in this manner was sub-optimal and hence a sampling port was designed and fitted to the system before cultivations could take place.

The MBR came equipped with a bulky condenser which occupied a large area of the headplate which made it difficult to operate the MBR particularly when using the direct driven configuration due to the size of the motor. A test was carried out to determine whether the condenser was necessary when operating the culture at 37°C. 300 ml of media was heated to 37°C and left for 3 days with the absence of the condenser, instead the system was merely connected to an empty bottle. Only 2 ml of water had collected in the bottle which was an insignificant volume, which meant that the condenser was not necessary.

A spare port in the headplate was modified into a septum port. Fortuitously, the size of the port could accommodate a standard septum which could fit tightly. The septum port was necessary to allow injection of feed and hence make bolus feeding possible. Before cultivation sterility tests were carried out to ensure that the technique of injecting feed through the septum could be done aseptically.

Chapter 3: Engineering Characterisation

3.1 Introduction

This chapter presents a detailed engineering characterisation of the MBR and 5L STR systems. Engineering characterisation is an important first step in understanding how a bioreactor system performs. There are minimum requirements that the reactor must meet in certain parameters to make optimal cell culture performance possible.

Engineering characterisation is also critical in order to conduct scale-up design. With process optimisation taking place at lab-scale this makes accurate scale-up a critically important step. In order to do this, important engineering parameters must be accurately characterised in order to achieve successful scale-up. For mammalian cell culture processes important parameters are power per unit volume (P/V), overall volumetric mass transfer coefficient (k_La) and mixing time (Varley and Birch, 1999).

Some of the physical characteristics that can affect bioreactor performance are vessel geometry, impeller type, size, shape and placement within the vessel as well as fill volume. Ideally the bioreactor should be operated to ensure optimal cell culture conditions as well as proving as efficient and cost effective as possible (Hockey and Nouri, 1996).

3.2 Characterisation of power number and power input

P/V is widely used for scale-up, scale-down and bioreactor design. The first definitive studies in power consumption were carried out by Rushton et al in the 1950's. He developed a number of dimensionless groups, including power number (N_p) (or Newton number) which relates resistance force to inertia force.

$$N_p = \frac{P}{\rho_L N^3 Di^5} \qquad 3.1$$

P = power input (W)
ρ_L = liquid density (kg/m^3)
N = rotational speed (rps)
Di = impeller diameter (m)
(Chapple et al, 2002)

N_p is closely linked to Re (refer to Fig. 3.1) which represents a ratio of inertial to viscous forces. Within laminar range (Re < 10), N_p is inversely proportional to Re, however within turbulent range (Re > 10,000) Rushton et al (1950) and Bates et al (1963) found that the impeller N_p of various impeller types and designs with baffled vessels remains almost constant. As a result, the N_p in the turbulent range is quoted as the N_p for a specific impeller geometry.

$$Re = \frac{\rho_L N Di^2}{\mu} \qquad 3.2$$

Di = impeller diameter (m)
N = impeller rotational speed (rps)
ρ_L = liquid density (kg/m^3)
μ = viscosity (kg/ms)

When the Re is in between laminar flow and turbulent flow it is classified as transition and is characterised by a variation in flow conditions within and external to the impeller region. This occurs because the flow conditions in the impeller region are more turbulent than in the rest of the bulk liquid. These regions of flow constantly mix with other regions in the bulk liquid and so form a transitional state of fluid flow (Dickey, 2010).

Figure 3.1: **A typical graph of the relationship between N_p and Re.** N_p becomes constant in the turbulent region which is roughly Re > 10^4 for most impeller types and designs (Harnby et al, 1992).

3.2.1 Power input

An important consideration for STRs is to minimise the mechanical stress damage exerted on the cells as mammalian cells can be fragile due to their lack of an outer cell wall. One of the factors that contribute to this is the power input into the reactor that is mainly determined by the impeller speed and gas sparging. It is preferable to employ impellers with pitched blades at lower impeller speeds as this can reduce shear stress at the same power per unit volume (Varley and Birch, 1999). Both the direct and magnetic impellers fitted to the MBRs are marine impellers that produce axial flow. Axial flow can be defined as generating currents that are parallel to the axis of the impeller as opposed to radial flow which produce currents that are in a tangential direction to the impeller shaft (refer to Fig. 3.2). Axial flow impellers can improve k_La by increasing the residence time of bubbles, this is particularly the case if gas is sparged underneath the impeller. They are also renowned for having a lower N_p and as a result being low shear. Radial impellers however, have higher power dissipation rates and hence break up bubbles, which can also improve k_La (Marks, 2003).

Table 3.1: N_p for a variety of impeller types.

(Taken from Dickey, 2010)

Figure 3.2: **Illustrations of the liquid flow patterns in a bioreactor.** A radial flow Rushton turbine impeller (a); an axial flow pitched blade turbine/marine impeller (b) and an axial flow hydrofoil impeller (c). (Taken from Dickey, 2010).

3.2.2 Power characterisation results

Gassed power (Pg) was not determined or calculated for the MBR. The reason for this is because gas sparging into the vessel can be conducted via surface aeration in which case gas bubbles are not present in the bulk culture. With regards to sparged aeration, this is intermittent, particularly in the early stages of a cultivation (days 0-4) where the gas demands of the system are low. As a result sparged aeration would have had an insignificant effect on power input (Lavery and Nienow, 1987) and hence it can be assumed that Pg = Pug.

As discussed previously, an important consideration for impeller choice for mammalian cell culture is to minimise mechanical stress damage and yet ensure low mixing times. Hence, the impeller should have a low N_p and high flow number which maximises flow for a given power input (Varley and Birch, 1999). Another important consideration is to operate the impeller at a tip speed that will not result in shear stress damage on the cells. It is widely recognised that an impeller tip speed above 1.5 m/s can begin to cause shear stress damage on cells (Varley and Birch, 1999).

The N_p of the magnetically driven impeller ranged from 0.47 – 1.20 and 0.39 – 0.53 for the directly driven impeller (refer to Fig 3.3). The N_p of the magnetic and directly driven impellers vary widely, especially at lower Re. This is because the design of the magnetically driven impeller creates less turbulence in the surrounding liquid and hence less power is lost to friction. As the liquid becomes more turbulent the N_p for both impeller types become more similar. The N_p of the magnetically driven impeller does reduce as Re increases, however it does not become constant in the turbulent regime. This could be partly due to the experimental design and operation of the power input experiments. The magnetically driven impeller is attached to a shaft which has a diameter of 0.31 cm. Due to the very small diameter of the shaft it was difficult to fit it perfectly into the motor lock that held and rotated the shaft. This resulted in a slight wobble that could have slightly distorted the power readings. These measurements compare favourably with those found in literature (Doran, 1995); Chisti (1992) used an assumed N_p of 0.4 for a marine impeller. These values are

lower than those for impellers used in microbial fermentations, like Rushton turbine impellers (generally $N_p > 1$), however low N_p impellers have been found to be generally better at gas dispersion than higher N_p impellers (Varley and Birch, 1999).

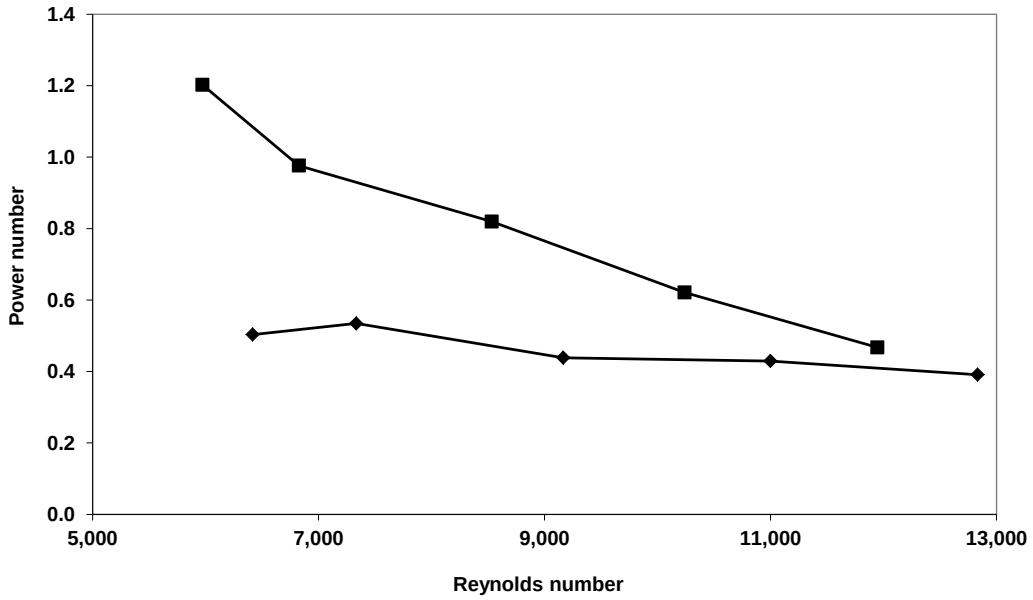

Figure 3.3: **Comparison of the N_p as a function of Re generated by the different impeller types at different speeds (350 – 700 rpm).** Magnetically driven impeller (■) and direct driven impeller (♦).

The power input for the magnetically driven impeller ranged from between 20.7 – 70.8 W/m^3 and 13.0 – 81.0 W/m^3 for the direct driven impeller. Between 350 rpm and 600 rpm the magnetically driven impeller has a higher power input, which could result in producing higher shear. The difference in power input decreases between the 2 impeller types and at 600 rpm, power input is virtually the same for both impeller types. At speeds greater than 600 rpm, the direct driven impeller has a marginally greater power input. It is difficult to make definitive conclusions as to why the magnetically driven impeller has a higher power input compared to the direct driven impeller at the lower impeller speeds as they are different designs. However, Nienow and Miles (1971) reported that pitched blade impellers with a clearance from the bottom of the vessel to tank height ratio of more than 1/3 have a higher power number than with a ratio of 1/3. The magnetically driven impeller was positioned with a smaller clearance than the direct driven impeller which may have resulted in the higher power

number and power input measurements. The magnetically driven impeller also has one more blade than the direct driven impeller which may also result in greater power input at the same impeller speeds due to the additional overall drag resistance on the impeller.

Power input measurements for the 5L STR were measured historically (Personal communication, Nick Silk). The P/V measurements for the MBRs and the 5L STR can be found in figures 3.4 and 3.5 respectively. At an impeller speed of 260 rpm; the impeller speed that has been previously determined to be optimal for the cell line used (Personal communication, Nick Silk), the 5L STR produces a P/V of 20.5 W/m^3. This P/V is matched by the directly driven MBR at an impeller speed of 410 rpm and by the magnetically driven MBR at an impeller speed of 350 rpm.

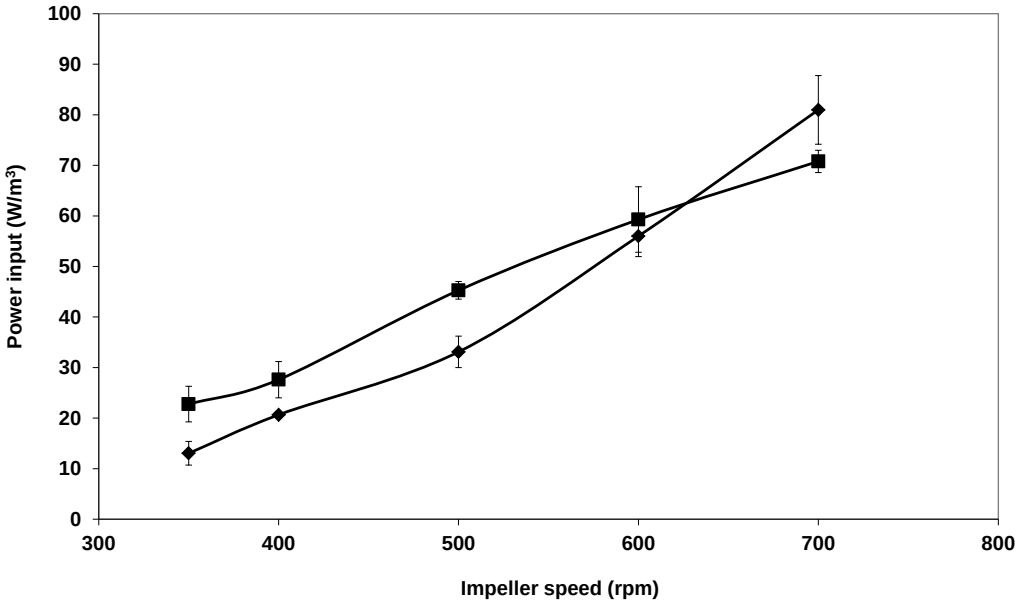

Figure 3.4: **Comparison of the volumetric power input generated by both MBR impeller types as a function of impeller speed.** Magnetically driven impeller (■) and direct driven impeller (♦). Experiments conducted as described in Section 2.11. Error bars represent one standard deviation about the mean (n=3).

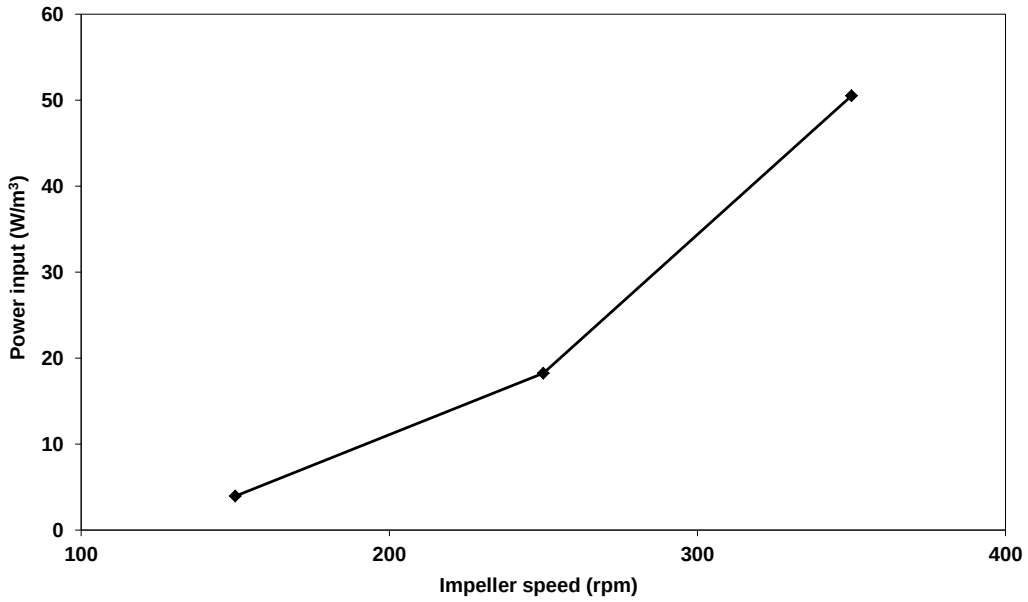

Figure 3.5: **Volumetric power input for the 5L STR over a range of impeller speeds.** These measurements were measured historically by Nick Silk (Personal communication) using the same equipment and methods as described for the MBR in Section 2.11.

3.3 Hydrodynamic conditions in the bioreactors

As has been previously discussed, mammalian cells are particularly shear sensitive and hence it is necessary to assess the shear stress produced by agitation as this is potentially the main cause of mechanical shear damage on the cells. As discussed in Section 1.7.4, fluid turbulence produces eddies, these eddies then break up into smaller eddies and so on. The smallest size eddies are called Kolmogorov eddies. Eddies contain kinetic energy and hence when they collide with cells they can exert enough mechanical shear stress to kill them. However, this only happens when the eddies are similar in size to the cells, which on average are 15 µm. Hence, it is important to calculate the Kolmogorov eddy size at various impeller speeds in the bioreactor systems to ascertain whether there is the potential for shear damage to occur.

The mean energy dissipation rate (average rate of dissipation of turbulence kinetic energy per unit mass) can be used to calculate the turbulent stresses acting on the impellers based on Kolmogorov's theory of local isotropic turbulence (Levich, 1962 and Harnby et al, 1992).

$$\overline{\varepsilon}_T = \frac{P}{\rho_L V} \qquad 3.3$$

P = power input (W)

ρ_L = liquid density (kg/m^3)

V = working volume (m^3)

For this theory to be most applicable, the Re must be in the turbulent region. Once the energy dissipation rate is known, the mean Kolmogorov length scale can be calculated and this is given by:

$$\overline{\lambda}_K = \left(\frac{\overline{\varepsilon}_T}{V^3} \right)^{-1/4} \qquad 3.4$$

$\overline{\varepsilon}_T$ = mean energy dissipation rate (W/kg)

v = kinematic viscosity (m^2/s)

The mean Kolmogorov length scale represents the mean length throughout the bulk liquid, however the maximum shear stress occurs in the impeller region where the energy dissipation rate is much greater than that in the rest of the bulk liquid (around 130 times more which is reflected in equation 3.5) (Cutter, 1966). Davies (1987) suggested that all the energy dissipated from the impellers is dissipated in half of the volume occupied by the impellers. Hence the Kolmogorov length scale in the impeller region is:

$$\lambda'_K = \left(\frac{\varepsilon'_T}{V^3} \right)^{-1/4} \qquad 3.5$$

$$\text{where } \varepsilon'_T = 130\, T$$

Table 3.2: Summary of the hydrodynamic conditions in the different bioreactors at different impeller speeds.

System	Impeller speed (rpm)	Energy dissipation rate (W/kg) x 10^3		Kolmogorov eddy size (µm)	
		$\overline{\varepsilon}_T$	ε'_T	$\overline{\lambda}_K$	λ'_K
MBR direct	350	0.020	2.6	84	25
MBR direct	700	0.080	10	60	18
MBR magnetic	350	0.023	2.6	82	24
MBR magnetic	700	0.070	9.1	62	18
5L STR	150	0.004	0.52	126	37
5L STR	260	0.020	2.6	84	25
5L STR	350	0.049	9.4	67	20

Table 3.2 clearly shows that none of the Kolmogorov eddy sizes produced by the various bioreactor systems are smaller than the average cell diameter, even when operated at high impeller speeds of 700 rpm in the MBRs. However, at these higher speeds the Kolmogorov eddy sizes are almost as small as the average cell size and could begin to cause cell damage (17.6 µm for the direct driven and 18.2 µm for the magnetically stirred). Hence, at slightly higher impeller speeds of around 800 rpm, Kolmogorov eddies smaller than 15 µm would be produced and could begin to cause mechanical stress damage on the cells. The impeller speed in the direct driven MBR that produces an impeller tip speed of 1.5 m/s is roughly 850 rpm and 800 rpm for the magnetically driven MBR, these are similar to the impeller speed that would produce Kolmogorov eddies that are smaller than 15 µm. Hence there does appear to be some evidence here that exceeding the maximum tolerable impeller tip speed of 1.5 m/s could initiate cell death due to the creation of Kolmogorov eddies that are smaller than cell size.

3.4 Characterisation of k_La

3.4.1 Introduction to static gassing out method

The static gassing out method was used in this study to measure k_La at various impeller speeds with a variety of sparger designs. This physical method has its advantages compared to chemical methods in that it can be conducted in cell culture media and hence provides an accurate representation of culture conditions.

3.4.2 Probe response time

DOT was measured in the reactor using the oxygen probe and so the probe response time could potentially affect k_La measurements as Tribe et al (1994), reported that not considering the probe response time can introduce significant errors in k_La measurements. According to Van't Riet (1979), the error in k_La is roughly 6% when k_La is smaller than the inverse of the probe response time. The response time of 6-8 seconds for the probe used in the following experiments is well below the inverse of k_La for any of the trials conducted in this study and hence probe response time was regarded as insignificant.

3.4.3 DO probe design and placement

Initial k_La measurements were carried out using the sparger provided with the MBR system, which was a hollow 0.31 cm diameter stainless steel shaft with a 15 μm sintered filter attached at the end. A major limitation of this sparger design was that it was a vertical hollow shaft that was located close to the vessel wall without a mechanism to sparge bubbles into the impeller region. This resulted in an uneven distribution of bubbles, with the majority remaining on the side where the sparger was placed.

There are 2 ports in the MBR headplate where the DOT probe and pH probes can be placed. There are also 8 positions where the sparger can be placed due to there being 8 x 0.31 cm ports in the headplate. Hence an initial study investigated the

effects on measured k_La due to the placement of the sparger and DOT probe in the headplate and their proximity to each other. The configurations trialled were with the DO probe nearest the sparger (1 cm away) and the DOT probe as far as possible from the sparger, on the opposite side of the headplate (5 cm away). It was expected that the difference in proximity would have an effect when using the 15 μm sparger due to the majority of the bubbles remaining on its side of the vessel. Another possible limitation of the reactor design is that the DOT probe is quite long and hence its sensor is located very close to the bottom of the vessel with a clearance of 1 cm. This makes it diametrically opposed to the area of the vessel where the majority of gas bubbles will collect.

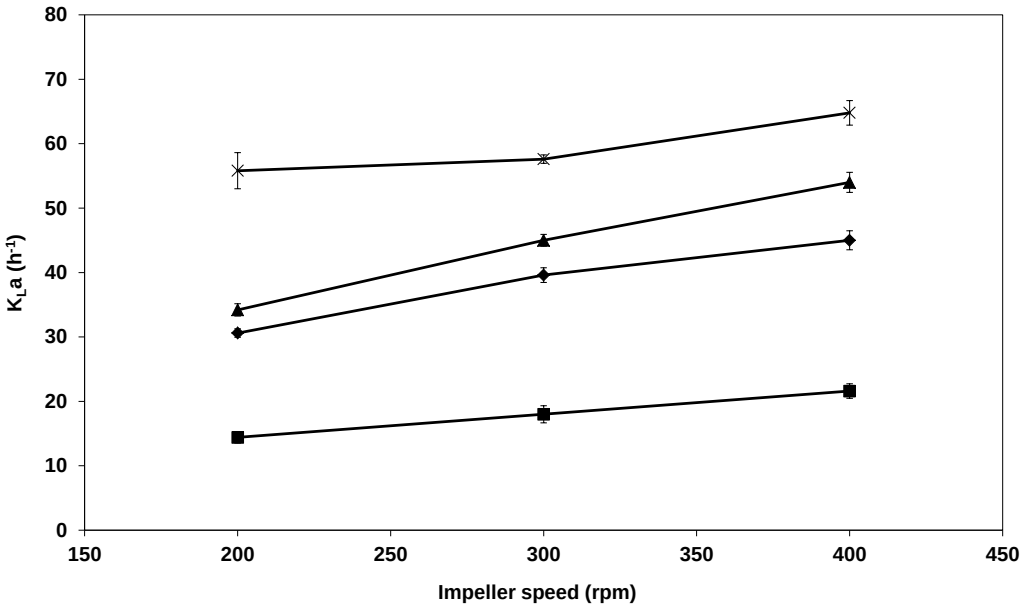

Figure 3.6: **Comparison of the k_La values for the direct and magnetic driven MBR impellers with the DOT probe in different positions in the bioreactor.** Magnetic far (■) represents the use of the magnetically driven impeller with the probe furthest away from the sparger (5 cm away) and magnetic near (♦) represents the use of the magnetically driven impeller with the probe nearest to the sparger (1 cm away). Direct far (▲) represents the use of the directly driven impeller with the probe furthest away from the sparger and direct near (x) represents the use of the directly driven impeller with the probe nearest to the impeller. All the DOT measurements were conducted using a constant gas flow rate of 0.33 vvm (100 ml/min). Error bars represent one standard deviation about the mean (n=3). These trials were conducted in water as described in Section 2.12.

All the DOT measurements were conducted using a constant gas flow rate of 0.33 vvm (100 ml/min). The k_La values measured when the DOT probe is close

to the sparger are significantly higher than those when the DOT probe is placed furthest away (refer to Fig. 3.6). This is not surprising as this sparger design is located on the side of the vessel pointing downwards. The directly driven impeller also provides higher k_La measurements. This could be due to its increased clearance from the bottom of the vessel and also because of its blade configuration which appears to provide increased turbulence to the liquid.

Based on the clear difference in measured k_La due to the bioreactor configuration, consequent trials were conducted with the DOT probe being placed opposite to the sparger in the headplate. This effect was heavily amplified due to the design and location of the 15 μm sparger and this difference is not anticipated when using spargers that direct bubble gas into the impeller region.

3.4.4 Alternative sparger designs

The 15 μm sparger was not a practical sparger design to use during cell cultivations because it produced a prohibitive amount of foam in CD-CHO media. Hence various other spargers were designed for use in the MBR. These spargers were designed to produce larger bubbles so as to reduce foaming and also to project the bubbles into the impeller region so as to produce better bubble and gas dispersion. The spargers used in the following experiments were a 90 μm sparger which was of a similar design to the 15 μm sparger except with larger pore sizes. A singular opening sparger which consisted of a 0.31 cm diameter hollow stainless steel shaft with a curved open end that could release bubbles into the impeller region. A horseshoe sparger design that again was fashioned from a 0.31 cm diameter hollow stainless steel shaft with 5 evenly spaced holes with a diameter of 0.05 cm that formed a semi-circle below the impellers. The fourth sparger design was 4 evenly spaced holes with a diameter of 0.05 cm drilled into the bottom of the impeller shaft of the magnetically driven impeller, which was again a 0.31 cm diameter hollow stainless steel shaft. Table 3.3 presents the values of k_La measured for each sparger design for both impeller types and as a function of impeller speed.

Table 3.3: Summary of k_La data obtained from different sparger and impeller designs at varying impeller speeds at an airflow rate of 0.33 vvm.

	k_La (hours^{-1})		
Impeller type	300 (rpm)	400 (rpm)	500 (rpm)
Horseshoe direct	8.1	8.2	9.7
Horseshoe magnetic	12	11	10
Singular hole direct	5.9	8.5	9.2
Singular hole magnetic	5.0	7.2	14
Impeller shaft	6.2	6.3	6.4
90 μm direct	16	17	22
90 μm magnetic	18	18	24

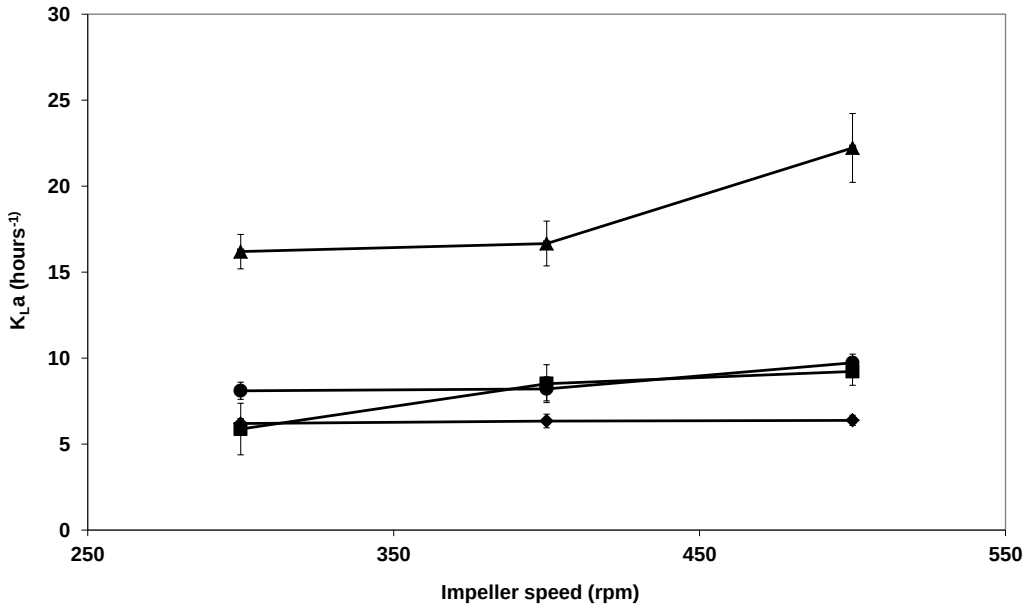

Figure 3.7: **k_La measurements for the different MBR sparger designs using the direct driven impeller and the magnetically driven impeller shaft sparger at an airflow rate of 0.33 vvm**. 90µm sintered sparger (▲); 0.31 cm diameter singular hole sparger (■); 4 hole impeller shaft sparger (♦) and horseshoe sparger (●). Error bars represent one standard deviation about the mean (n=3). These trials were conducted in CD-CHO media at 37°C as described in Section 2.12.

As k_La is a function of aeration rate, bubble size and agitation rate, it was not surprising to see that the 90 µm sparger provided the highest k_La (refer to Fig. 3.7). There was no significant difference between the other sparger designs with all the other sparger configurations providing k_La values in the same region (Table 3.3). k_La measurements obtained using the direct driven impeller clearly show that the k_La produced by the 0.31 cm diameter singular opening sparger and the horseshoe sparger were very similar. All the other sparger designs except the 90 µm sparger were facing the impeller. The horseshoe sparger had a glaring limitation in that bubbles only came out of one hole, the one nearest the shaft. The flow rates used did not generate enough pressure to release bubbles from the other holes which clearly limits its ability to increase k_La. This is not the case with the horseshoe sparger in the 5L STR which could release bubbles from each of its holes. The horseshoe sparger design is meant to aid bubble distribution as bubbles are sparged underneath the impeller and from multiple points.

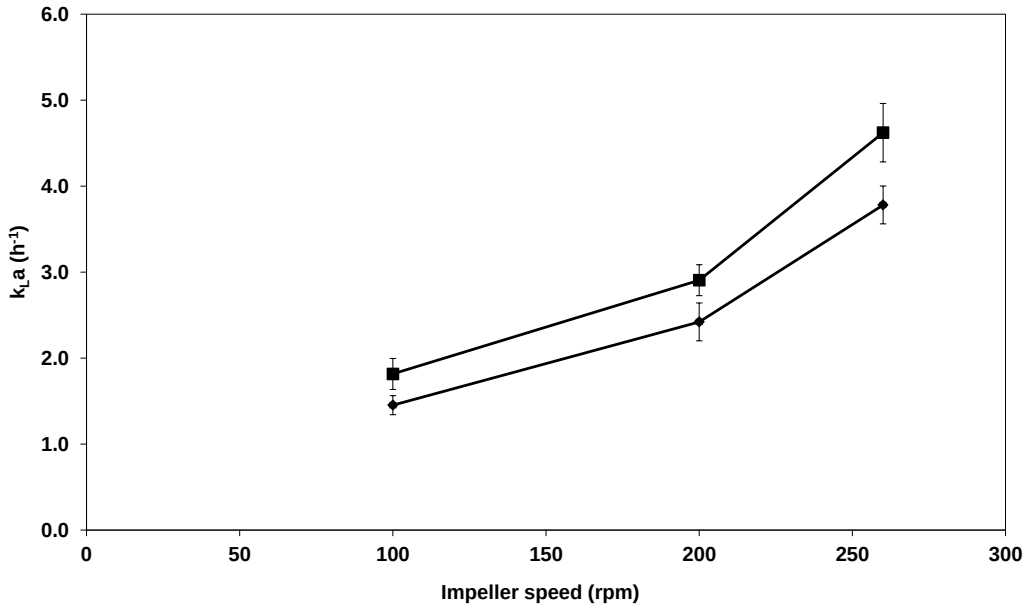

Figure 3.8: **k_La measurements in the 5L STR at different impeller speeds and airflow rates**. 0.03 vvm airflow (♦) and 0.06 vvm airflow (■). Error bars represent one standard deviation about the mean (n=3) These trials were conducted in CD-CHO media at 37°C as described in Section 2.12.

k_La measurements in the 5L STR (refer to Fig. 3.8) increase with both increasing impeller speed and higher gas flow rate. As expected higher airflow rates produce higher $k_L$as at corresponding impeller speeds due to k_La being a function of aeration rate.

The k_La results achieved in the MBR compare favourably with those found in literature for mammalian cell culture systems. Typical values of k_La found in mammalian cell culture processes is within 1-15 h^{-1} (Diao et al, 2007, Nienow 2006 and Moreira et al 1995).

3.4.5 k_La measurements using surface aeration

k_La was measured while operating the directly driven MBR with surface aeration. MBRs have been successfully operated while using surface aeration primarily because their smaller liquid volume can facilitate enough gas diffusion to occur to achieve a k_La that can support cell growth at high cell densities. This is the case with regards to shake flasks which rely on surface aeration for gas delivery and exchange. With regards to the k_La measurements undertaken, they

were carried out in the same way as those with direct sparging except that surface aeration was used. Kamen et al (1995) suggested that there are 4 conditions that must be met in order to calculate accurate k_La values using the static gassing out method. These conditions are that the gas side and interfacial resistances are negligible, the gas phase and liquid phase are well mixed, the response time of the probe is at least five fold shorter than rate of absorption and that the residence time of the gas phase in the bioreactor is short so that the interfacial concentration of oxygen at equilibrium may be considered constant. The first condition is met as it is well known that the gas-liquid interface itself contributes negligible resistance (Doran, 1995) and that the liquid-phase mass-transfer resistance dominates due to the poor solubility of oxygen in culture media. Section 3.7 of this thesis shows that the liquid phase is well mixed and it is assumed that the gas phase would be well mixed due to the relatively small headspace and high airflow rate (0.66 vvm). Section 3.4.2 has already shown that the probe response time is negligible. As for the fourth condition, the gas residence time is a measure of how long it takes for the gas concentration to significantly change in a given volume. The gas residence time in the headspace is governed primarily by the size of the headspace and the gas flow rate. If the reactor has a large headspace and low gas flow rate then gas mixing in the headspace will be slow and hence the gas residence time will be significant. If the headspace is small and the gas flow rate is higher, then gas mixing in the headspace will be quicker and hence the gas residence time will reduce.

The residence time was not measured in this experiment but can be assumed to be insignificant as the reactor headspace is relatively small at < 200 ml and the airflow rate used in surface aeration at 200 ml/min = 0.66 vvm which is relatively high. Also, k_La is calculated by measuring the gradient of the linear slope which is often between 20-80% DOT and hence there is an opportunity for appropriate gas removal to occur in the headspace before the DOT reaches 20% and hence accurate measurements of k_La can occur.

Surface aeration in the directly driven MBR produced k_La values ranging from 1.3 h^{-1} at 300 rpm to 2.3 h^{-1} at 500 rpm (refer to Fig. 3.9). These are significantly lower than the k_Las measured using sparged aeration and may inhibit cell growth

if high cell densities (> 10^6 cells/mL) are reached. The MBR system can however compensate for these lower k_La values by separately sparging enriched oxygen into the reactors to supplement the air inlet.

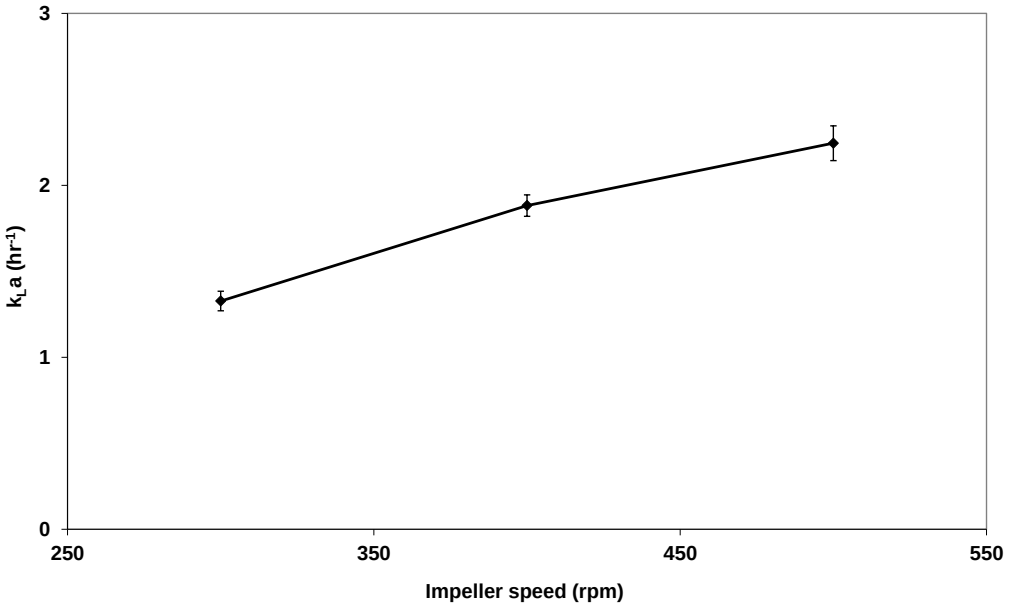

Figure 3.9: **k_La measurements for the direct driven MBR at a range of impeller speeds with surface aeration at 0.66 vvm**. Error bars represent one standard deviation about the mean (n=3).

3.5 Mixing time

Mixing time is a very important parameter for mammalian cell culture processes. Mixing should be optimised so that a homogenous environment is produced within the reactor. Otherwise the cells will travel through a variety of environments within the reactor, which can have adverse effects on the cells growth kinetics and productivity. Mixing times should also be minimised so that responses to any changes in operating conditions like temperature and pH can be as fast as possible. Efficient mixing is particularly important during fed-batch operation to avoid the creation of local nutrient gradients

3.5.1 Decolourisation method

Mixing times were evaluated in the MBR for both impeller types at working volumes of 200 and 300 ml using the decolourisation method. This method has been widely used for determining mixing times (Bujalski et al, 1999 and Hirati et al, 2007) as the reaction between iodine and sodium thiosulphate is quick and hence the rate limiting step will be liquid mixing.

Figure 3.10 shows that mixing time is inversely proportional to impeller speed and that it is reduced at smaller fill volumes. Lower mixing times are expected at smaller fill volumes as there is a constant amount of energy being transferred to the liquid to a reduced volume, which results in more turbulence leading to faster circulation. The direct driven impeller provides shorter mixing times than the magnetically driven impeller particularly at lower speeds. This is likely due to the direct driven impeller having a greater clearance from the bottom of the vessel and also due to its three blade configuration which creates more turbulence in the liquid (Nienow 2006). The magnetically driven impeller provides mixing times of between 4 – 15 seconds and the directly driven impeller provides mixing times of between 3 – 13 seconds over the same impeller speeds. At a constant P/V of 20.5 W/m^3 the mixing times are similar when the MBR is run at a working volume of 300 ml. At a matched P/V the 5L STR provides a mixing time of 6 seconds which is very similar to both MBR configurations which produce mixing times of 6 and 9 seconds for the direct and magnetically driven impellers respectively. The mixing times in the 5L STR and MBR are consistent with those found in literature. It was reported that mixing times for a 5L STR for CHO cell culture is 2-5 seconds (Lara et al, 2006).

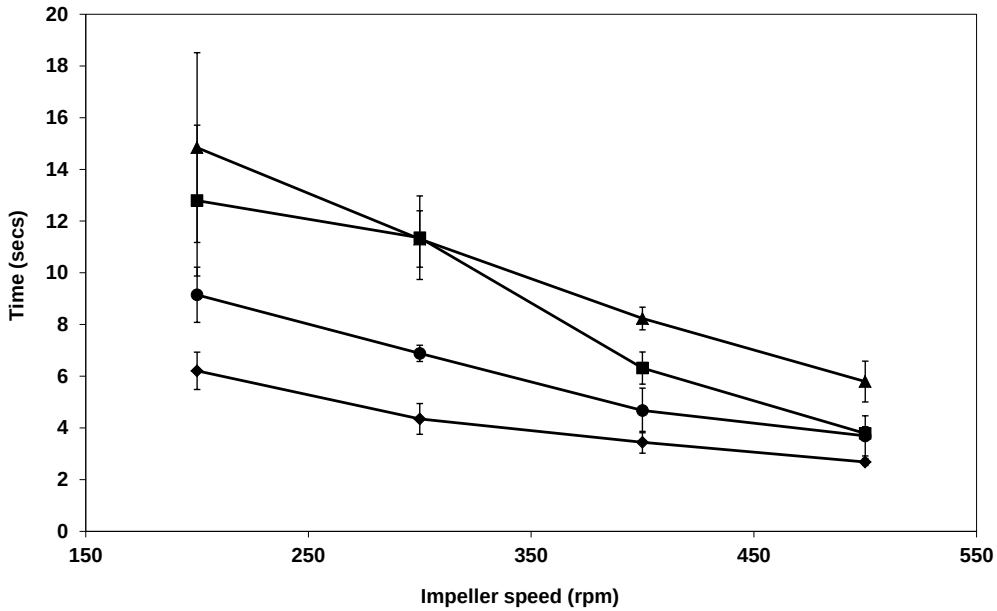

Figure 3.10: **Comparison of the mixing times for the direct and magnetically driven impellers in working volumes of 200 and 300 ml using the decolourisation method.** Directly driven impeller with a fill volume of 300 ml (■); directly driven impeller with fill volume of 200 ml (♦); magnetically driven impeller with a fill volume of 300 ml (▲); magnetically driven impeller with a fill volume of 200 ml (●). Trials were conducted according to the method described in Section 2.13.1. Error bars represent one standard deviation about the mean (n=3).

It has been reported that on increasing bioreactor scale that mixing time should increase (Marks, 2003). However, there are reasons why this is not the case when comparing the MBR and the 5L STR.

a) The 5L STR has a curved base which improves mixing by better facilitating the circular flow of liquid. Due to the shape of the MBR port in the polyblock, the MBR vessel has to have a flat base to fit tightly into the block. Also the vessel is heated via the base of the polyblock port and hence there must be full contact between the MBR vessel and the polyblock port.

b) As detailed in Section 2.3, the impeller design of the direct driven MBR is different to that of the 5L STR. The direct driven MBR impeller is a marine impeller with a blade angle of 30° while the 5L STR is fitted with an elephant ear impeller with a blade angle of 45°.

To evaluate the impact of blade angle on mixing times, a scale down model of the 5L STR impeller was constructed and evaluated in the MBR system. The impeller was scaled down by maintaining a constant impeller diameter to tank diameter ratio, blade width to impeller diameter ratio and blade length to impeller diameter ratio. The mixing time produced by the scaled down impeller was evaluated with two blade angles; 30° and 60°; over a range of impeller speeds using the decolourisation method as detailed in section 2.13.1. Figure 3.11 clearly shows that the angle of the blade has a significant impact on mixing time with the 60° angle blades producing much shorter mixing times than the blades inclined at 30°. This indicates that larger blade angles can produce shorter mixing times and could explain why the mixing times in the 5L STR are shorter than expected.

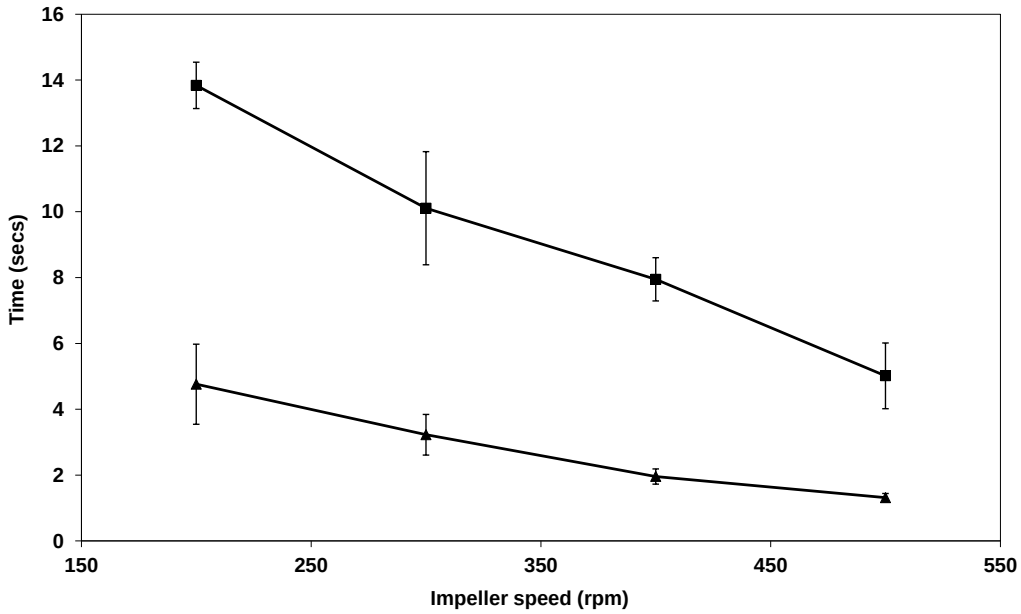

Figure 3.11: **Mixing times at a variety of impeller speeds using a pitched blade impeller in the directly driven MBR**. 30° blade angle (■) and 60° blade angle (▲). Error bars represent one standard deviation about the mean (n=3).

3.5.2 pH tracer method

The pH tracer method was used to measure the mixing time in the MBR (refer to Fig. 3.12). The trends achieved using this method were very similar to that used in the decolourisation method. Mixing times were shortest at 200 ml culture volumes and were also shortest using the direct agitation method. The direct

driven impeller provides mixing times of 7-20 seconds and the magnetic driven impeller provides mixing times of 7-24 seconds. The limitation of this method was that there was a slight delay due to the response time of the probe which may have caused the readings to be similar at the shortest mixing times.

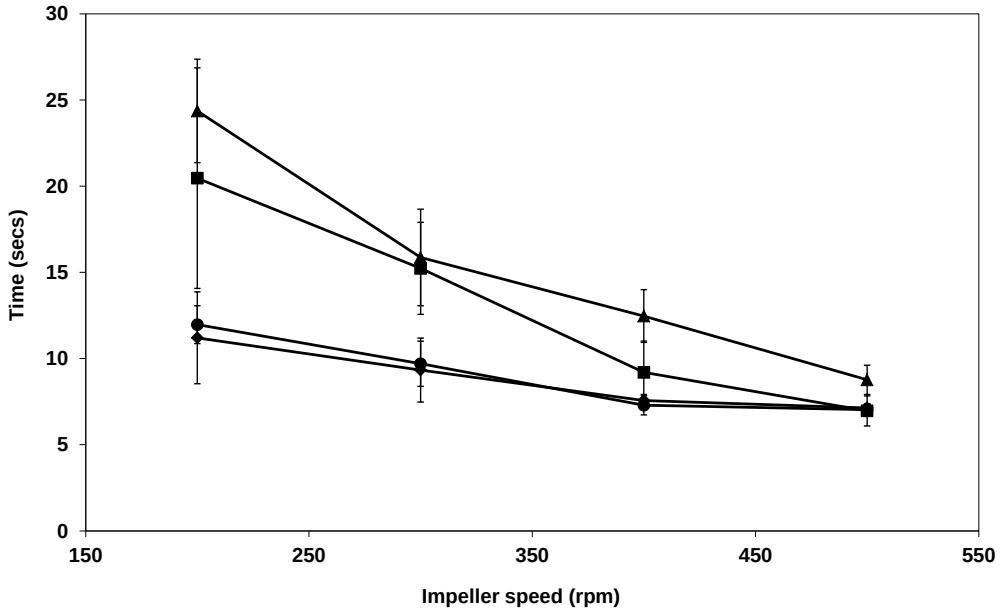

Figure 3.12: **Comparison of the mixing times for the direct and magnetically driven impellers in working volumes of 200 and 300 ml using the pH tracer method.** Directly driven impeller with a fill volume of 300 ml (■); direct driven impeller with fill volume of 200 ml (♦); magnetically driven impeller with a fill volume of 300 ml (▲); magnetically driven impeller with a fill volume of 200 ml (●). Trials were conducted according to the method described in Section 2.13.2. Error bars represent one standard deviation about the mean (n=3).

3.5.3 Mixing time correlation

Nienow reported in 1998 that mixing time could be predicted by using equation 3.6 with bioreactors that have a 1:1 aspect ratio.

$$T_m = 5.9 D_T^{2/3} (\overline{\varepsilon}_T)^{-1/3} (Di/D_T)^{-1/3} \qquad 3.6$$

D_T = Tank diameter (m)

$\overline{\varepsilon}_T$ = Mean energy dissipation rate (W/kg)

Di = Impeller diameter (m)

Nienow's equation was used to compare predicted mixing time values with actual values obtained in the 5L STR and the direct driven MBR. The equation accurately predicts the mixing times in the directly driven MBR except at 300 rpm where there is a significant difference of 3.3 seconds (40% difference) (refer to Fig. 3.13). With regards to the 5L STR, the actual and predicted values are very similar except at 50 rpm where the actual mixing time is significantly higher at 96 seconds than the predicted value i.e. 50 seconds (refer to Fig. 3.14).

Table 3.4: Nienow's correlation accurately predicts the mixing time obtained in the direct driven MBR system.

	Average mixing time (secs)	
N (rpm)	MBR	Nienow
200	13	12
300	11	8.1
400	6.3	6.0
500	3.8	4.8

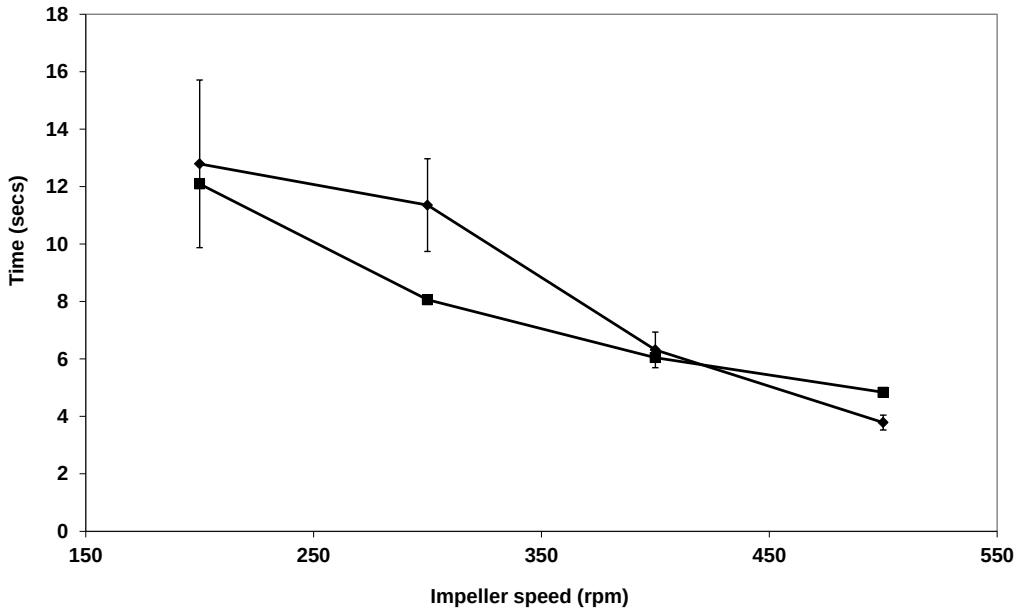

Figure 3.13: **Comparison of the mixing times in the directly driven MBR with a fill volume of 300 ml derived from the decolourisation method and predicted mixing times.** The directly driven MBR is represented by the (♦) and the Nienow predicted values are represented by the (■). Error bars represent one standard deviation about the mean (n=3).

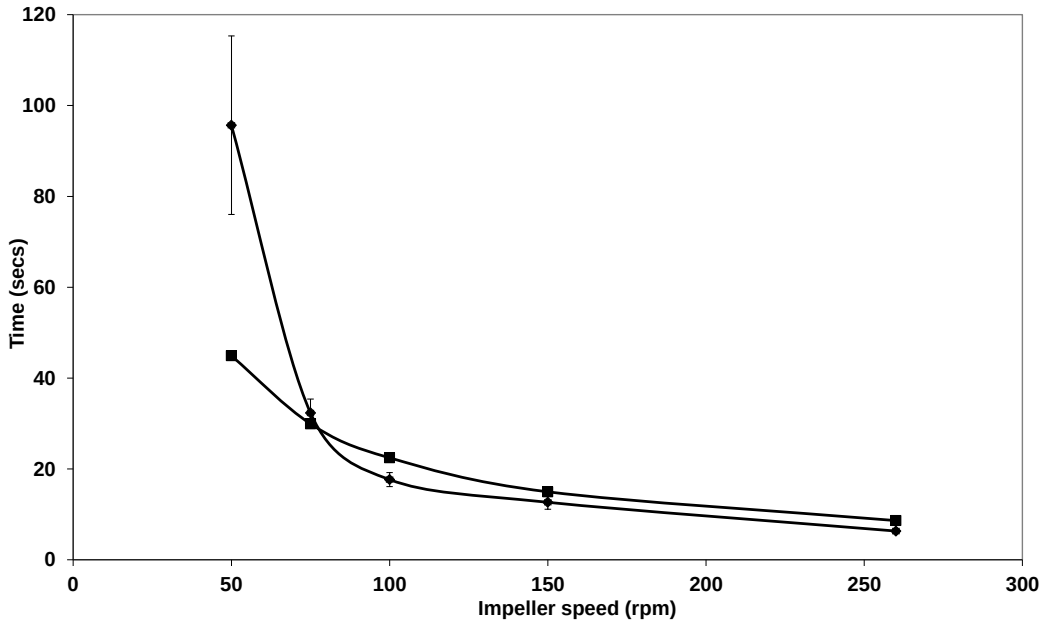

Figure 3.14: **Comparison of the mixing times in the 5L STR and Nienow's predicted values.** 5L STR (♦) and Nienow's predicted values (■). The 5L STR mixing times were measured using the decolourisation method as described in Section 2.13.1. Error bars represent one standard deviation about the mean (n=3).

3.6 P/V and mixing times at large scale

Mixing is an important parameter and it would be desirable to keep mixing time constant upon scale-up (refer to Section 1.7.2), however due to its relationship with power consumption, it is rarely possible to maintain a constant mixing time on scale-up. This is because larger fluid volumes result in longer flow paths for bulk circulation, which require faster fluid flows to achieve the same mixing times. As reactor scale increases, a significantly greater amount of power input is required to achieve faster fluid flows. To keep mixing time constant the velocity of the fluid in the tank must be increased in proportion to tank size.

Generally for geometrically similar bioreactors, P/V is directly proportional to fluid velocity squared:

$$P/V \propto v^2 \qquad 3.7$$

P = Power (W)
V = Volume of liquid (m^3)
v = Linear fluid velocity (m/s)
(Doran, 1995)

It is clear from the above relationship that increasing fluid velocity requires a significant increase in power input. Doran (1995) explained that scaling-up a $1m^3$ pilot-scale stirred tank to a $100m^3$ tank (assuming geometric similarity) would result in a 4.5 fold increase in fluid flow path length. Therefore to keep the same mixing time, fluid flow in the larger tank must be 4.5 fold faster, which would require a 20-fold increase in P/V. This is a significant increase in power requirement, which could produce a prohibitive level of shear stress.

Zlokarnic and Judat (1998) also discussed the impact of scale-up on mixing time and found that if P/V is kept constant, mixing time increases in proportion to vessel diameter raised to the power 0.67. Applying this to the scale-up of the 5L STR used in this study to a 5000L industrial scale STR; mixing time would be expected to increase by 4.7 fold or from 6 seconds to around 30 seconds. Xing et

al (2009) studied the impact of scale-up on a CHO cell culture process and found that mixing times varied between 50-200 seconds in a 5000L reactor and that significant DO and pH gradients were formed.

For these reasons mixing time is not a commonly used scale-up criteria for mammalian cell culture processes because a potentially prohibitive power input could be required to generate higher agitation rates (Xing et al 2009). Due to the shear sensitivity of mammalian cells and to ensure shear stress is kept within acceptable limits, constant P/V is commonly used as a scale-up criterion (Langheinrich and Nienow, 1999, Valery and Birch, 1999 and Marks, 2003).

3.6.1 Improving mixing times at large scale

Measures can be taken to minimise mixing time when scaling up using constant P/V. If geometric similarity is relaxed, Varley and Birch (1999) claim that larger impellers rotating slower would produce shorter mixing times than smaller impellers rotating faster. Marks (2003) proposed that mixing times at large scale could be reduced by employing the largest power input within the acceptable range so that agitation rate is increased but not to a speed that results in shear damage. Varley and Birch (1999) also suggest that making feed and acid additions in the impeller region as opposed to the culture surface could also reduce mixing times and the formation of concentration gradients.

3.7 Mixing time test images in the MBR

A selection of the mixing time trials were filmed using a high speed camera to confirm the times measured using the decolourisation method and to provide images of the mixing profile in the vessels. The images in figure 3.14 clearly show the downward axial flow generated by the direct driven impeller. Decolourisation and hence mixing occurs around and under the impeller region first and then occurs in the top half of the vessel. This can be partly explained by the injection of sodium thiosulphate which is injected just above the liquid surface downwards into the impeller region. This was done to mimic the addition of feed which is carried out in the same fashion. There were concerns that the surface tension around the DOT and pH probes could restrict mixing, however

from the images it is clear that this is not the case. Even the very slight gap between the DO probe and the vessel wall appears to be well mixed.

a) Time 0 seconds

b) Time 2 seconds

c) Time 6 seconds

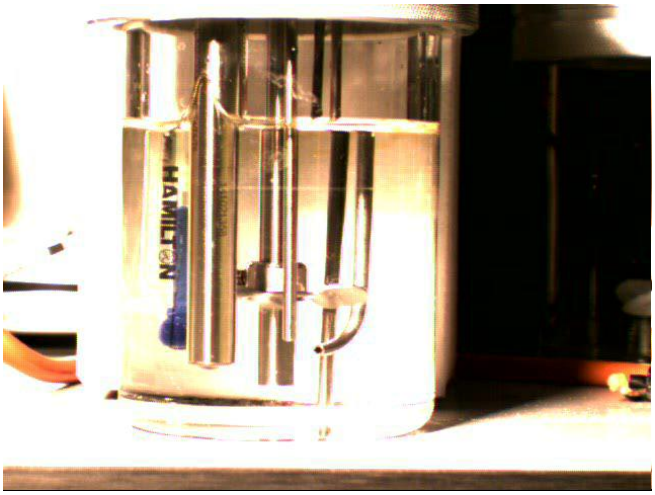

Figure 3.15: **Still images of the decolourisation experiment in the 500 ml MBR with a working volume of 300 ml and impeller speed of 410 rpm**. a) before sodium thiosulphate was added; b) 2 seconds after the addition of sodium thiosulphate and c) 6 seconds after the addition of sodium thiosulphate.

3.8 Conclusions

This chapter has presented a detailed engineering characterisation of the MBR system as well as an engineering characterisation of a 5L STR. This work was carried out to better understand the performance capability of the MBR with regards to power input, k_La and mixing time. These parameters have a significant impact on the feasibility and efficiency of carrying out cell culture and the potential to carry out cultivations at high cell density. These parameters were also measured in the 5L STR in order to conduct scale comparison studies which is an essential exercise in determining whether the MBR system is a feasible scale-down model for process development and optimisation.

Power input was measured for the directly and magnetically driven MBRs by using a small scale air bearing dyanometer; the setup of which was similar to that described by Nienow and Miles (1969). The N_p was calculated for both agitation configurations with the N_p for the direct driven impeller equalling 0.42. The N_p for the magnetically driven impeller was not accurately measured due to the experimental design; however it is estimated to be similar to that of the directly driven impeller. These figures are consistent with those found in literature

(Doran, 1995, Sandadi et al 2011) for marine impellers of around 0.4 – 0.5. The N_p of the 5L STR was measured historically as 0.97 (Personnel communication, Nick Silk) and when run at 260 rpm produced a P/V of 20.5 W/m^3. At matched P/V the agitation speed in the directly driven MBR is 410 rpm and 350 rpm in the magnetically driven MBR.

k_La was measured for the MBR system and the 5L STR as a function of agitation rate using the static gassing out method with CD-CHO media at 37°C, as this mimicked cell culture conditions. The sparger supplied with the MBR system (15 µm sintered sparger) was not suitable for use in CD-CHO media due to excessive foaming and hence a variety of alternate sparger designs were developed. k_La values were highest using the 90 µm sintered sparger design for both the directly and magnetically driven impellers (16-24 h^{-1}). On average the k_La values obtained for the other sparger designs were similar and varied between 5-14 h^{-1} which are values that are again consistent with those found in literature (Diao et al, 2007, Nienow, 2006 and Moreira et al, 1995) with regards to mammalian cell culture. k_La was also measured for the MBR using surface aeration and these values ranged from 1.3-2.3 h^{-1}. The k_La for the 5L STR was measured at different agitation and gas flow rates (100-260 rpm and 0.03-0.06 vvm). The k_La measured with an airflow rate of 0.03 vvm and at P/V = 20.5 W/m^3 was 3.8 h^{-1}, and doubling the gas flow rate to 0.06 vvm only increased k_La to 4.6 h^{-1}. It was found that agitation rate had a more profound effect on k_La than gas flow rate.

Mixing times were measured in the MBR system using the decolourisation and the pH tracer method as a function of both agitation rate and fill volume. Mixing times reduced significantly at faster agitation rates and smaller fill volumes. The directly driven impeller produced lower mixing times compared to the magnetically driven impeller. The 5L STR had a mixing time of 6 seconds at P/V = 20.5 W/m^3 which was very similar to the directly driven MBR which produced a mixing time of 6.3 seconds at the same P/V. It was found that the mixing times measured using the decolourisation method with the directly driven impeller were similar to those predicted by a correlation developed by Nienow (1998).

The engineering characterisation work presented in this chapter demonstrates that the MBR performs well in core engineering parameters like mixing time and k_La. The MBR was able to produce mixing times and k_La values that are comparable or better than the 5L STR at matched P/V. This indicates that it may have the potential to support cultivations that produce similar growth and productivity if a suitable scale-down criterion is used. To evaluate the MBR's potential to conduct comparable cultivations, an initial scale comparison cultivation is required, which will allow comparison between the 5L STR and both the magnetically and directly driven MBRs.

Chapter 4: Optimisation of gas delivery to the MBR system

4.1 Introduction

The findings of the engineering characterisation studies in the previous chapter indicate that the MBR system has the potential to facilitate high cell density cultivations. The work in this chapter evaluates the performance of the MBR system compared to a 5L STR using a constant scale-down criterion. This chapter also details a series of cultivations aimed at optimising the performance of the MBR system.

4.2 Initial comparison cultivations based on matched P/V

An initial scale comparison experiment was carried out to compare the performance of the 5L STR and the MBR system employing both the directly driven and magnetically driven impellers. Generally, the scale-down criterion chosen will very much depend upon the type of bioprocess being operated and the type of cell line. For fast growing cell lines that have high oxygen demands, like microbial cell lines, an appropriate scale-down criterion could be equal k_La, as oxygen supply will be the limiting factor. This is particularly the case as shear forces are not a major concern. However, mammalian cell cultivations have relatively low oxygen demands even at high cell densities and hence k_La is not often a limiting factor. P/V is often the scale-down criterion used for mammalian cell culture processes due to concerns of potential hydrodynamic cell damage. P/V is important for both mixing time and k_La (Varley and Birch, 1999), so it is important that the P/V constant used produces adequate mixing and k_La to support high cell densities, but is low enough to ensure hydrodynamic cell damage does not occur.

The scale-down factor that was used was a constant P/V of 20.5 W/m^3 as this was the P/V produced by the 5L STR when run at its recommended impeller speed of 260 rpm. A P/V of 20.5 W/m^3 falls within the typical range of values

(10-100 W/m^3) used for mammalian cell culture processes (Xing et al, 2009 and Gimenez et al, 2013). Scaling down based on matched P/V also produced the same mixing time of 6 seconds for the 5L STR and directly driven MBR. The mixing time of the magnetically driven impeller at matched P/V was higher at 9 seconds.

4.2.1 Fluid flow and hydrodynamic conditions

Generally, there is a concern as to how accurate scale-down can be carried out at miniature scale, particularly when the mechanisms used for mixing and k_La are often very different (for example the lack of mechanical agitation). It becomes more difficult to predict the flow patterns that occur at this scale and hence how effective mixing and k_La will be.

Most MBRs are modelled on lab-scale bioreactors and hence have common vessel geometry; this of course helps to ensure scale-down is as accurate as possible. In the case of the MBR used in this study, it is mechanically similar to conventional lab-scale bioreactors. The most significant difference in design however, is the shape of the bottom of the vessel. The MBR has a flat bottom which differs from the more curved bottom of conventional lab-scale bioreactors. This will have an effect on fluid flow as the curved bottom of the vessel helps to distribute gas and liquid flow above the impeller region and towards the top of the vessel. The MBR doesn't have this curved design and hence when the fluid flows approach the bottom of the vessels they are broken up which creates more turbulence.

The other notable difference is that the DOT and pH probes in the MBR occupy a significant volume within the vessel. The height of the vessel is 0.13 m and the shaft length of the probe is 0.12 m. The vessel diameter is 0.08 m while the probe shaft diameter is 0.012 m. This forms 15% of the vessels diameter which is significant, particularly as the pH probe has a similar diameter. Hence, the probes occupy roughly 30% of the vessel diameter. This makes the probes substantial baffles which are not required for mammalian cell culture. Bioreactors used for

microbial fermentations often employ 4 baffles with diameters that do not exceed 1/10 or 1/12 D_T and so the probes in the MBR mimic large baffles (Chisti and Moo-Young, 2002).

4.2.2 Growth comparison

The initial scale comparison cultivations were carried out according to the process parameters detailed in Sections 2.5 and 2.6 using fed-batch operation as detailed in Section 2.9. The maximum VCC of the 5L STR was significantly higher than that obtained in the MBRs; the 5L STR had a maximum VCC of 9.9 x 10^6 cells/ml, the maximum VCC for the magnetically driven MBR was 5.1 x 10^6 cells/ml and 4.9 x 10^6 cells/ml for the directly driven MBR (refer to Fig. 4.1). There was also a significant difference between the integral viable cell concentration (IVCC) of the 5L STR and that of the MBRs. The IVCC for the 5L STR was 78 x 10^6 cells.day/mL, 43 x 10^6 cells.day/mL for the magnetically driven MBR and 38 x 10^6 cells.day/mL for the directly driven MBR.

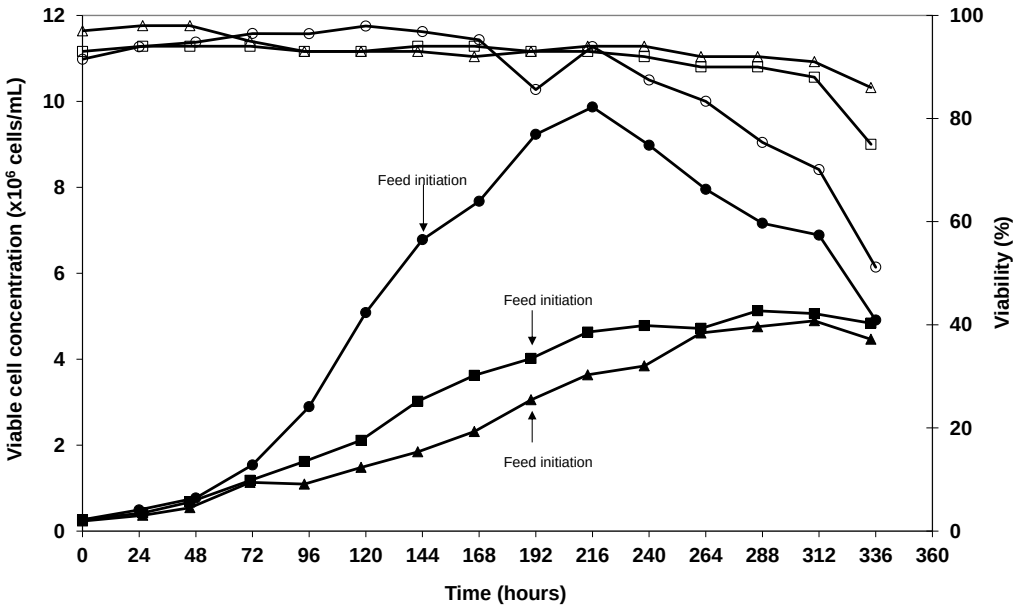

Figure 4.1: **Growth profile comparisons of the initial fed-batch 5L STR, magnetically driven MBR and directly driven MBR.** Both MBR configurations were directly sparged using a 0.31 cm diameter singular opening sparger with 100% enriched oxygen enabled from the beginning of the cultivations. Gas inlet pressure was unregulated in the MBR system. VCCs for the 5L STR (●); the magnetically driven MBR (■) and the directly driven MBR (▲). Cell culture viability for the 5L STR (o); the magnetically driven MBR (□) and the directly driven MBR (Δ). Process parameters are detailed in Sections 2.5 and 2.6 and the feeding strategy is detailed in Section 2.9.

In order to identify the exponential growth phase and calculate the maximum specific growth rate (μ_{max}), a semi-logarithmic plot (logarithmic VCC axis and linear time axis) was plotted (refer to Fig. 4.2) as it clearly presents changes in the rate of growth. In a semi-logarithmic plot, the linear part of the curve represents growth that is increasing at a constant rate with each consecutive time period and represents the exponential growth rate.

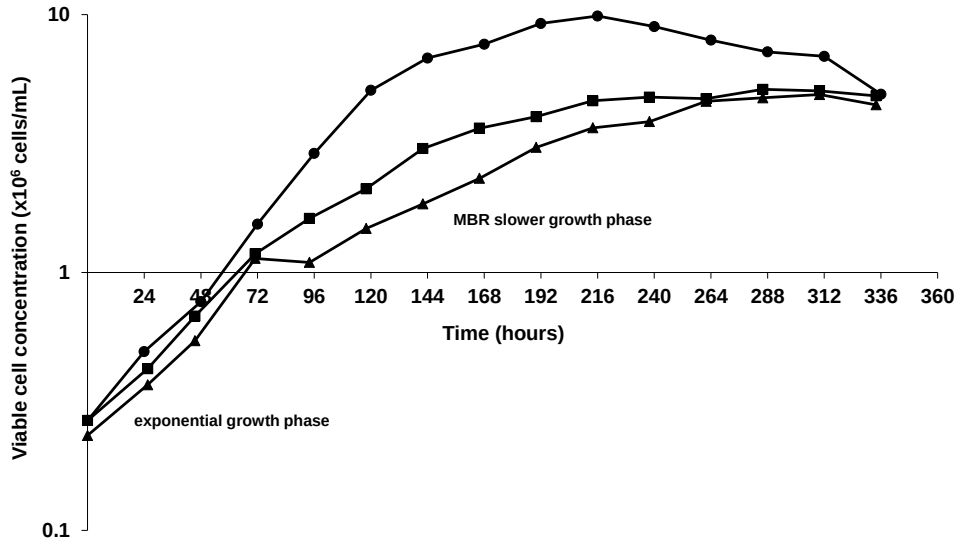

Figure 4.2: **Growth profile comparisons of the initial fed-batch 5L STR, magnetically driven MBR and directly driven MBR cultivations with the VCC plotted on a logarithmic axis and culture time plotted on a linear axis.** VCCs for the 5L STR (●); the magnetically driven MBR (■) and the directly driven MBR (▲).

The 5L STR maintains a constant and exponential growth rate from time 0 hours to 120 hours, identified by the linear part of the curve. The slope of this part of the curve is 0.025 hr^{-1} and as this represents growth during the exponential growth phase this also represents the maximum specific growth rate (μ_{max}).

Both MBR cultivations have two distinct growth phases during the same period (0 to 120 hours) (refer to Fig. 4.3). In the first phase of growth (0 to 72 hours), growth was exponential, indicated by the linear part of the curve with the steepest slope. During this period, the growth rate of the magnetically driven MBR was 0.021 hr^{-1} and 0.022 hr^{-1} for the directly driven MBR. The growth rate for both MBR cultivations reduced after 72 hours and this marks the beginning of a second distinct growth phase (72 to 144 hours for the magnetically driven

MBR and 96 to 144 hours for the directly driven MBR). In this phase, the growth rate for the magnetically driven MBR was 0.0095 hr^{-1} and 0.011 hr^{-1} for the directly driven MBR. This represents a significant reduction in growth rate compared to the 5L STR during a similar period.

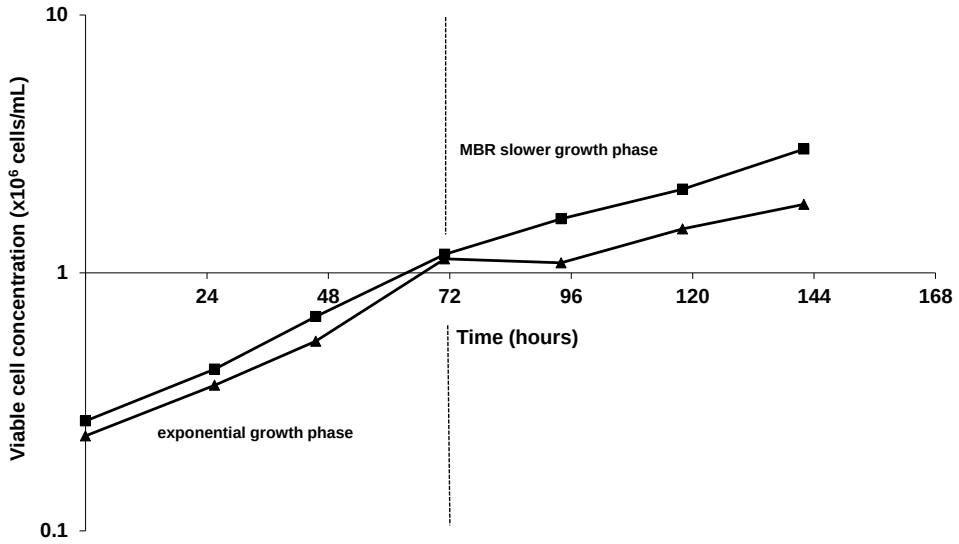

Figure 4.3: **Growth profile comparisons of the initial fed-batch magnetically driven MBR and directly driven MBR for time 0 – 144 hours with the VCC plotted on a logarithmic axis and culture time plotted on a linear axis.** VCCs for the magnetically driven MBR (■) and the directly driven MBR (▲).

At this stage it was unclear why the growth rates in the MBRs reduced after 72 hours as the main process parameters (temperature, DOT and pH) were closely controlled around the set points. What may have initiated the reduction in growth rate are factors relating to gas delivery. In the first 48-72 hours, mammalian cell cultivations have minimal oxygen requirements due to low cell numbers and thus minimal gassing occurs in this period. However, after 48-72 hours the oxygen demand of the culture begins to increase resulting in more frequent gassing of the reactor. As a result, factors related to the gassing of the system may have contributed to the reduction in growth rate after 72 hours and the subsequent lower maximum VCCs and final IVCCs produced by the MBRs.

Interestingly, it was noticed that the cells in the MBR were larger in size after 72 hours than those in the 5L STR. The cells in the 5L STR did not exceed 17 µm in diameter throughout the culture, however the cells in the MBRs both

reached a cell size of over 17.5 µm by 120 hours and remained around this size until 288 hours after which they began to reduce in size.

4.2.3 Antibody productivity comparison

Whilst some useful information can be inferred from the overall trends in product concentration data plotted against culture time in Figure 4.4, it is of note that there is significant variability in the data compared to expected trends. The data in Figure 4.4 presents a number of spikes which are unexpected and not observed in unpublished historical data and in other product concentration data presented in this thesis (Figures 4.11, 4.17 and 5.2). There are also data points in Figure 4.4 which show product concentration decrease with culture time (5L STR 288 to 336 hours; directly driven MBR 288 to 336 hours); this should not occur as product concentration could remain constant if the cells are not producing product or increase if the cells are producing product. Product concentration may decrease if the product breaks down; however there is no reason why this could have occurred during the cultivations as the main process parameters (DOT, pH and temperature) remained well controlled. Unexpected variability in the product concentration measured by HPLC could have been caused by inaccuracies during sample preparation or aliquoting.

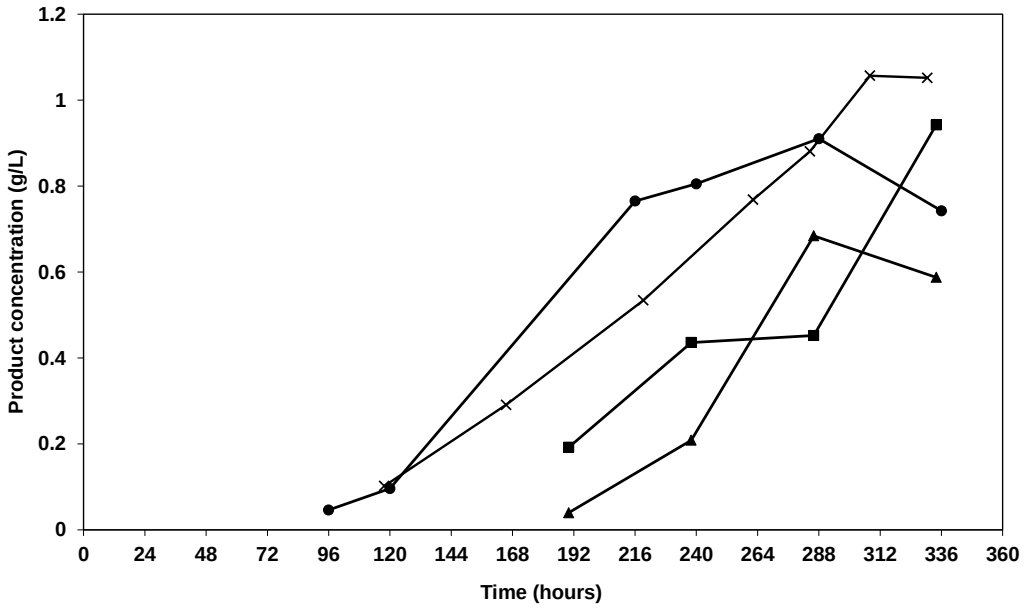

Figure 4.4: **Product concentration profile comparisons of the initial fed-batch 5L STR, a fed-batch 5L STR cultivation reported in Chapter 5 of this thesis (provided for comparison), magnetically driven MBR and directly driven MBR.** Initial fed-batch 5L STR (●); fed-batch 5L STR cultivation reported in Chapter 5 presented here for comparison (x); magnetically driven MBR (■) and directly driven MBR (▲). Antibody concentration was measured using HPLC as detailed in Section 2.15.

Given the variability in this data it would be inaccurate to make comparisons between the three cultivations based on the final product concentrations alone. The variability in the product concentration data also makes it difficult to calculate accurate cell specific productivity ($Q_{p)}$ values for each cultivation. Q_p can be calculated by plotting the product concentration vs IVCC (Sunley et al, 2008, Yanga et al, 2010 and Barrat et al, 2012) with the slope of this relationship representing cell specific productivity. This method of calculating Q_p would compensate for some of the variability by taking into account more of the data and thus reducing the effect of inaccuracies in the data; however as there are a limited number of data points on each curve (four for each MBR and six for the 5L STR), the Q_p values could still maintain a degree of inaccuracy.

Plotting the product concentration vs IVCC for all data points (refer to Fig. 4.5) results in a Q_p of 24 pg/cell/day for both the magnetically and directly driven MBRs compared to 12 pg/cell/day for the 5L STR. The R squared values of the trendlines for each bioreactor indicate that the relationship of product

concentration and IVCC does not explain some of the variation of the data about the mean (R squared 0.79 for the 5L STR; 0.87 for the magnetically driven MBR; and 0.78 for the directly driven MBR).

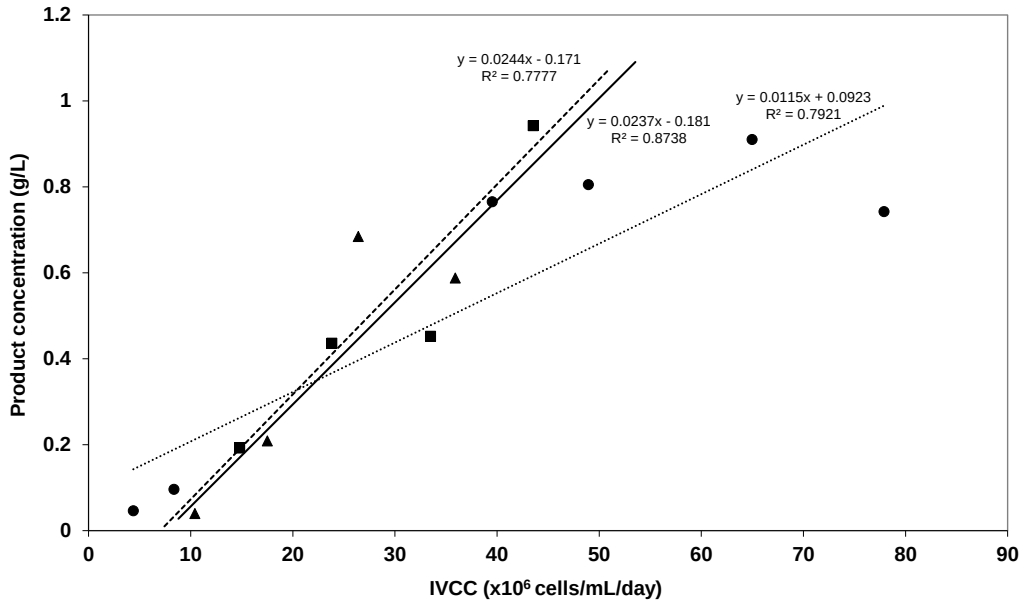

Figure 4.5: **Comparison plots of product concentration vs IVCC for the initial fed-batch 5L STR, magnetically driven MBR and directly driven MBR.** 5L STR (●); magnetically driven MBR (■) and the directly driven MBR (▲). Trend lines have been added to the plots for each reactor system with the dotted line representing the 5L STR; the solid line representing the magnetically driven MBR and the dashed line representing the directly driven MBR.

To reduce unexplained variation and to produce the best fitting trendline, a data point was removed from each cultivation (product concentration of 0.74 g/L at IVCC 77.9 x 10^6 cells.day/mL for the 5L STR; product concentration of 0.45 g/L at IVCC 34 x 10^6 cells.day/mL for the magnetically driven MBR; and product concentration 0.68 g/L at IVCC 26 x 10^6 cells.day/mL for the directly driven MBR) (refer to Fig. 4.6). When plotted in this way, the R squared values are closer to 1 making the trendlines fit the data better (R squared 0.95 for the 5L STR; 1.00 for the magnetically driven MBR; 1.00 for the directly driven MBR). Plotting the data in this way results in a Q_p of 16 pg/cell/day for the 5L STR; 26 pg/cell/day for the magnetically driven MBR and 21 pg/cell/day for the directly driven MBR. As these trendlines fit the data better, the Q_p values obtained from these trendlines would appear to be a better estimate of the Q_p of each cultivation.

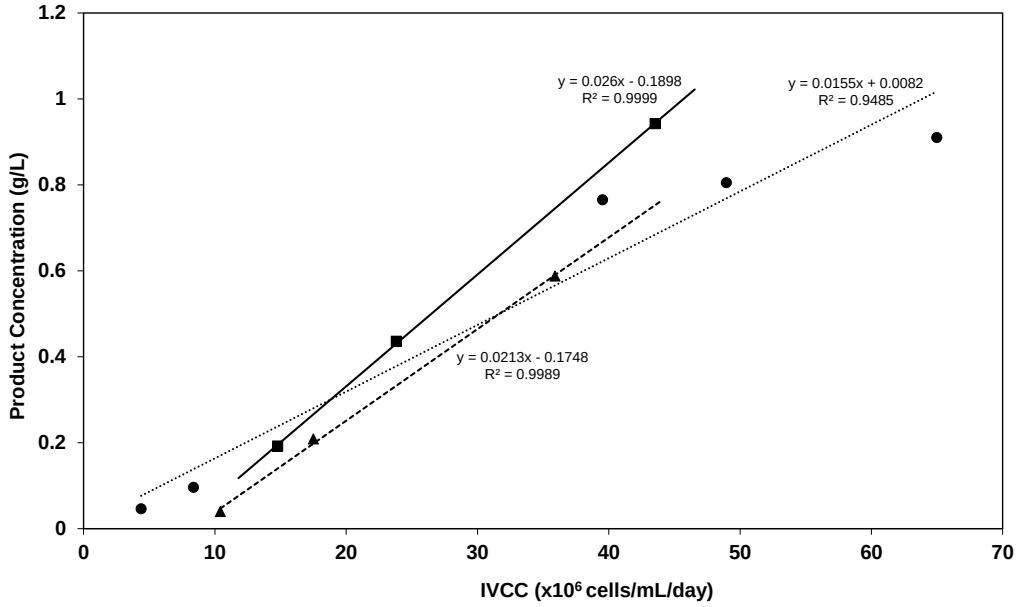

Figure 4.6: **Comparison plots of product concentration vs IVCC for the initial fed-batch 5L STR, magnetically driven MBR and directly driven MBR with one data point removed for each cultivation to reduce variation and to produce trendlines of best fit.** The data points removed are; the product concentration of 0.74 g/L at IVCC 78 x 10^6 cells.day/mL for the 5L STR; the product concentration of 0.45 g/L at IVCC 34 x 10^6 cells.day/mL for the magnetically driven MBR; and 0.68 g/L at IVCC 26 x 10^6 cells.day/mL for the directly driven MBR. 5L STR (●); magnetically driven MBR (■) and the directly driven MBR (▲). Trend lines have been added to the plots for each reactor system with the dotted line representing the 5L STR; the solid line representing the magnetically driven MBR and the dashed line representing the directly driven MBR.

4.2.4 Main findings and next steps

This initial fed-batch comparison cultivation showed that the 5L STR performed very differently to the MBRs when operated at a constant P/V of 20.5 W/m^3 (refer to Table 4.1). Both the growth and cell specific productivity profiles highlighted differences in performance between the 5L STR and the MBRs.

Table 4.1: Summary of the key growth and productivity data for the initial 5L STR and MBR cultivations based on a constant P/V.

	Direct driven MBR	**Magnetically driven MBR**	**5L STR**
Max VCC (x10^6 cells/ml)	4.9	5.1	9.9
μ_{max} (hr^{-1})	0.022 (0-72 hours) 0.011 (72-144 hours)	0.021 (0-72 hours) 0.0095 (96-144 hours)	0.025 (0-120 hours)
IVCC (x10^6 cells/mL/day)	36	43	78
Q_p based on all product concentration data points (pg/cell/day)	24	24	12
Q_p based on lines of best fit (pg/cell/day)	21	26	16

The increased Q_p and slower growth could indicate that the growth of the cells in the MBRs was arrested at a stage in the cell cycle that was particularly productive. Al-Rubeai et al (1992) reported that when hybridoma cells were arrested at the G1 phase using thymidine the Q_p increased and that cell volume was larger. They also reported that Q_p can increase when the cells are subjected to non-lethal hydrodynamic stress (Al-Rubeai et al, 1992). Throughout the literature there have been many similar studies involving different cell lines that have reported that there is an inverse relationship between Q_p and growth rate. This has been observed under a variety of different cell stresses including; the over expression of endogenous cell cycle inhibitors, exposing cells to chemicals that are known to induce growth arrest and using lower temperature shifts (hypothermic growth) (Sunley et al, 2008). The viability of the cultivations in the

MBRs was similar to that in the 5L STR and was consistently higher after 216 hours. Hence it would appear that the cells in the MBRs had been stressed to some degree that could have caused growth arrest, however this stress was not enough to result in reduced cell viability. It is not clear at this stage what could have caused this elevated level of cell stress as the MBR system accurately controlled the main process parameters including, temperature, pH and DOT.

It is unlikely that hydrodynamic stress damage could have been induced by the impellers using a matched P/V of 20.5 W/m^3. This is because the impeller tip speed for the directly driven impeller was 0.71 m/s and 0.65 m/s for the magnetically driven impeller, these speeds are both significantly below the impeller tip speed of 1.5 m/s which is recognised as being the speed at which cell damage may begin (Varley and Birch, 1999). Nienow (2006) contests that there are large-scale bioreactor mammalian cell culture processes that employ impeller tip speeds higher than 1.5 m/s which do not produce cell damage and so higher tip speeds can be tolerated by mammalian cells. The impeller tip speeds for the MBRs were also lower than that of the 5L STR which was 0.84 m/s, again indicating that the impeller tip speed should not have produced prohibitive amounts of shear stress on the cells. Another point to consider is that the impellers used in the MBR cultivations are pitched blade impellers with an angle of 30°, which is again a design aimed at reducing the production of shear stresses.

The gas delivery system of the MBR system may have caused the difference in growth and productivity between the 5L STR and the MBRs.

1. The MBR system was not capable of gas mixing and so the system could not continuously sparge each reactor. This resulted in the system having to deliver regular bursts of gas into the reactors in order to control process parameters (refer to Section 4.3.2). It was noticed that after each burst of gas, cells were drawn up the sparger shaft, and sometimes up into the gas filter. This would have been caused by the pressure differential that had been created between the sparger shaft and the bulk culture. The cells were then discharged back into the

bulk culture during the next burst of gas. This could have stressed the cells in two ways.

a) The cells that are drawn into the sparger shaft would have been isolated from the controlled environment in the bulk culture. This could have stressed the cells, particularly if they remained out of the bulk culture for some time or were drawn up into the air filter.

b) The cells could also have been exposed to shear stresses due to the shear forces created by the sparger wall as the cells flowed through the sparger shaft back into the bulk culture. The pressure in the gas inlet taps in the MBR system were not controlled, so the bursts of gas into the MBR may have occurred at a force high enough to induce shear stress on the cells.

2. The MBR was setup to control DOT using both air and 100% enriched oxygen, while the 5L STR controlled DOT by gradually increasing the oxygen concentration in the sparged gas when required. Extended use of 100% enriched oxygen may have had a toxic effect on the culture. This is discussed further in Section 4.3.3.

Flow cytometry could have been used in this study to further analyse the physiological state of the cells in the MBR and 5L STR cultures. Flow cytometry has been used to analyse mammalian cell culture cultivations since the 1990's and has been used to measure cell viability, cell number, cell cycle, apoptosis and many more physiological parameters (Kuystermans et al, 2012). This study could have benefitted from the use of flow cytometry to evaluate the cell cycle characteristics of the cultures, which could have provided a greater insight into the factors that caused the difference in growth in the MBR and 5L STR cultures. For example, Rubeai et al (1991) suggested that analysing the proportion of cells in the S phase of the cell cycle could provide an indication of the culture's proliferative capacity. It has also been reported that cultures undergoing growth arrest will have a higher proportion of cells in the G1 phase (Kumar and Borth, 2012).

Flow cytometry has also been used to study the impact of hydrodynamic stresses on hybridoma cells caused by gas bubble and agitation interactions. Rubeai et al (1993) used flow cytometry to conclude that cell damage occurred due to bubble entrainment and bubble bursting caused by vortex formation due to intense agitation. Hence flow cytometry could also have been used to study the impact of hydrodynamic forces created by direct sparging in the MBRs.

The rest of this chapter will discuss the principles of gas delivery and evaluate a number of batch cultivations that aim to optimise gas delivery to the MBRs.

4.3 Gas delivery to the MBR system

Gas delivery to a bioreactor forms a fundamental aspect of a bioreactor system's design. This is obviously because cells rely on a combination of gases to metabolise and grow and to synthesise the required protein product. In Section 1.7.4 of this thesis the potential shear effects of aeration have been discussed and in Section 3.4 the impact that the mode of aeration and sparger design have on k_La were also discussed. As aeration is so fundamental to the operation of bioreactor systems, optimising its design and operation is essential. The work in this chapter will focus on evaluating the MBR performance when employing a 90 μm sintered sparger, a 0.31 cm singular opening sparger as well as evaluating the performance of surface aeration.

The 90 μm sintered sparger was evaluated due to the high k_La values it produced, which would result in efficient oxygen transfer (refer to Section 3.4.4). The foam it produced was manageable with the additions of antifoam and hence it had the potential to be a viable configuration for mammalian cell culture.

The 0.31 cm singular opening sparger design was also used because it produced a sufficient k_La to maintain high cell densities (8.5 h^{-1}) at matched P/V to the 5L STR and represented a simple and effective design that generated large air bubbles. The formation of large air bubbles is an advantage because it results in less foam formation and reduces the potential shear effects on the cells.

Surface aeration was also investigated as a mechanism to mitigate the potential harmful effects of direct sparging (bubble creation and foaming). The higher surface area to volume ratio of MBRs can allow for sufficient levels of gas diffusivity and hence meet the cell culture's gas demands.

4.3.1 Gases supplied by the MBR system

4.3.1.1 Air and enriched oxygen

The most fundamental gas cells require is of course oxygen and hence supply of an adequate amount of oxygen to the culture is a key function of a MBR system. However, oxygen is the first gas that becomes limiting at high cell densities due to its poor solubility in culture media and so the oxygen supplied through air needs to be enriched with pure oxygen, often when the culture is in exponential and stationary growth phase. Also it is important for the system to have an adequately high k_La to ensure efficient oxygen transfer to the cells, particularly at high cell densities. Ideally, the oxygen concentration in the air/oxygen inlet should be increased gradually throughout the culture to meet the cells' oxygen demands. Gradually increasing the oxygen concentration with oxygen demand as opposed to sparging 100% oxygen into the culture will help maintain tighter control around the DOT setpoint and avoid any potential toxic effects associated with hyperoxia (over oxygenation). The toxic effects of oxygen have been reported (Cacciuttolo et al, 1992) and involve increased DNA strand breakage and adversely affecting the cells' metabolic functions like glucose consumption rate, lactate production rate and cell growth. The MBR system does not have gas mixing capability so these two gases are sparged to the vessels independently, which limits the system's capability of gradually enriching the air inlet with enriched oxygen.

4.3.1.2 Carbon dioxide

Cell culture media is normally buffered using CO_2 in the gaseous phase in equilibrium with sodium bicarbonate ($NaHCO_3$) (equation 4.1 and 4.2). In the early stages of the culture, pH will drift upwards due to the insignificant amounts

of CO_2 being produced as a result of cellular metabolism and because this CO_2 is being stripped out of the culture. As the culture progresses and the cells metabolise glucose to produce lactate, the culture pH will start to become more acidic, which would necessitate the addition of bicarbonate. It is important to try and maintain a tight control of pH and to keep the additions of CO_2 and bicarbonate to a minimum. The accumulation of dissolved CO_2 (DCO_2) in culture can have a toxic effect on cells adversely affecting their growth, productivity and on product formation. As a result it is important that a high level of DCO_2 does not accumulate in the culture and is hence stripped out (Matsunaga et al, 2009). CO_2 stripping will naturally occur when other gases are sparged into the culture displacing CO_2. A problem could occur if excessive amounts of CO_2 are sparged into the culture to control pH. CO_2 stripping becomes more of a challenge as the scale of bioreactor increases due to the liquid surface to volume ratio reducing. Matsunaga et al (2009) conducted a study that showed that the efficiency of gas stripping using surface aeration at small volumes (80 and 500L) was much greater than at larger scales (2000 and 10,000L). Hence, at miniaturised scale, gas stripping is more efficient due to k_La^{CO2} being higher. The factors that affect gas stripping are virtually the same as those that affect k_La^{O2} like vessel geometry, liquid volume, impeller tip speed, aeration rate, the sparger pore size as well as others (Matsunaga et al, 2009). Additions of bicarbonate should be minimised wherever possible as it will increase the culture's osmolality, which can also be harmful to cells at inhibitive levels (Zhu, 2012).

Although the concentration of DCO_2 can have a significant effect on cell culture, DCO_2 monitoring is not a standard feature of MBR systems. The main reasons for this are that DCO_2 probes are expensive, which can significantly increase the cost of a MBR if many vessels are run in parallel. Also due to a MBR's small scale, space in the headplate and within the volume of the vessel are at a premium (Frahm et al, 2002) and so DCO_2 monitoring is often compromised.

$$CO_2 + H_2O \longleftrightarrow H_2CO_3 \longleftrightarrow H^+ + HCO_3^- \quad 4.1$$

$$NaHCO_3 \longleftrightarrow Na^+ + HCO_3^- \quad 4.2$$

4.3.1.3 Nitrogen gas

The other gas that is sparged into the system is nitrogen. Primarily nitrogen is used to control DOT levels by stripping out excess oxygen.

4.3.2 Mechanism of gas delivery to the MBR system

Originally the system was designed to deliver oxygen to the MBR via air at 21% or through 100% oxygen. The MBR system does not have gas mixing capabilities and hence only one gas can be sparged into a vessel at any one time. Also if a gas is being sparged into a vessel, that same gas cannot be sparged into another vessel at the same time. The system can however sparge different gases into different vessels at the same time.

With regards to controlling process parameters the system addresses the needs of each bioreactor in order of priority. This priority is dictated by a combination of factors including how far the process parameter is from the setpoint, how far it is from the deadband (an acceptable range above and below the setpoint) and the rate at which it is drifting towards or away from the setpoint. For example, if the DOT level is well below the setpoint and the pH level is just marginally above the setpoint in 2 separate vessels it would prioritise sparging in air/oxygen to raise the DOT level and then move on to addressing the pH level in the other vessel.

4.3.3 Toxicity of 100% oxygen

It is widely understood that oxygen at high concentrations can have toxic effects on cell growth and productivity and hence DOT levels should be maintained at around 30-60% (Castilho et al, 2008).

A problem arises with the DOT control when 2 vessels require oxygen. In this situation the MBR could control a vessel by sparging air into one and pure

oxygen in the other vessel. Quite often air will be sparged into vessel 1 and pure oxygen in the following vessel. This poses three problems.

1. A vessel will be sparged with pure oxygen from the beginning of the culture even though it has a low oxygen demand. This sparging of pure oxygen may prove to be toxic to the cells if oxygen gradients are formed. This would seem unlikely as the mixing time of the system is very low and from studying the mixing images it is clear the system is well mixed (refer to Fig. 3.15 Section 3.7).

2. There is a difference in which gases are being sparged to the vessels and hence this affects consistency. If one vessel is predominantly being sparged with air while the other is being sparged with pure oxygen this forms a significant process change that could result in a variation of growth. It would be more desirable that both vessels were subjected to similar gas inputs to maintain consistent culture conditions.

3. The vessel that is sparged with pure oxygen will overshoot the DOT setpoint more frequently and more severely. This will result in more nitrogen being sparged into the vessel to strip out the excess oxygen. This again will lead to a difference in culture conditions as a vessel will be sparged with more nitrogen then the other.

Also with regards to scale comparison, the lab-scale bioreactor system used in this research did have gas mixing capability and hence it would have gradually increased oxygen concentration in the sparged gas to meet the culture's oxygen demand.

4.3.4 Sparger design – 90 µm sintered sparger

The MBR was operated using a 90 µm sintered sparger with sparging into the culture and employing direct driven agitation. The benefits of using a sintered sparger is that the small pores produce small bubbles which results in gas being delivered to the culture more efficiently. Smaller bubbles increase the rate of

gaseous transfer into the liquid due to their larger interfacial area per unit of gas volume and hence reach gas equilibrium quicker resulting in quicker gas transfer into the liquid. Small bubbles also rise slower through the liquid than larger bubbles and hence there is a greater opportunity for gas transfer to occur into the liquid. The disadvantage of creating smaller bubbles is that they have a greater shear effect on the cells when they burst (Wu, 1995). Another disadvantage of creating smaller bubbles in mammalian cell culture and in particular when utilising CD-CHO media is the amount of foaming that is produced. If foaming becomes too excessive, it can rise and block air filters and lead to the failure of a cultivation. Also, excessive foaming can have damaging effects on mammalian cells and can result in cell death. To mitigate these effects, antifoam must be used to reduce the levels of foam.

4.4 Mechanism of cell damage due to bubble bursting

The mechanism of bubble bursting is illustrated in figure 4.6. When a bubble reaches the top of the air-liquid interface, half of it forms a liquid film which protrudes out of the liquid and the other half depresses the liquid below it. The process of bubble rupture begins when the liquid film thins at its apex (its thinnest point) forming a hole. There is then a rapid expansion of the hole which forces the liquid to flow underneath the bubble cavity. This liquid flow produces 2 liquid jets, one that shoots up above the bubble cavity and one below into the liquid. These fast moving liquid jets can create enough shear stress to damage cells. It has been reported that this phenomenon is more pronounced with smaller bubbles as they rupture faster creating faster liquid jets. These faster liquid jets then create more intense hydrodynamic shear stresses in the liquid which are then exerted on the cells (Wu, 1995 and Kilonzo and Margaritis 2004).

Figure 4.7: **A schematic illustrating the different stages of bubble bursting** (Taken from Wu, 1995).

4.5 Toxic effects of antifoam

Antifoam emulsions are usually silicon or mineral oil droplets which encapsulate hydrophobic particles consisting of silica or wax (Pelton, 1996). Antifoam must be formulated as an emulsion so that it is dispersed into small droplets which help the antifoam agents spread fast and wide in the foam. These encapsulated hydrophobic particles are what induce lamella rupture and hence bubble bursting which results in a reduction in foam.

Foam that is found on the top of liquid media can be formed by both primary and secondary bubbles. Primary bubbles are formed from the sparger and rise to the top of the liquid. Secondary bubbles are formed by primary bubbles that coalesce with other primary bubbles while they rise towards the top of the liquid. Antifoam particles bind to bubbles in the liquid phase by heterocoagulation which leaves at least one hydrophobic particle on the bubble wall. As these bubbles rise they coalesce with other bubbles forming secondary bubbles. As the secondary bubbles grow the buoyancy force exceeds the yield stress of the foam resulting in the bubble rising quickly through the foam and bursting releasing nitrogen into the headspace (Pelton, 1996**)**

Excessive foaming and the formation of a significant layer of foam can lead to cell death due to the effects of excessive hydrodynamic shear stress due to bubble bursting. Also cells that are attached to bubbles can rise into the foam layer and remain stuck there no longer passing through the rest of the bulk culture. This is particularly the case in serum free media (Zhang et al, 1992). Cells that remain in the foam layer become deprived of essential nutrients and gases that are found in the bulk culture which leads to cell death.

It is known that excessive amounts of antifoam can have toxic effects on cells and they can also compound the damaging effect of direct sparging on cells (Zhang et al, 1992). Hence the amount of antifoam additions should be just enough to clear the formation of foam.

4.6 Cell protection

Before the advent of chemically defined animal component free media (CDACFM), mammalian cell culture media was supplemented with serum. The presence of serum in media offered advantages and disadvantages, however one of its benefits was that it provided some protection to cells from shear forces (Van der Valk et al, 2010). In the absence of serum, Pluronic F-68, a non-ionic, synthetic polymeric surfactant, is added to cell culture media to provide protection to the cells against shear forces (Stoll et al, 1992). Pluronic F-68

works by reducing the amount of cell to bubble attachment therefore reducing the number of cells that are exposed to the shear forces resulting from bubble bursting. This occurs because Pluronic F-68 interacts with cells reducing the cell surface hydrophobicity therefore reducing the hydrophobic attachment of the cell to the bubble (Ghebeh et al, 2002).

4.7 Gas delivery evaluation

This section presents a set of batch fermentations carried out to evaluate the optimal gas delivery mechanism for the MBR system. The directly driven MBR was used as it provided faster mixing times and a higher k_La at a matched P/V of 20.5 W/m^3 compared to the magnetically driven MBR; all cultivations were carried out in duplicate. In all the following batch cultivations, the pressure in the gas taps was regulated to ensure that gas was delivered to the system in gentle bursts where applicable. Table 4.2 summarises the reactor configurations that were evaluated.

Table 4.2: Summary of the reactor configurations used in optimising the gas delivery to the directly driven MBR system.

	Reactor configuration	
Initial cultivation (Section 4.2)	Cultivation mode	Single, fed-batch
	Impeller	Direct and magnetically driven
	Sparger type	Singular opening 0.31 cm diameter
	Gas delivery	- Direct sparging (100 ml/min) - Pressure unregulated - 100% enriched oxygen enabled
90 µm sintered sparger (Section 4.7.1)	Cultivation mode	Duplicate batch cultivations
	Impeller	Direct driven
	Sparger type	90 µm sintered sparger
	Gas delivery	- Direct sparging (50 ml/min) - Pressure regulated delivery - Enriched oxygen disabled
Direct sparge – 0.31 cm (Section 4.7.2)	Cultivation mode	Duplicate batch cultivations
	Impeller	Direct driven
	Sparger type	Singular opening 0.31 cm diameter
	Gas delivery	- Direct sparging (100 ml/min) - Pressure regulated delivery - 40% enriched oxygen on demand
Surface aeration (Section 4.7.3)	Cultivation mode	Duplicate batch cultivations
	Impeller	Direct driven
	Sparger type	Surface aeration
	Gas delivery	- Surface aeration (200 ml/min) - Pressure regulated delivery - 40% and 100% enriched oxygen on demand

4.7.1 90 μm sintered sparger

The desirability of achieving a high k_La in cell culture has been discussed (introduction Section 1.7). One way of increasing k_La is by delivering gas through small bubbles as they represent a higher surface area to volume ratio and therefore in total a greater amount of gas will be transferred into the culture, resulting in efficient gas transfer. An effective way of producing small gas bubbles is to utilise a sintered or porous metal sparger. The sintered sparger provided with the prototype MBR had a pore size of 15 μm and produced extremely small bubbles. In water, this sparger design was practical as the small bubbles did not create a significant amount of foaming, however when utilised in CD-CHO media, foaming was excessive almost immediately upon sparging, even at low gas flow rates (0.05-0.1 vvm). The foaming was so excessive that foam had risen to the top of the vessel and was flowing through the outlet tubing upon seconds of gas sparging. As a result cell culture was not conducted with the 15 μm sparger as the excessive foaming would have required almost constant addition of antifoam. Instead a sintered sparger with 90 μm sized pores was utilised and operated at an airflow rate of 50 mL/min (0.17 vvm). A lower airflow rate was used for this sparger design to reduce foam formation, however foaming did occur and had to be controlled with a daily addition of antifoam (1 ml or 0.003 v/v). Although the bubbles produced were larger than those produced using a 15 μm pore size, the bubble size was significantly smaller than those produced by the other sparger design used in this trial.

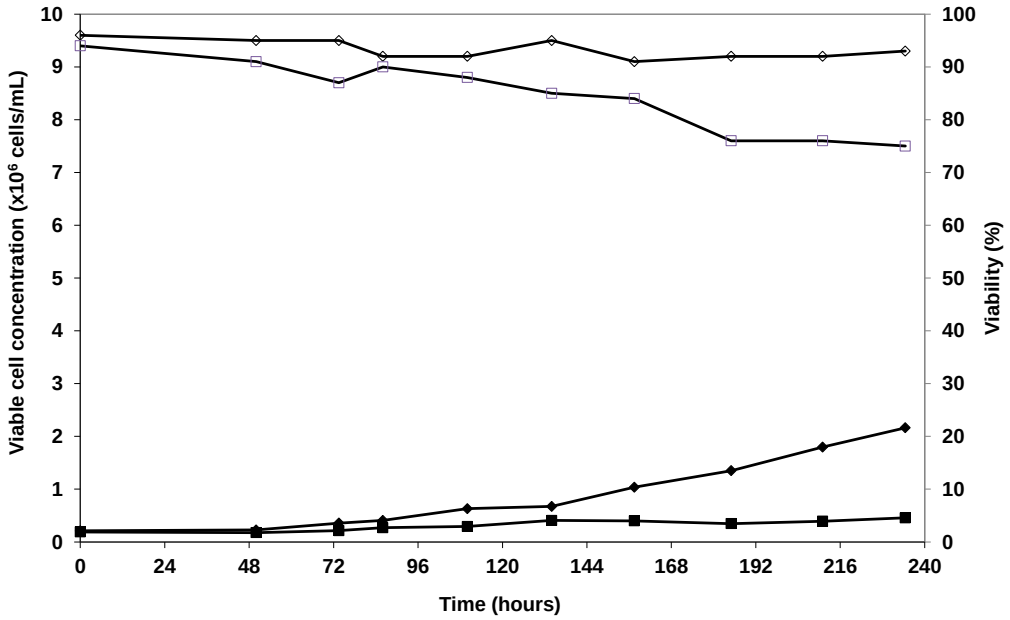

Figure 4.8: **Growth profiles of duplicate batch cultivations in the MBRs using a 90 µm sintered sparger.** VCC for MBR 1 (♦); VCC for MBR 2 (■); cell culture viability for MBR 1 (◊) and cell culture viability for MBR 2 (□). Operated at an airflow rate of 50 mL/min (0.17 vvm). Process parameters are detailed in Sections 2.5 and 2.6.

It is clear from the growth profiles in figure 4.8, that the 90 µm sintered sparger did not provide adequate cell culture conditions. Both the duplicate cell cultures did not perform well with little cell growth until 120 hours. In MBR 1, growth improves after this point but is still minimal. The culture does grow at a steady rate until 240 hours peaking at 2.2 x 10^6 cells/ml and with a culture viability of 93%. In MBR 2, the VCC shows a very slight increase throughout the entirety of the culture peaking at 0.48 x 10^6 cells/ml at 134 hours with no growth or significant cell death after this point. At 240 hours when the culture was stopped the culture viability was 75%. It is clear from this growth data that the 90 µm sintered sparger is not suitable for operation with the CY01 cell line used. Although the culture maintained relatively high cell viability throughout, the poor growth was most likely caused by the shear effects of the small bubbles bursting. The shear stresses exerted on the cells may not have been enough to rupture the cells but may have provided enough stress to inhibit cell division and arrest growth.

Researchers have also reported another limitation in using microspargers like the one utilised in this cultivation. To support the same VCC, microspargers are

required to use almost 10 times less gas flow than larger macrospargers. This can lead to a reduction in CO_2 removal as the fine bubbles saturate with CO_2 quickly and the large reduction in bubble volume results in a loss of CO_2 mass transfer efficiency (Czermak et al, 2009 and Ozturk, 2014). This could have led to a build-up of metabolically produced CO_2 which could have adversely impacted on cell growth (refer to section 4.3.1.2).

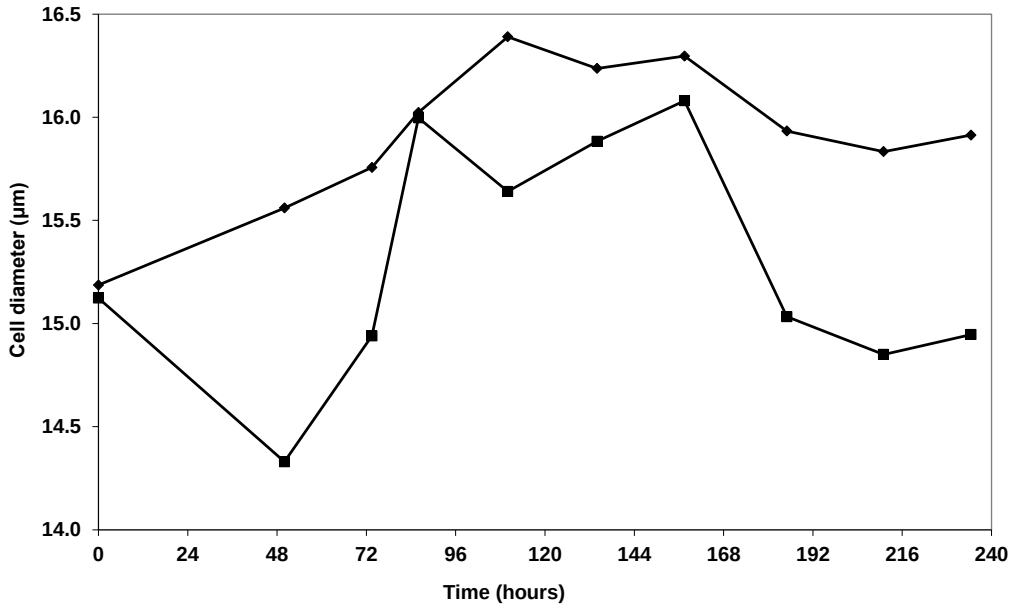

Figure 4.9: **Cell diameter measurements of duplicate batch cultivations in the MBRs using a 90 µm sintered sparger.** Cell diameter for MBR 1 (♦) and cell diameter for MBR 2 (■). Cell size was measured by using the Vi-CELL as described in Section 2.7.

As shown in figure 4.9 the cell diameter profiles diverge in the early stages of the culture between 0 and 48 hours. However, after 72 hours the profiles become similar until around 160 hours. After this point the profiles diverge again with the cells in MBR 2 becoming on average smaller than those in MBR 1. This could be due to poorer cell viability in MBR 2 indicating that the cells were dying and hence leading to cell shrinkage (refer to Fig. 4.8)

4.7.2 Direct sparging – 0.31 cm opening sparger

This configuration utilised a sparger with a hollow shaft and hole with a diameter of 0.31 cm. The shaft bends at the bottom forming a right angle ensuring that the

hole faces the impeller which directs sparged bubbles into the impeller zone (refer to Fig. 4.10). The pictures below show that there is good bubble mixing within the impeller region and that bubbles are evenly distributed at the top of the liquid surface. This is consistent with the fact that the system has a low mixing time of 6 seconds at 400 rpm. This should ensure that gas mixing is as efficient as possible as the gas enters the impeller zone and is then effectively distributed to the rest of the culture.

Direct sparging results in higher k_La, however the effects of this mechanism of sparging on the cells is unknown. Generally speaking the creation of bubbles can lead to detrimental effects on cell viability and it is clear that this was the case when using a 90 μm sintered sparger. However, the bubbles created using a 0.31 cm diameter opening are much larger and hence should reduce the shear effects on the cells. The bubbles produced using this sparger did not produce a significant amount of foam, resulting in the culture requiring only two additions of antifoam of 1 ml throughout the cultivation (at 144 and 192 h). In this culture the gas inlets that contained oxygen were atmospheric air and 40% enriched oxygen. Initially only the air inlet was enabled and the enriched oxygen was disabled due to low oxygen demand in the early stages of the culture. The enriched oxygen was only enabled for MBR 1 at 216 hours as the system could no longer maintain the DOT within the lower end of the deadband around the DOT setpoint. MBR 2 did not quite reach the same maximum VCC as MBR 1 making oxygen enrichment unnecessary.

Figure 4.10: **Image of the MBR vessel filled with 300 ml CD-CHO media being sparged with air.** This configuration consisted of direct driven agitation (410 rpm) and direct sparging via the singular opening 0.31 cm diameter sparger shaft with a gas flow rate of 100 ml/min.

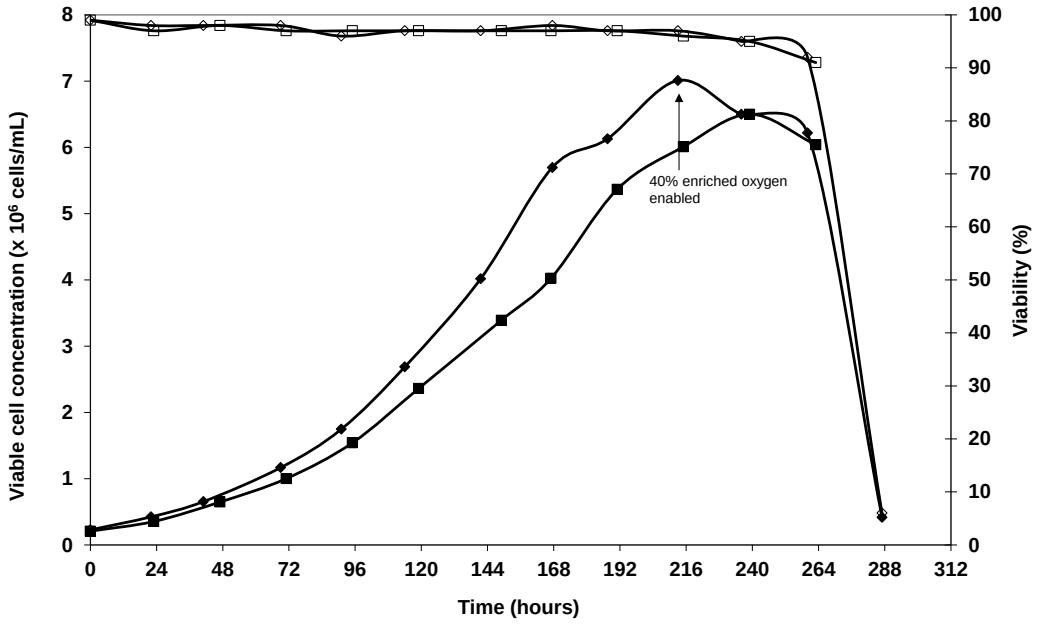

Figure 4.11: **Growth profiles of duplicate batch cultivations in the MBRs using a 0.31 cm diameter singular opening sparger sparging directly into the culture.** VCC for MBR 1 (♦); VCC for MBR 2 (■); cell culture viability for MBR 1 (◊) and cell culture viability for MBR 2 (□). 40% enriched oxygen was

switched on for MBR 1 at 216 hours. Process parameters are detailed in Sections 2.5 and 2.6.

Both the cultures in MBR 1 and MBR 2 performed similarly (refer to Fig. 4.11). MBR 1 reached a maximum VCC of 7.0 x 10^6 cells/ml at 213 hours and MBR 2 reached a maximum VCC of 6.5 x 10^6 cells/ml at 239 hours. Viability for both cultures remained above 90% until 260 hours after which culture viability for both cultures dropped abruptly to below 10%. This occurred because the glucose concentration in both cultures was exhausted leaving the cells with no energy source resulting in rapid cell death (refer to Fig. 4.13). The μ_{max} for MBR 1 was 0.024 h^{-1} and 0.022 h^{-1} for MBR 2 (calculated using a semi-logarithmic plot as discussed in Section 4.2.2). The IVCC for MBR 1 till 260 hours was 39 x 10^6 cells.day/mL and 34 x 10^6 cell day/mL for MBR 2.

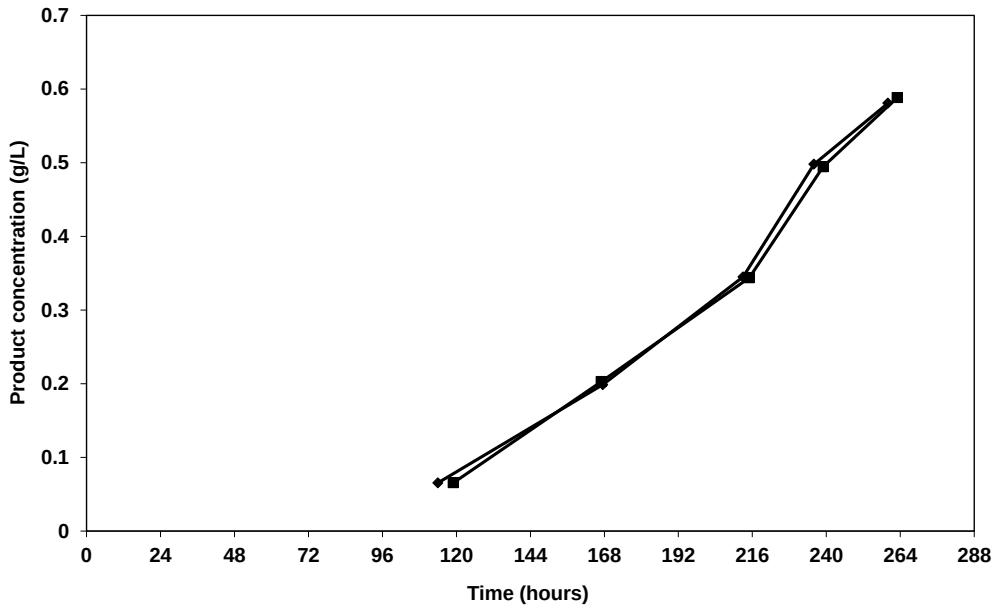

Figure 4.12: **Product concentration profiles of duplicate batch cultivations in the MBRs using a 0.31 cm diameter singular opening sparger sparging upto 40% enriched oxygen into the culture.** Protein concentration profiles for MBR 1 (♦), MBR 2 (■). Antibody concentration was measured using HPLC as detailed in Section 2.15.

Both the cultures produced virtually the same product titres with MBR 1 producing 0.58 g/L and MBR 2 producing 0.59 g/L (refer to Fig. 4.12).

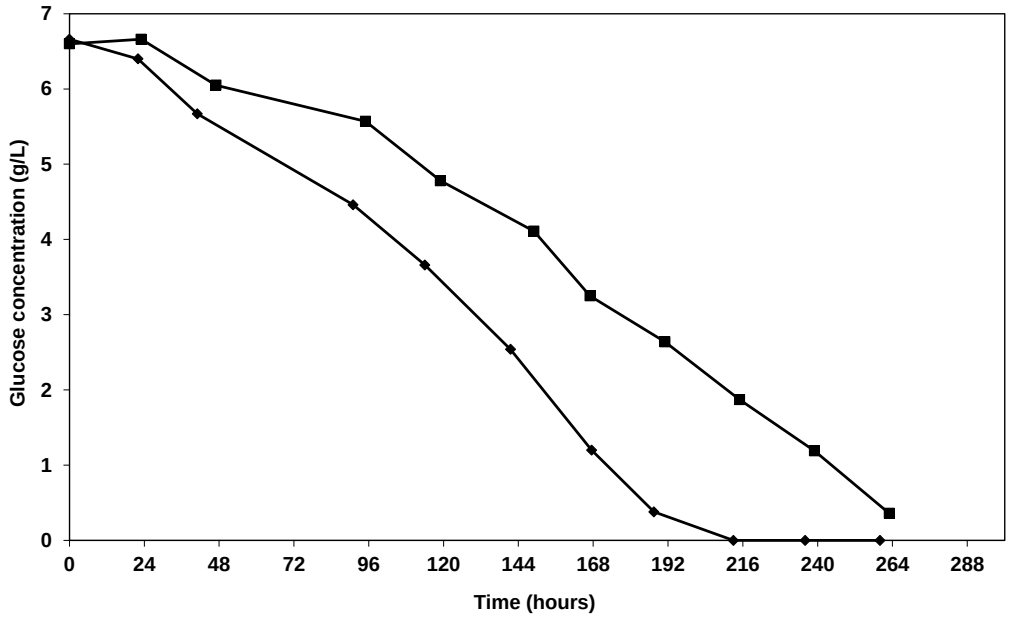

Figure 4.13: **Glucose concentration profiles of duplicate batch cultivations in the MBRs using a 0.31 cm diameter singular opening sparger sparging up to 40% enriched oxygen into the culture.** Glucose concentration profiles for MBR 1 (♦) and MBR 2 (■). Glucose concentration was measured using the NOVA Bioprofile as described in Section 2.8.

As would be expected glucose concentration in both cultures decreases throughout the culture. As these are batch runs the culture is not replenished with nutrients resulting in glucose being exhausted from the culture. The glucose concentration in MBR 2 is consistently slightly higher than that in MBR 1 and this is because the IVCC in MBR 2 was consistently lower than that in MBR 1 at corresponding time points (refer to Fig. 4.13).

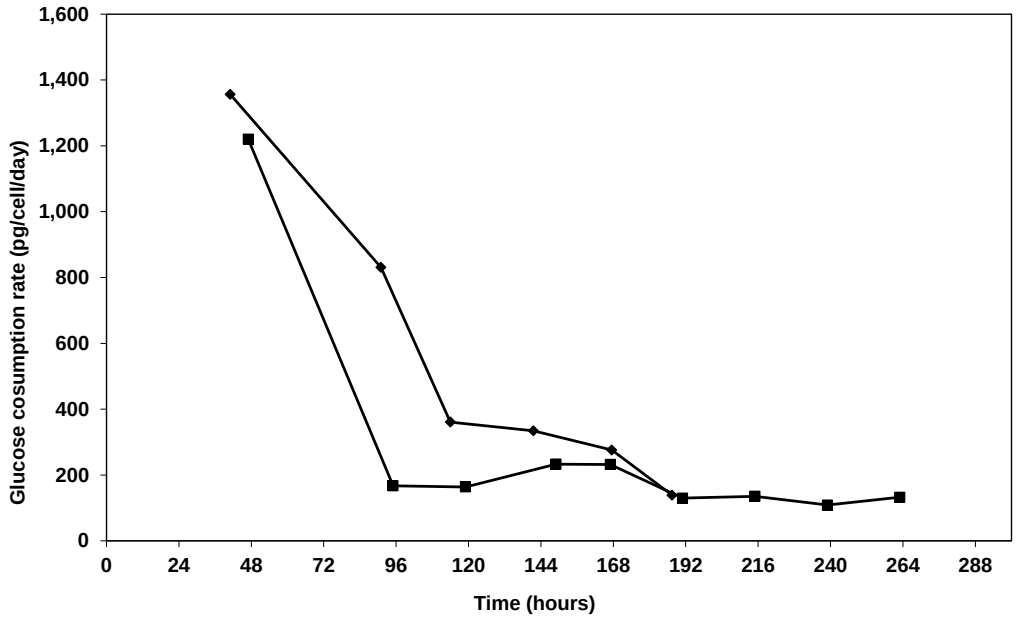

Figure 4.14: **Glucose consumption rate profiles of duplicate batch cultivations in the MBRs using a 0.31 cm diameter singular opening sparger sparging up to 40% enriched oxygen into the culture.** Glucose concentration profiles for MBR 1 (♦) and MBR 2 (■). Glucose concentration was measured using the NOVA Bioprofile as described in Section 2.8. These rates were calculated by dividing the glucose consumed per day by the delta IVCC per day. Delta IVCC is the IVCC for a specific day and the IVCC is the sum of the delta IVCC for each day.

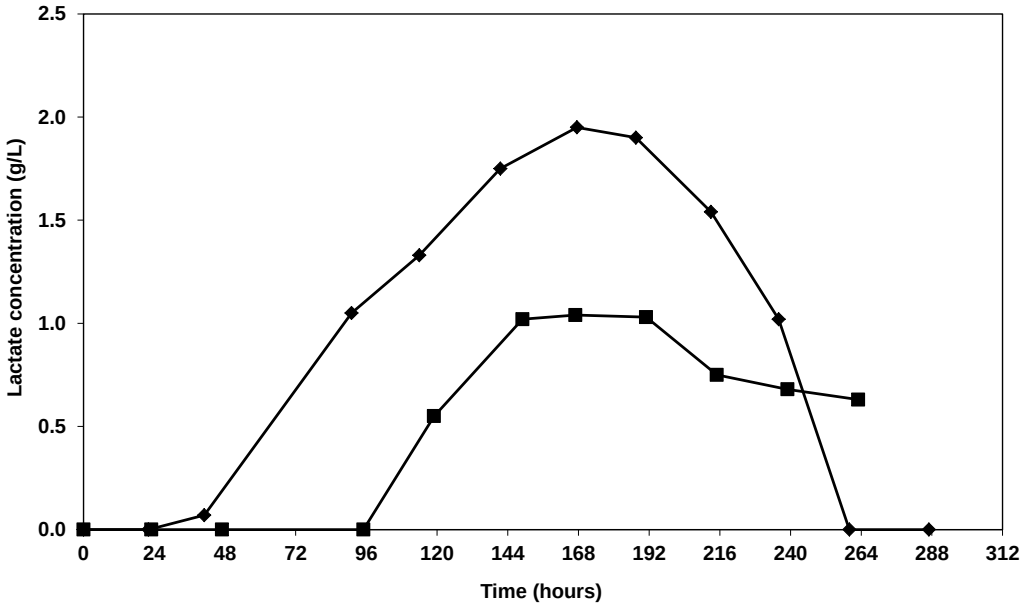

Figure 4.15: **Lactate concentration profiles of duplicate batch cultivations in the MBRs using a 0.31 cm diameter singular opening sparger sparging up to 40% enriched oxygen into the culture.** Lactate concentration profiles for MBR 1 (♦) and MBR 2 (■). Lactate concentration was measured using the NOVA Bioprofile as described in Section 2.8.

The lactate concentration profiles follow the same pattern with lactate accumulation until day 7 occurring for both MBRs. After 168 hours there is lactate consumption which coincides with reduced culture glucose concentration. MBR 1 consumes lactate at a faster rate than MBR 2 probably because it has a lower glucose concentration at the same culture time. These lactate profiles correspond accurately with the glucose concentration profiles (refer to Figs. 4.13 and 4.15). Lactate is produced as a result of incomplete oxidation of glucose by the glycolytic pathway (Schneider et al, 1996). So, a higher glucose consumption would result in a higher lactate production rate and hence the higher concentration of lactate throughout the culture until 168 hours in MBR 1. Lactate can be consumed when there is a low glucose concentration (1-2 g/L, Butler, 2005) and hence the lactate concentration in MBR 1 reduces rapidly after 168 hours when glucose is exhausted from the culture. This phenomenon happens in MBR 2 for the same reason although at a slower rate.

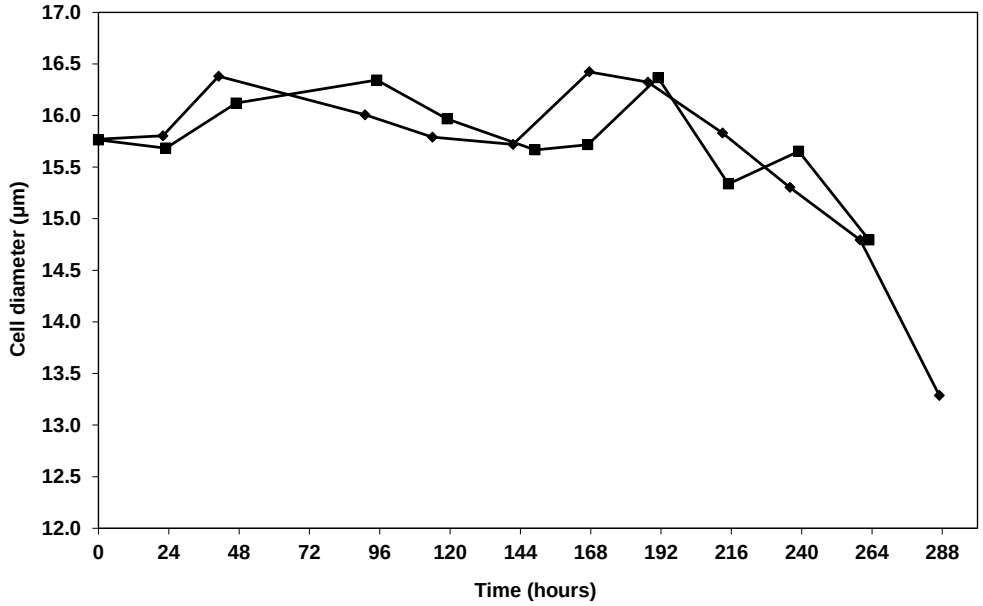

Figure 4.16: **Cell diameter measurements of duplicate batch cultivations in the MBRs using a singular opening sparger sparging up to 40% enriched oxygen into the culture.** Cell diameter for MBR 1 (♦) and cell diameter for MBR 2 (■). Cell size was measured by using the Vi-CELL as described in Section 2.7.

The diameter of cells grown in both MBRs was similar throughout the culture with both MBRs producing similar profiles as shown in figure 4.16. As expected the average cell diameter reduces as the culture starts to decline after time 192 hours.

Cell growth improved using the configuration detailed in this section (direct sparging; regulated pressure gas delivery; 40% enriched oxygen) compared to the initial configuration used in Section 4.2 (direct sparging; unregulated pressure gas delivery; 100% enriched oxygen). For the directly driven MBR, growth improved from a maximum VCC of 4.9 $x10^6$ cells/ml in the initial cultivation to 6.5 x 10^6 cells/ml and 7.0 x 10^6 cells/ml for the MBR cultivations using this configuration. Specific growth rates were similar for all three reactors between 0 to 72 hours, 0.022 hr^{-1} for the initial cultivation and 0.024 hr^{-1} and 0.022 hr^{-1} for the cultivations using this configuration. However between 72 to 96 hours VCC remained fairly constant in the initial cultivation. Between around 96 hours and 144 hours the specific growth rate in the initial cultivation was 0.011 hr^{-1} compared to 0.015 hr^{-1} and 0.016 hr^{-1} for the directly driven MBRs used in this configuration. Gassing of the system increases steadily after the culture reaches 48-72 hours as the cells proliferate and require more oxygen. The impact of gassing the system may have contributed to the reduction in growth rate after 72 hours in the initial cultivation and may explain why growth was better using this configuration.

The main modifications made for the cultivation described in this section are detailed below:

a) The initial configuration did not regulate pressure in the gas taps; however in this configuration pressure was regulated ensuring that the bursts of gas into the reactors were more gentle. This would have resulted in lower back pressure up the sparger shaft which may have resulted in a smaller volume of cell culture being withdrawn from the bulk culture. The lower pressure would also minimise potential shear effects of discharging the cells back into the culture through the sparger shaft.

b) This configuration only used enriched oxygen when necessary, minimising its use throughout the culture. When enriched oxygen was enabled, only 40% enriched oxygen was used compared to 100% in the initial cultivation. This provided better DOT control as the use of enriched oxygen can lead to more frequent DOT spiking. This also reduced the cells exposure to potentially harmful concentrations of oxygen.

4.7.3 Surface aeration

Surface aeration was carried out to overcome the potential problems caused by the intermittent nature of the gassing mechanism. Surface aeration has clear limitations regarding k_La with values far lower than those achieved using direct sparging (refer to Section 3.4.5). This is wholly due to the gas having to diffuse from the headspace into the liquid and then being distributed through the culture via impeller induced mixing. Oxygen concentration gradients within the vessel could arise resulting in cells potentially entering in and out of areas of the vessel which have a limited amount of oxygen which could stress the cells. Another limitation of surface aeration is poorer control of process parameters relating to DOT and pH as these rely on concentrations of oxygen, nitrogen and carbon dioxide. As it will take longer for these gases to diffuse into the liquid and then be adequately mixed in the culture the system will often overshoot and then have to compensate. This process will result in less tight control around set points as the system is not able to respond quickly enough to a change in conditions. The low k_La this configuration delivers poses a particular problem for meeting the oxygen demands of the culture particularly when there is a high VCC. To overcome oxygen limitation at this stage, oxygen enrichment must take place to compensate for the low k_La. As the system was not configured to blend gasses, a pre-blended gas canister of 40% oxygen was utilised to provide oxygen enriched air. The next increment used was 100% oxygen. It was thought that utilising 100% oxygen could be problematic due to the toxicity of high oxygen concentration.

This gassing regime entailed using air and 40% oxygen and then removing air and using 100% oxygen when oxygen demand increased. So in the latter stages

of the culture the system would be receiving 40% and 100% oxygen on demand. Air was no longer sufficient at 84 hours hence 40% oxygen was turned on to supplement it. At 130 hours, 40% oxygen was no longer sufficient and hence 100% oxygen was enabled to supplement it leaving the 40% oxygen and 100% oxygen gas inlets enabled.

The growth curves for both MBR 1 and 2 were virtually identical with MBR 1 reaching a maximum VCC of 8.2 x 10^6 cells/ml and MBR 2 reaching a maximum VCC of 7.9 x 10^6 cells/ml. Viability for both cultures remained above 90% until around 250 hours after which culture viability for both cultures began to drop abruptly. This occurred again because the glucose concentration in both cultures was exhausted leaving the cells with no energy source resulting in rapid cell death. The μ_{max} for MBR 1 was 0.027 h^{-1} and 0.030 h^{-1} for MBR 2 (calculated using a semi-logarithmic plot as discussed in Section 4.2.2). The IVCC for MBR 1 was 53 x 10^6 cells.day/mL and 57 x 10^6 cells.day/mL for MBR 2 (refer to Fig. 4.17).

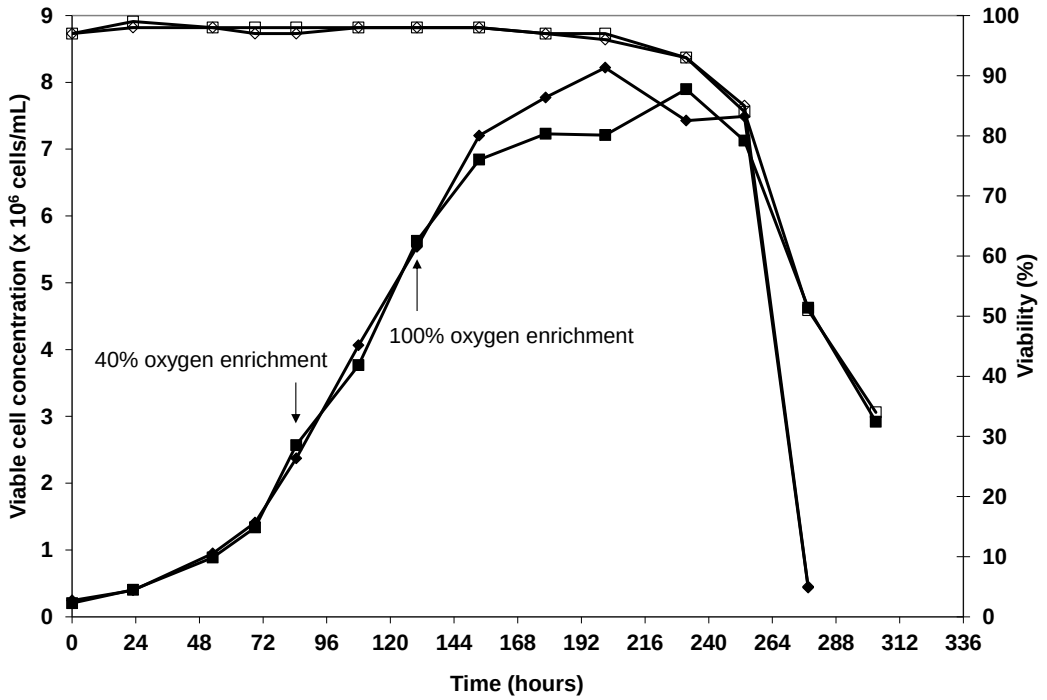

Figure 4.17: **Growth profiles of duplicate batch cultivations in the MBRs operated with surface aeration.** VCC for MBR 1 (♦); VCC for MBR 2 (■); cell culture viability for MBR 1 (◊) and cell culture viability for MBR 2 (□). 40% enriched oxygen was enabled at 84 hours and 100% enriched oxygen was enabled at 130 hours. Process parameters are detailed in Sections 2.5 and 2.6.

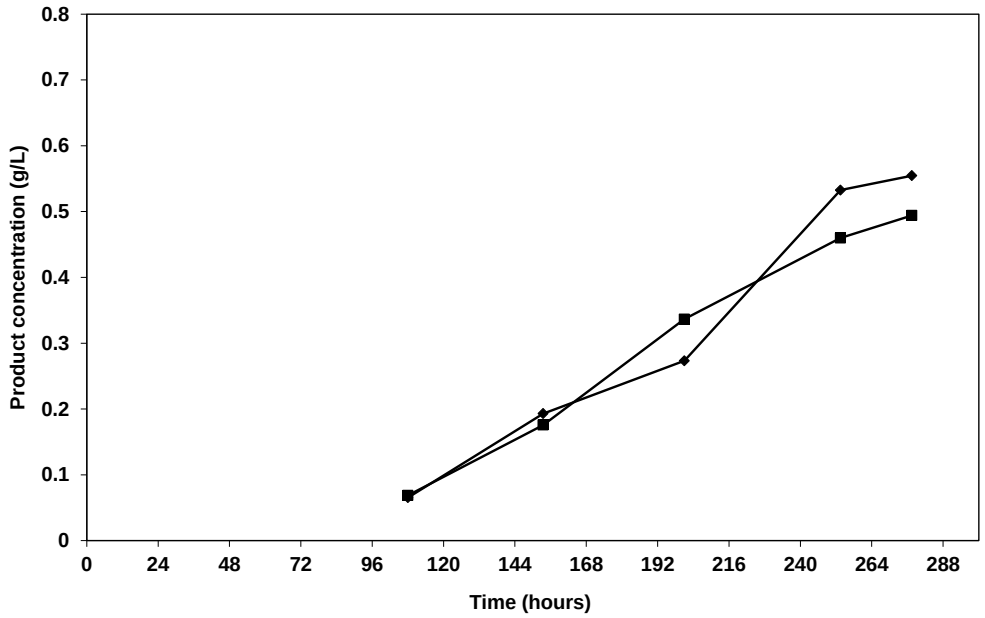

Figure 4.18: **Product concentration profiles of duplicate batch cultivations in the MBRs operated with surface aeration.** Product concentration profiles for MBR 1 (♦) and MBR 2 (■). Antibody concentration was measured using HPLC as detailed in Section 2.15.

As was expected both the cultures produced similar product titres with MBR 1 producing 0.49 g/L and MBR 2 producing 0.55 g/L as shown in figure 4.18.

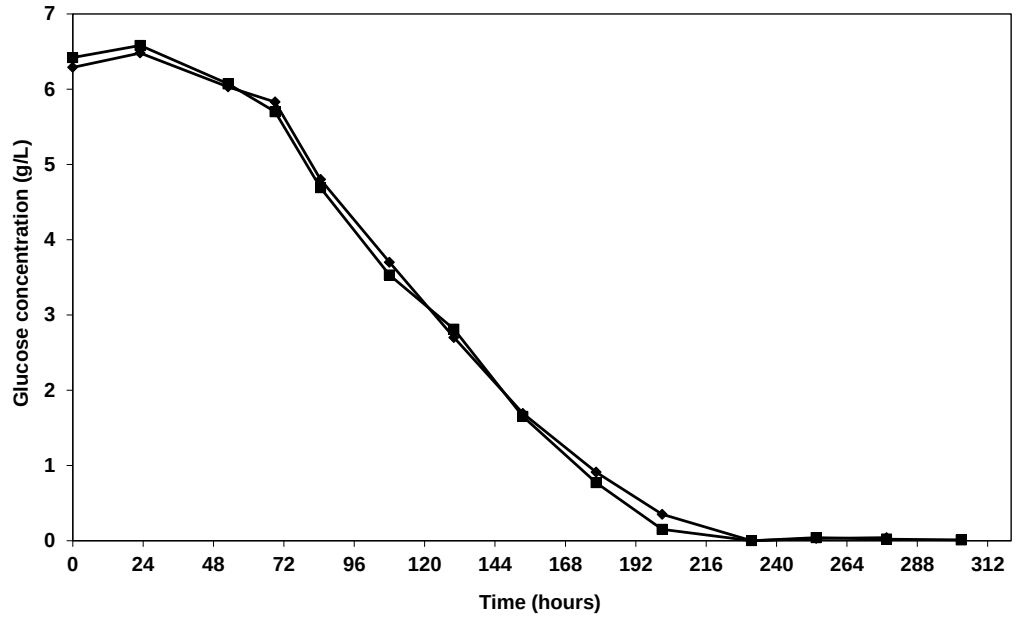

Figure 4.19**: Glucose concentration profiles of duplicate batch cultivations in the MBRs operated with surface aeration.** Glucose concentration profiles for batch cultivations MBR 1 (♦) and MBR 2 (■). Glucose concentration was measured using the NOVA Bioprofile as described in Section 2.8.

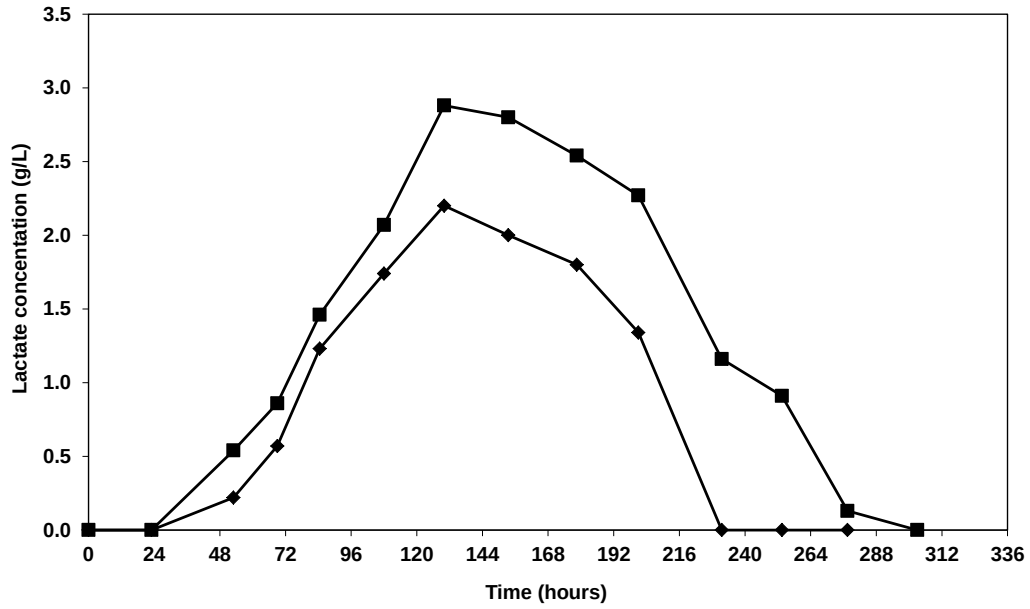

Figure 4.20: **Lactate concentration profiles of duplicate batch cultivations in the MBRs operated with surface aeration.** Lactate concentration profiles for batch cultivations MBR 1 (♦) and MBR 2 (■). Lactate concentration was measured using the NOVA Bioprofile as described in Section 2.8.

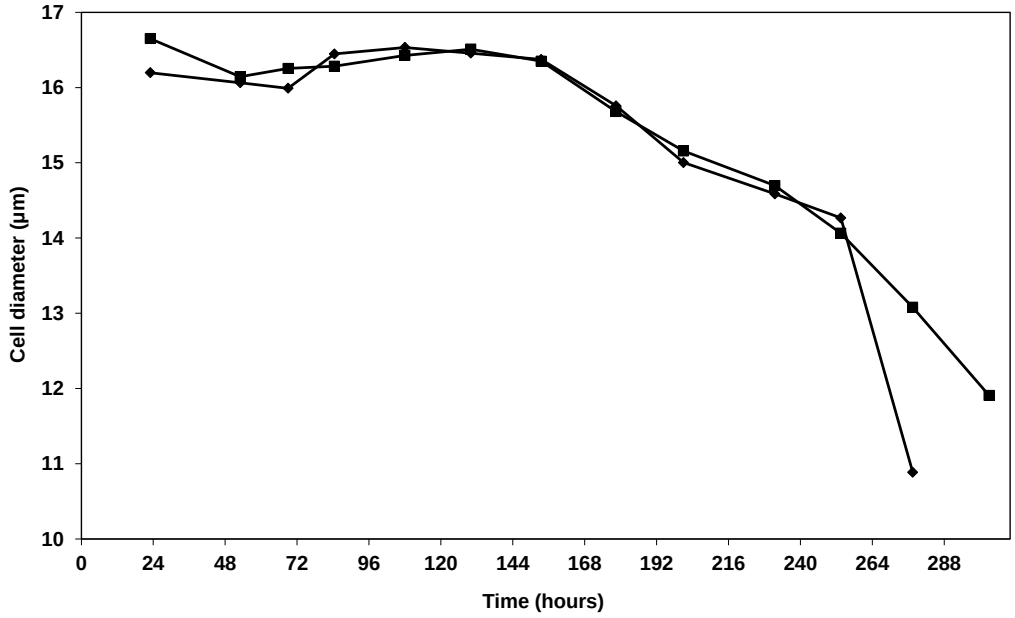

Figure 4.21: **Cell diameter measurement profiles of duplicate batch cultivations in the MBRs operated with surface aeration.** Cell diameter profiles for batch cultivations MBR 1 (♦) and MBR 2 (■). Cell size was measured by using the Vi-CELL as described in Section 2.7.

Both the MBRs produced very similar glucose concentration (refer to Fig. 4.19), lactate concentration (refer to Fig. 4.20) and cell diameter profiles (refer to Fig. 4.21) indicating good reproducibility of the MBR system.

4.8 Evaluation of the effects of antifoam on cell growth

To eliminate the possibility that antifoam added to the cultures employing direct sparging may have contributed to the reduced growth in these cultures, a shake flask experiment was conducted to evaluate the effects that antifoam can have on growth. One flask was run as a control with no antifoam addition. The experimental flask received 0.004 v/v of 3% antifoam solution every day from day 2 onwards which is slightly more than that which would have been added to the MBR using the 90 μm sintered sparger. This experiment utilised 1 L shake flasks with a culture volume of 300 ml to best mimic the culture volume in the MBR.

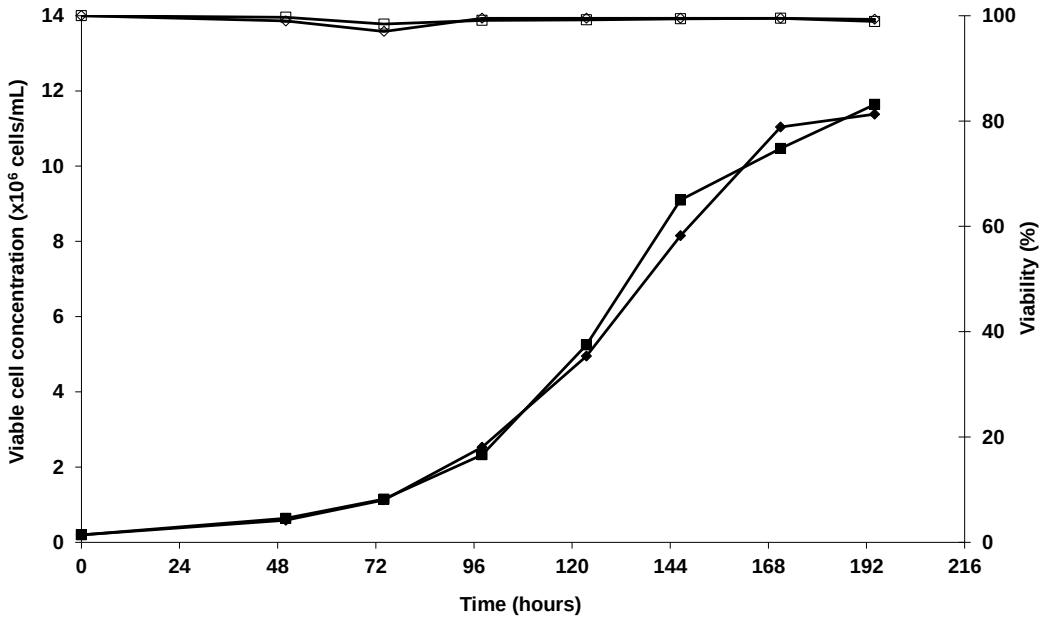

Figure 4.22: **Growth profiles for batch flask cultivations run at 37°C, 140 rpm and 5% CO_2.** VCC for control flask 1 with no antifoam (♦); VCC for flask with 0.004 v/v of 3% antifoam added daily from day 2 (■); cell culture viability for control flask (◊) and cell culture viability for flask with antifoam added (□).

The growth curves in figure 4.22 are almost identical which would indicate that the quantity and concentration of antifoam added to the cultures did not have any effect on growth. Culture viability for both flasks remains above 95% at the end of the exponential phase at around 192 hours.

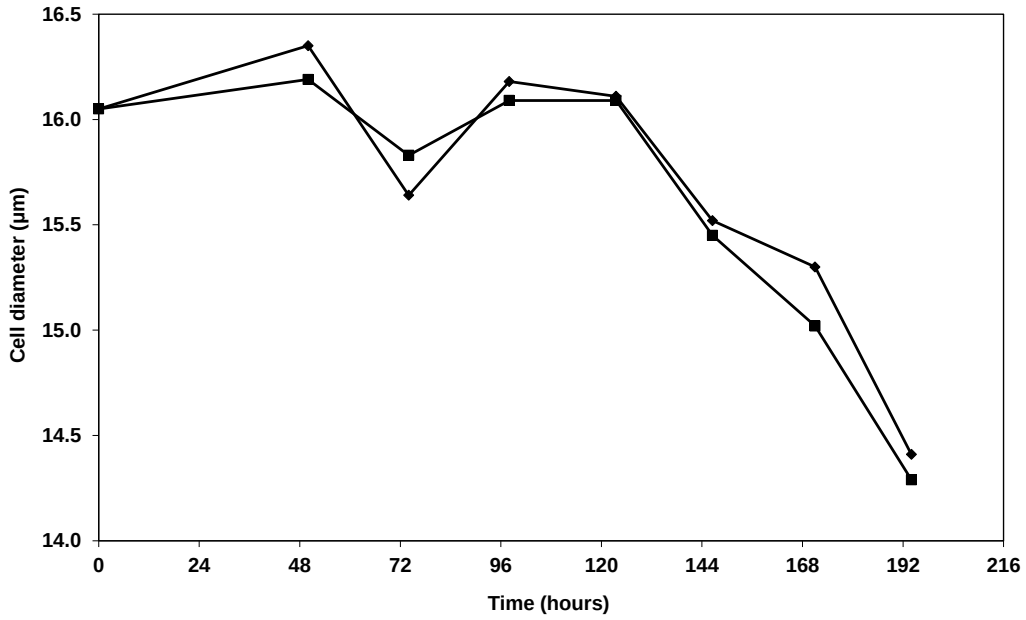

Figure 4.23: **Cell diameter measurement profiles of the control and experimental batch flask cultivations.** Control flask (♦) and experimental flask (■). Cell size was measured using the Vi-CELL as described in Section 2.7.

The cell size profiles are also similar for both the experimental conditions which would also indicate that there was no effect on cell physiology (refer to Fig. 4.23). A metabolite analysis was undertaken at 192 hours (day 7) near the end of the evaluation (refer to Table 4.3). The final metabolite concentration and osmolality of both culture conditions were very similar again indicating that the difference in culture conditions did not have a significant effect.

This evaluation indicates that the quantities of antifoam added to the MBR would not have contributed to poorer growth as the same concentration of antifoam added to shake flask cultures did not affect growth.

Table 4.3: Metabolite concentrations and osmolality of the control (flask 1) and the flask with added antifoam (flask 2). Samples were taken at 192 hours.

	Flask 1							
Metabolite	Gluc (g/L)	lac (g/L)	Gln (mmol/L)	NH4+ (mmol/L)	Glu (mmol/L)	Na+ (mmol/L)	K+ (mmol/L)	Osm (mOsm/Kg)
Concentration	1.89	1.47	0	2.63	0.33	117	7.3	322.9
	Flask 2							
Metabolite	Gluc (g/L)	lac (g/L)	Gln (mmol/L)	NH4+ (mmol/L)	Glu (mmol/L)	Na+ (mmol/L)	K+ (mmol/L)	Osm (mOsm/Kg)
Concentration	1.7	1.67	0	2.38	0.004	114	7.8	318.9

4.9 Conclusions

These experiments have shown that the design and operation of different gas delivery configurations can have profound effects on cell culture performance.

An initial scale comparison was conducted comparing the performance of the directly and magnetically driven MBRs and a 5L STR. Constant P/V was used as a scale-down criterion which also resulted in a constant mixing time for the 5L STR and the directly driven MBR. There was a significant difference between the maximum VCC of the 5L STR (9.9 x 10^6 cells/ml) and both the magnetic and direct driven MBRs (5.1 and 4.9 x 10^6 cells/ml respectively).

The Q_p of the magnetically and directly driven MBRs were twice that of the 5L STR (24 vs 12 pg/cell/day) when plotting all of the product concentration data points against IVCC. Q_p values differed however, when lines of best fit were plotted resulting in a Q_p of 26 pg/cell/day for the magnetically driven MBR, 21 pg/cell/day for the directly driven MBR and 16 pg/cell/day for the 5L STR. It must be noted that these Q_p figures are estimates and may have a certain degree of error due to variability in the product concentration data.

It was found that the 90 μm sintered sparger is not suitable for use with the cell line trialled in these experiments. Compared to the sintered sparger, the configuration that involved sparging directly into the culture using the singular opening 0.31 cm sparger design yielded far better culture performance. It produced a maximum VCC of 6.8 x 10^6 cells/mL, a μ_{max} of 0.023 h^{-1} and a product titre of 0.58 g/L. Furthermore, the configuration that involved surface aeration produced even better cell growth reaching a maximum VCC of 8.1 x 10^6 cells/mL and a μ_{max} of 0.028 h^{-1}, however it produced a slightly lower titre of 0.52 g/L. Interestingly, the culture that involved direct sparging produced cells that had a significantly higher cell specific productivity of 16 pg/cell/day compared to 10 pg/cell/day in the cultivations that employed surface aeration. The main results are summarised in table 4.4.

Table 4.4: Summary of the main performance parameters for each gas delivery configuration. These figures are averages based on duplicate MBR runs. The numbers in the brackets are ± 1 standard deviation about the mean.

Configuration	Maximum VCC ($x10^6$ cells/mL)	μ_{max} (h^{-1})	Titre (g/L)	Qp (pg/cell/day)
90 μm sintered	1.34	NA	NA	NA
Direct sparging - 0.31 cm	6.8 (± 0.36)	0.023 (± 0.0011)	0.58 (± 0.0057)	16 (± 1.7)
Surface aeration	8.1 (± 0.22)	0.028 (± 0.0022)	0.52 (± 0.042)	10 (± 0.92)

The difference in performance between the cultivations operated with the direct gas sparging method (singular opening 0.31 cm sparger) and cultivations operated with surface aeration could be due to the effects of the culture being drawn up the sparger shaft in between sparging. This phenomenon could have stressed the cells by removing them from the controlled environment within the bulk culture into an uncontrolled and potentially hostile environment within the sparger shaft. The cells may also have been impacted by shear forces when being discharged out of the sparger shaft back into the culture due to shear forces created by wall of the sparger shaft.

The work in this chapter has shown that optimising the gas delivery system of the directly driven MBR improved cell growth. These cultivations, however, do not provide a direct comparison with the 5L STR because the optimisation cultivations were run in batch mode while the initial cultivations (Section 4.2) were run in fed-batch mode. In order to progress the scale-down comparison work further; a direct comparison between the directly driven MBR system and the 5L STR run in fed-batch mode at a matched P/V of 20.5 W/m^3 is therefore required.

As surface aeration in the MBR produced better growth compared to the direct sparging configuration; this mode of gas sparging is used in the next comparison cultivation. Although operation of surface aeration produces a different hydrodynamic environment in the MBR to that produced by direct sparging in

the 5L STR; using surface aeration in a scale-down comparison will evaluate if the MBR system has the potential to match the performance of the 5L STR and sustain high cell density cultures. If performance is found to be comparable, then future work should focus on optimising the MBR to achieve comparable scale-down cultivations using direct sparging.

Chapter 5: Comparison of fed-batch operations and development of an advanced feeding strategy

5.1 Introduction

In chapter 4, a scale comparison of fed-batch cultures was carried out in order to compare the performance of the MBR with the larger 5L STR. It was seen that cell growth in the MBR was significantly lower than that in the 5L STR. This chapter will evaluate the performance of an optimised MBR design drawing on the conclusions made in chapter 4. The optimised MBR setup utilises surface aeration as opposed to direct gas sparging (refer to Section 4.7.3 and 4.9). The feed utilised in this experiment was 10 x CD-CHO with supplemented glucose with a final feed glucose concentration of around 150 g/L.

Fed-batch processes have been for many years the most popular choice for MAB production. Feeding regimes developed over the years ranging from simple glucose feeds to more complex multi-nutrient feeds introduced at different stages of growth. Modern industrial bioreactor processes employ feeding regimes to prolong culture life and increase product titres. Feeding regimes are designed to replenish nutrients that are exhausted from the cell culture, particularly the carbon energy source. Feeding can increase product titres by increasing the IVCC which is a measure of the total number of cells accumulated throughout the culture. This obviously has a direct effect on product titre which increases with higher IVCC at a constant Q_p, as there are more cells producing product (Bibila and Robinson, 1995). The benefits that can be achieved by developing an effective feeding regime can be significant; with product titres potentially increasing 2-4 fold from those achieved using batch culture.

It is hence essential to demonstrate that the MBR can facilitate fed-batch operation and still be an accurate predictor of cell culture performance at larger scale.

5.2 Fed-batch fermentation scale comparison

5.2.1 Growth and antibody productivity

All growth profiles in this section are based on duplicate fed-batch cell cultivations. The growth profiles for the 5L STR and the MBR show good similarity (refer to Fig. 5.1). The maximum VCC for the 5L STR was 9.8 x 10^6 cells/mL and 10.4 x 10^6 cells/mL for the MBR. There was also good similarity in the IVCC for both the reactors. The IVCC in the 5L STR was 86 x 10^6 cells.day/mL and the IVCC for the MBR was 76 x 10^6 cells.day/mL. The 5L STR reaches its maximum VCC at 237 hours compared to 261 hours for the MBR. Also, feeding is initiated at 168 hours for the 5L STR compared to 192 hours for the MBR. Both the reactors produced very similar product titres with the 5L STR producing 1.05 g/L and the MBR producing 1.07 g/L antibody (refer to Fig. 5.2).

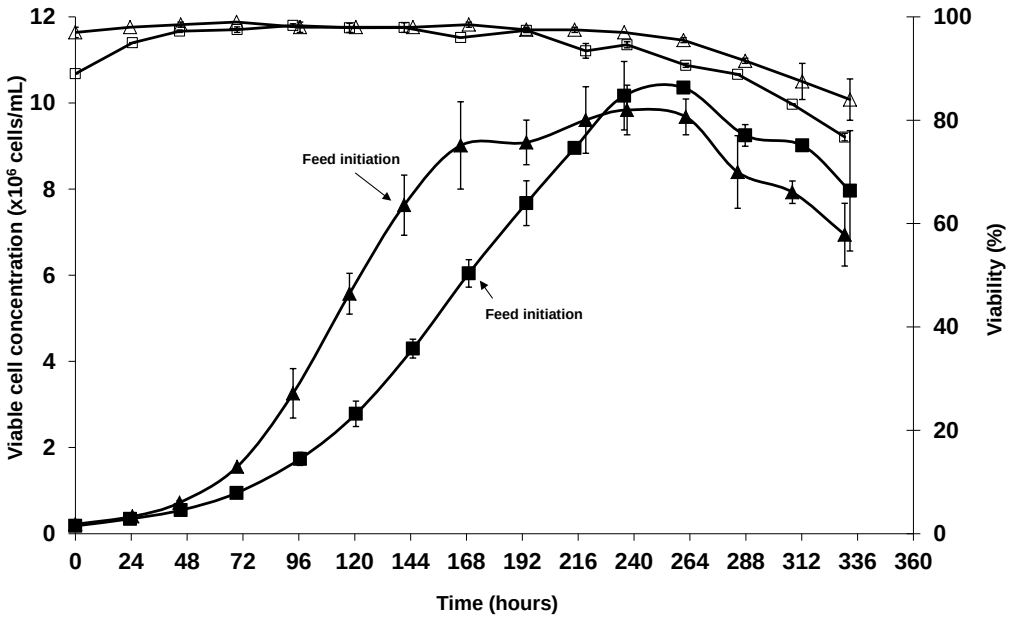

Figure 5.1: **Comparison of the fed-batch cell culture growth and viability profiles of the 5L STR operated with direct sparging and the MBR operated with surface aeration.** VCC for the 5L STR (▲) and VCC for the MBR (■) and. Cell culture viability for the 5 L STR (Δ) and cell culture viability for the MBR (□). Feeding was initiated for the 5L STR at 168 hours and at 192 hours for the MBR. The data points are mean values from duplicate cell culture runs. Error bars represent ± 1 standard deviation from the mean (n=2). The cell culture method is described in Sections 2.5, 2.6 and 2.9.

μ_{max} for both the 5L STR and directly driven MBR were similar. μ_{max} for the 5L STR occurred between 0 and 96 hours and was 0.029 h^{-1} and for the MBR μ_{max} occurred between 0 and 96 hours and was 0.024 h^{-1} (refer to Fig. 5.2).

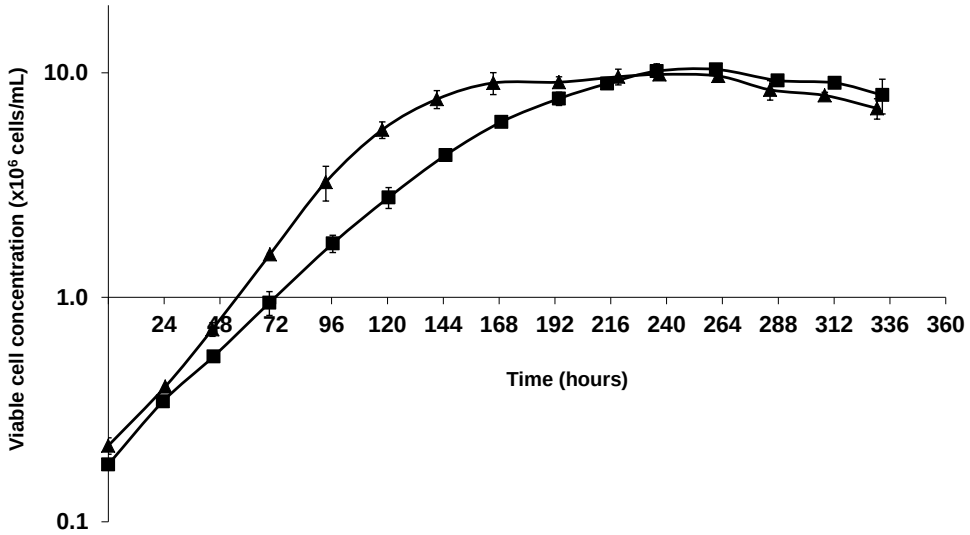

Figure 5.2: **Semi-logarithmic growth profile comparisons of the fed-batch 5L STR operated with direct sparging and the directly driven MBR operated with surface aeration.** 5L STR (▲) and MBR (■).

The product titres as well as the growth profiles and IVCC are similar for both reactor systems which would indicate that the Q_p for both would be quite similar (see Table 5.1). As discussed in section 4.2.3, Q_p can be calculated by plotting product concentration vs IVCC (refer to Fig. 5.4). Using this method the calculated Q_p of the MBR was 16 pg/cell/day and 13 pg/cell/day for the 5L STR.

The growth and productivity data would indicate that the fed-batch MBR cultivations operated with an optimised surface aeration mode did not have the same hostile environment as that produced during the initial fed-batch comparison cultivation (Section 4.2). However the conditions in the MBR may have been slightly more hostile than in the 5L STR.

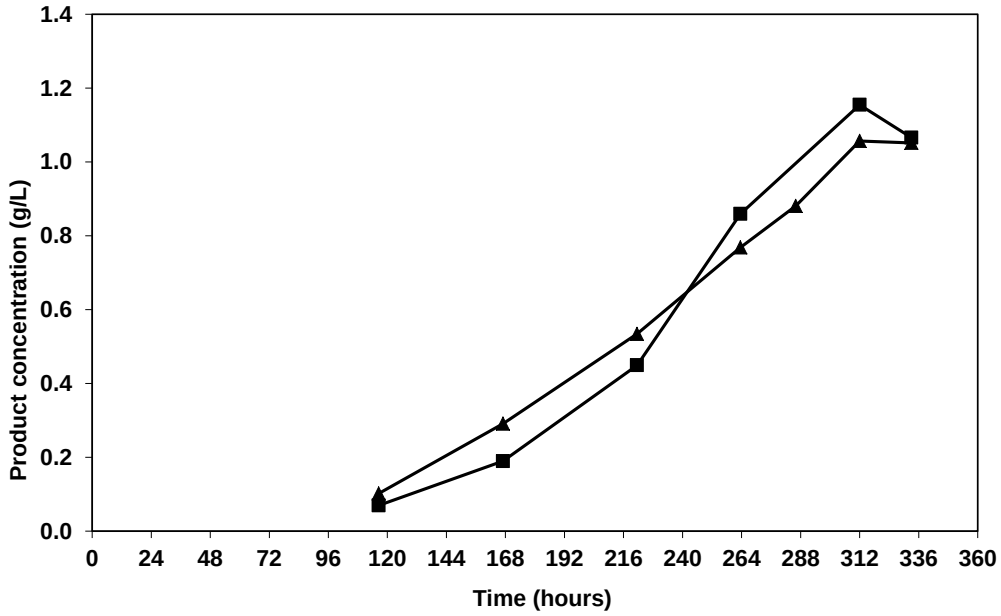

Figure 5.3: **Comparison of the product concentration profiles of the fed-batch 5L STR operated with direct sparging and the directly driven MBR operated with surface aeration.** The 5L STR (▲) and the MBR (■). Product concentration was measured using HPLC as detailed in Section 2.15.

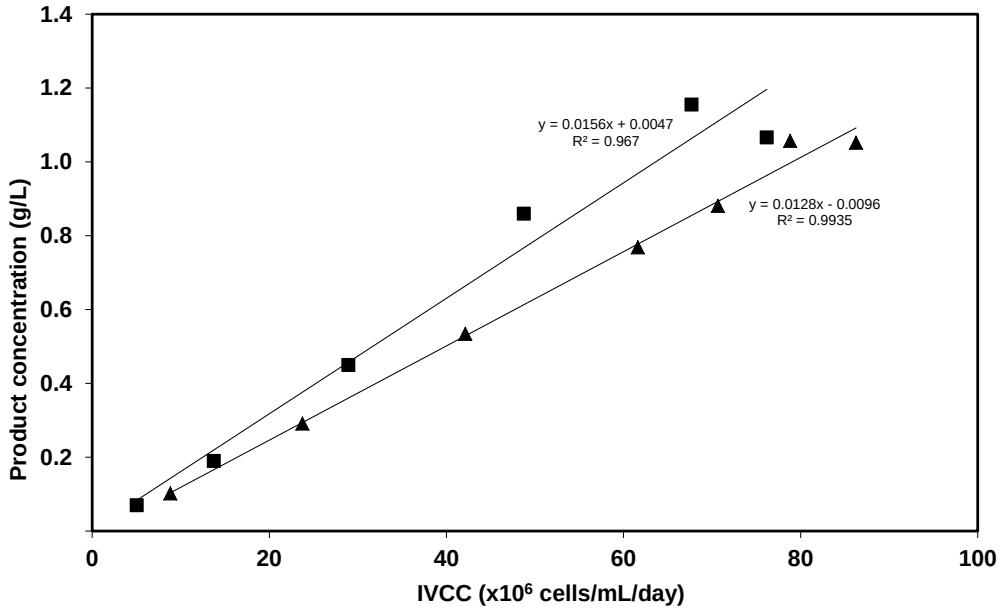

Figure 5.4: **Comparison plots of product concentration vs IVCC for the 5L STR operated with direct sparging and the directly driven MBR operated with surface aeration.** Product concentration of the 5L STR (▲) and the directly driven MBR (■).

Table 5.1: Summary of the growth and productivity performance in the MBR and 5L STR. The data points are mean values from duplicate cell culture runs. Triplicate VCC measurements were carried out daily for each cell culture run, so the maximum VCC figures represent the average of 6 VCC measurements. The numbers in the brackets are ± 1 standard deviation about the mean. The ranges show a relatively low level of variability between measurements, therefore displaying the maximum VCC figures to one decimal place is an appropriate degree of precision. There appears to be no significant difference between the maximum VCC values of the MBR and 5L STR as the mean values are within one standard deviation of each other.

	Directly driven MBR	**5L STR**
Max VCC ($x10^6$ cells/ml)	10.4 (±0.6)	9.8 (±0.6)
μ_{max} (h^{-1})	0.024	0.029
IVCC ($x10^6$ cells.day/mL)	76	86
Max. MAB Titre (g/L)	1.07	1.05
Q_p (pg/cell/day)	16	13

The size of the cells in both the reactors follows a fairly similar trend throughout the cultivations (refer to Fig. 5.5). The cell size in the 5L STR is however consistently smaller than that in the MBR. This is particularly the case after 48 hours and again after 288 hours. The larger cell size in the MBR in the early stages does correspond to slightly slower growth in the MBR at the same time period. The largest difference occurs at 96 hours with the MBR having an average cell diameter of 1.5 µm larger than that in the 5L STR. This time point corresponds to the time when the 5L STR enters into the exponential growth phase. The MBR appears to enter the exponential growth phase around 24 hours later. After 240 hours the cell size in the 5L STR drops significantly and remains lower than that in the MBR. This appears to correspond with the consistently lower viability found in the 5L STR after this time point. It is generally expected

that the average measured cell diameter would start to drop at the end of a cultivation to reflect the start of the death phase. Cell death at this phase of the culture is often associated with apoptosis (Arden and Betenbaugh, 2004). This occurs when cells are subjected to non-lethal stresses that activate a series of cellular responses which culminate in cell death. At a late stage in the culture the accumulation of toxins or the depletion of an essential amino acid or nutrient is often the cause of apoptosis. However, whatever the cause of cell death, a reduction in the measured cell diameter is usual and this is because of the shrinkage that occurs during apoptosis and also the rupturing that occurs due to the breakdown of the cell membrane.

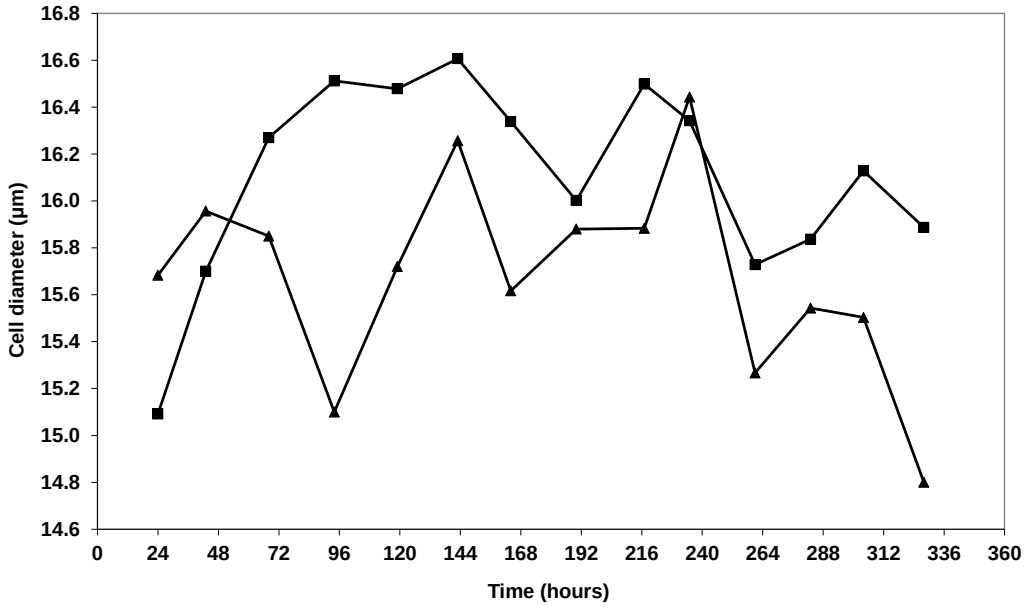

Figure 5.5: **Comparison of the cell size profiles of the fed-batch 5L STR operated with direct sparging and the directly driven MBR operated with surface aeration.** The 5L STR (▲) and fed-batch MBR (■). Cell size was measured using the Vi-CELL as described in Section 2.7.

5.3 Comparison of process parameter control

Culture pH, temperature and DOT have a significant impact on cell growth, metabolism and productivity, hence it is important to review profiles of these process parameters when comparing bioreactor performance. The data in this section is from one directly driven MBR cultivation and one 5L STR cultivation from the cultivations described in Section 5.2.

5.3.1 DOT

Both the MBR and 5L STR were operated with a DOT setpoint of 30% and a deadband of 10%. Over the course of the cultivation, both bioreactor systems controlled DOT within their respective deadbands with the exception of a minimal number of spikes. DOT control in the 5L STR was tightest about the setpoint between 0 to 130 hours after which DOT control drifts further from the setpoint to around 30 ± 5%. This may have been the point during which the system began to utilise enriched oxygen to cope with the culture's increased oxygen demand during the exponential growth phase. The introduction of enriched oxygen can make it more difficult for the system to control tightly about the setpoint due to the increased concentration of oxygen being sparged into the system which can result in DOT overshoots.

This effect did not occur in the MBR because it was operated using surface aeration, which would have resulted in a more gradual change to DOT control due to the system's lower k_La. There is, however, a gradual reduction in average DOT readings as the culture progresses to reach high cell density. It can be seen in figure 5.6A that the DOT readings move closer to the lower end of the deadband (20% DOT). This is caused by the culture's higher oxygen demands, which make it more difficult for the system to control DOT at the setpoint. For the directly driven MBR there are three spikes at around 216, 288 and 312 hours where the DOT deviates markedly from the setpoint. These increased DOT readings were caused by the delivery of air from a syringe during bolus feed additions. Feed additions can impact on DOT levels in miniature scale, surface aerated bioreactors, as feeding can disturb the reactor's headspace (Hsu et al, 2012).

A

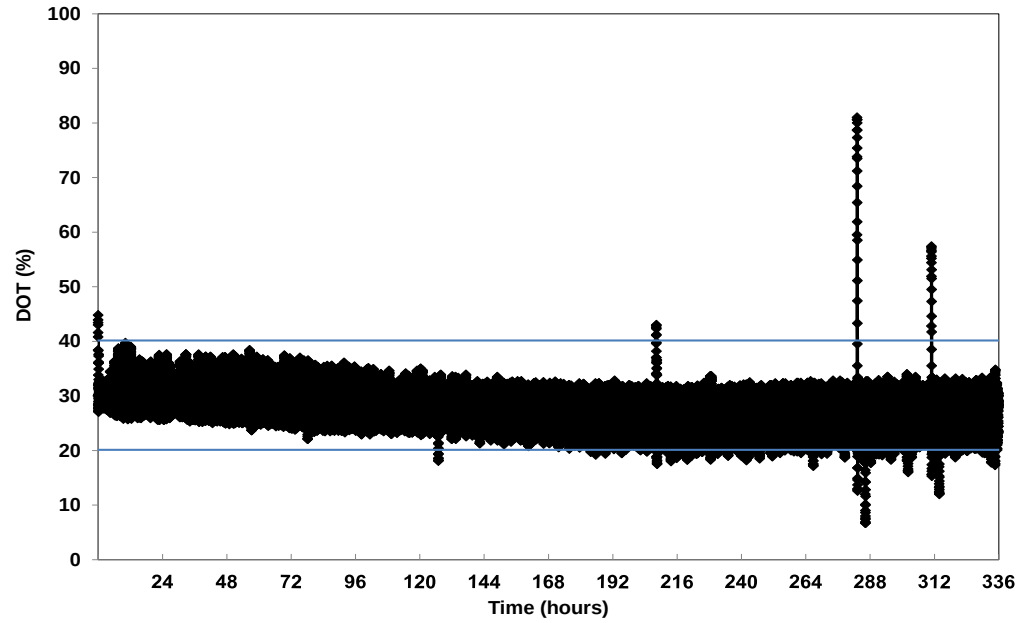

B

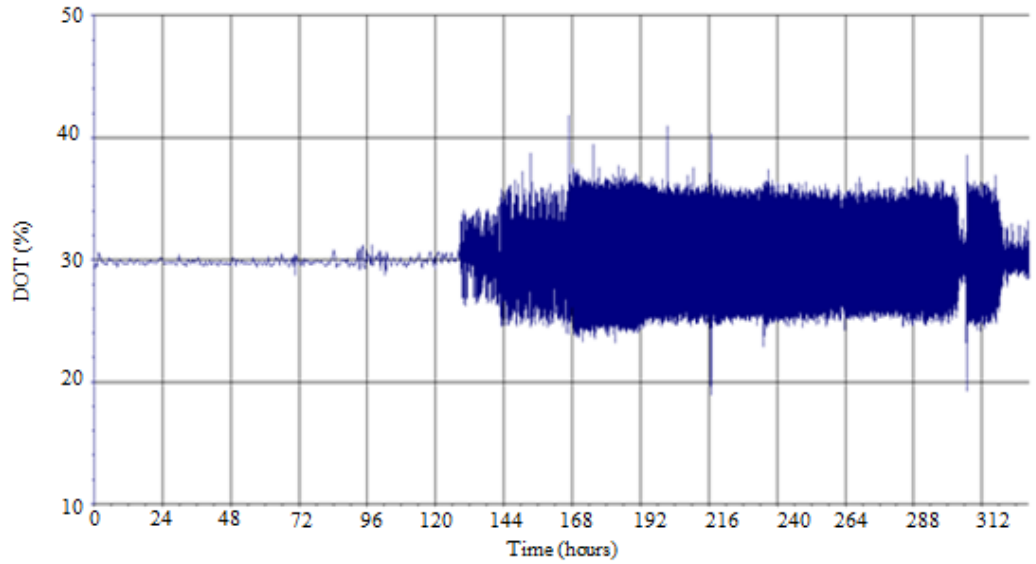

Figure 5.6: **DOT profiles for the fed-batch directly driven MBR operated with surface aeration and the fed-batch 5L STR.** A) data logged every 20 seconds from one MBR to one decimal place B) data logged every 30 seconds from one 5L STR to one decimal place. Data for the complete 5L STR cultivation could not be exported from the Biostat BDCU software as the software is only able to export the first 6,000 data points, which only covers the first four days of the cultivation. This is a screen shot of a plot produced by the software for the cultivation.

5.3.2 pH

The MBR was operated with a pH setpoint of 7.10 and a deadband of 0.1 and the 5L STR was operated with a pH setpoint of 7.10 and a deadband of 0.05. It is difficult to accurately compare the pH profiles of the two systems (refer to Fig. 5.7) as the MBR's data is recorded to one decimal place whereas the 5L STR data is recorded to two decimal places. Although the MBR data was logged to one decimal place, pH was controlled to two decimal places.

Overall, pH control was similar for both systems with the pH measurement often at the higher end of the deadband of ± 0.1 for the MBR and ± 0.05 for the 5L STR. The pH in the 5L STR drops for around 24 to 48 hours (between 110 and 144 hours) which may have been caused by accumulation of lactate (Bibilia and Robinson, 1995) which peaks between 120 and 140 hours. In the MBR, lactate concentration peaks between 168 and 216 hours and this corresponds to a drop in pH from the higher end of the deadband to the setpoint during those hours.

There are a number of pH spikes in the 5L STR profile during which pH increases (every 24 hours between 168 hours and 312 hours); this is due to daily alkali bolus feed additions which momentarily increase pH on addition. This is also noticeable in the MBR between 192 and 216 hours, at around 240 hours and after around 288 hours.

A

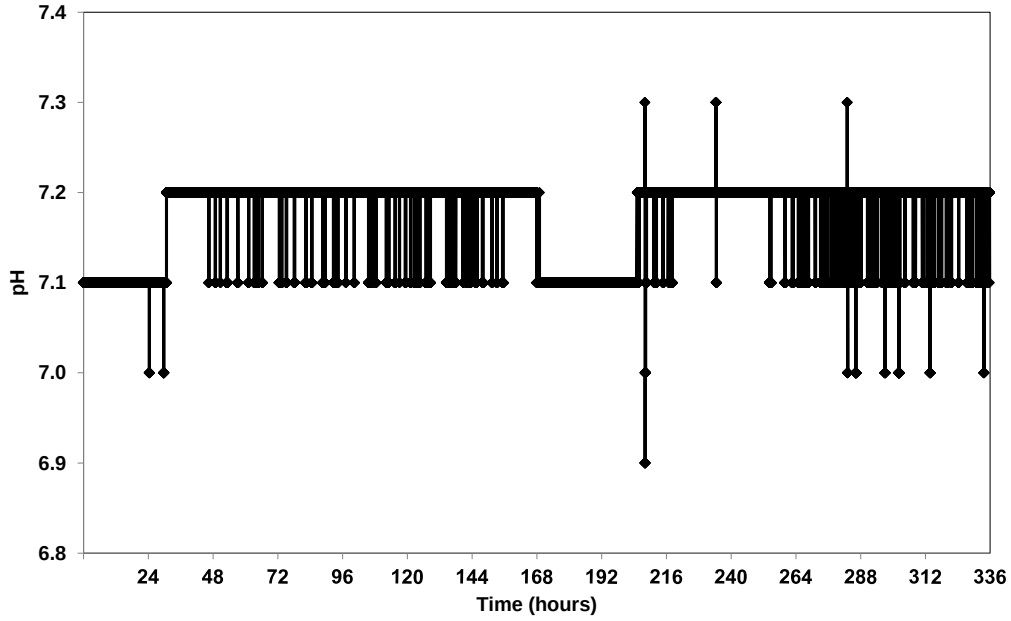

B

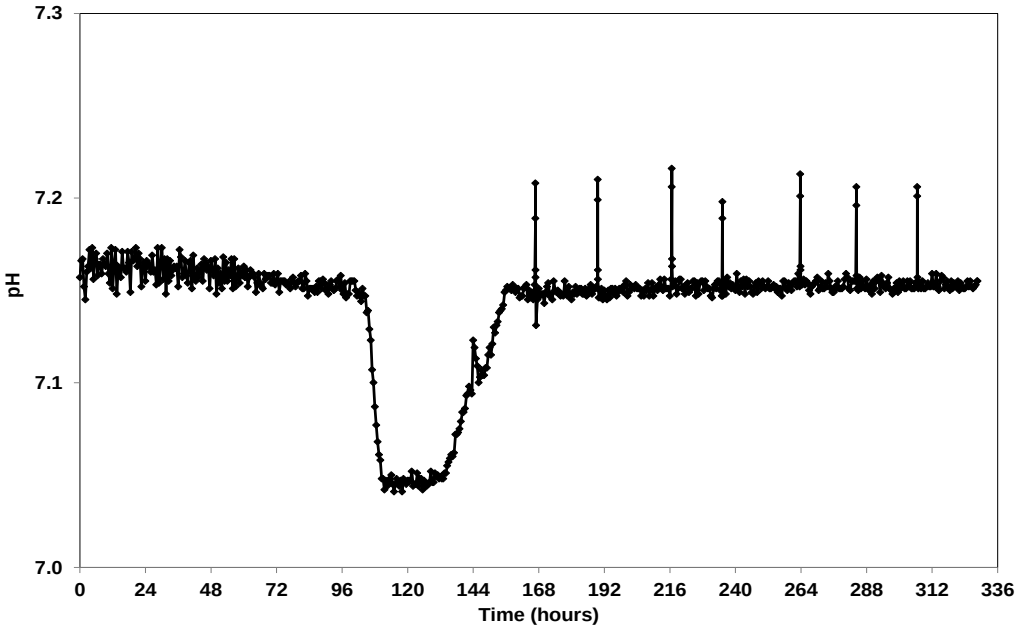

Figure 5.7: **pH profiles for the fed-batch directly driven MBR operated with surface aeration and the fed-batch 5L STR.** A) data logged every 20 seconds from one MBR and to one decimal place B) data logged every 30 minutes from one 5L STR to two decimal places. Data covering the whole of the cultivation was exported from the Biostat BDCU software as it had fewer than 6,000 data points.

5.3.3 Temperature

The temperature profiles were very similar between the two systems (refer to Fig. 5.8). Temperature control around the setpoint of 37°C was very tight in the 5L STR and at around ± 0.1°C in the MBR system. There are a number of downward spikes in the 5L STR every 24 hours from 168 hours, again this is due to the addition of refrigerated bolus feed additions which momentarily reduce culture temperature. This is also noticed in the MBR system between 192 and 216 hours and at around 288 hours.

5.3.4 Summary

Temperature and pH spikes that occurred at the time of feeding are generally more noticeable in the 5L STR profiles than the MBR's. This may have occurred because feed additions in the 5L STR were made at the bottom of the reactor near the probes while feed additions in the MBR were made at the surface further away from the probes. It is also difficult to compare the pH and temperature profiles when there are very slight changes because the MBR recorded data to one decimal place while the 5L STR recorded data to two decimal places.

The DOT, pH and temperature profiles of the 5L STR and MBR generally showed good similarity throughout the cultivations. The process parameters were largely controlled within their respective deadbands except when feeding occurred, which resulted in temporary overshoots.

A

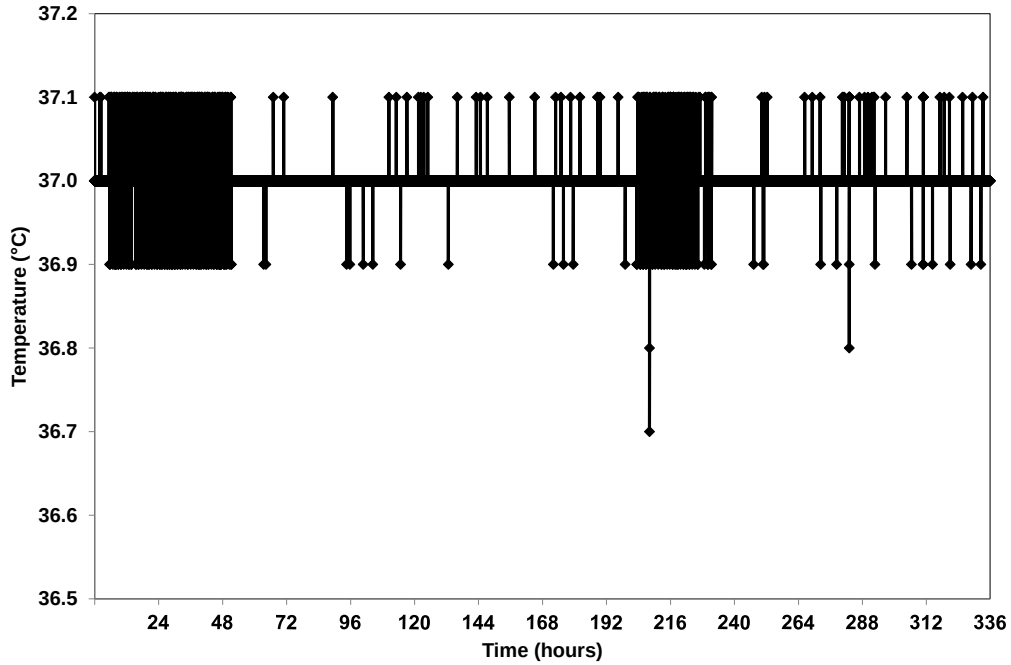

B

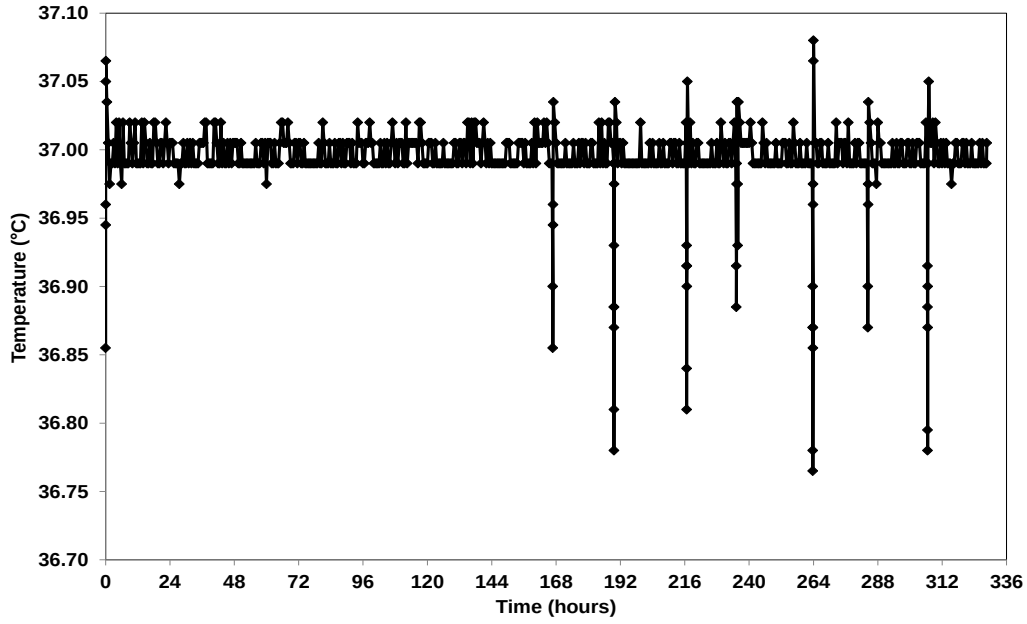

Figure 5.8: **Temperature profiles for the fed-batch directly driven MBR operated with surface aeration and the fed-batch 5L STR.** A) data logged every 20 seconds from one MBR and to one decimal place B) data logged every 30 minutes from one 5L STR to two decimal places. This complete data set was exported from the Biostat BDCU software as it had fewer than 6000 data points.

5.4 Metabolite analysis

5.4.1 Glucose and lactate

Generally, specific glucose consumption rates are the highest during the exponential growth phase and then reduce and level off during the stationary growth stage and death phase. High levels of glucose are present in the basal media to support the high rates of growth in the early stages of the culture but as the growth rate reduces the demand for glucose reduces.

The glucose consumption rates of both the MBR and 5L STR are similar throughout the cultivations and follow the same trend (refer to Fig. 5.10). The 5L STR does have a slightly higher specific glucose consumption rate during the earlier stages of the culture primarily due to it entering the exponential growth phase earlier and also due to its higher μ_{max}. The MBR then has a higher specific glucose consumption rate starting from 120 hours to 192 hours because this is when it enters the exponential growth phase. After 192 hours the specific glucose consumption rates for both reactors are very similar and this is because they are both approaching the stationary growth phase. The overall glucose consumption rate for both cultivations was fairly similar with the 5L STR producing an average specific glucose consumption rate (Q_{glc}) of 282 pg/cell/day and the MBR producing an average Q_{glc} of 250 pg/cell/day.

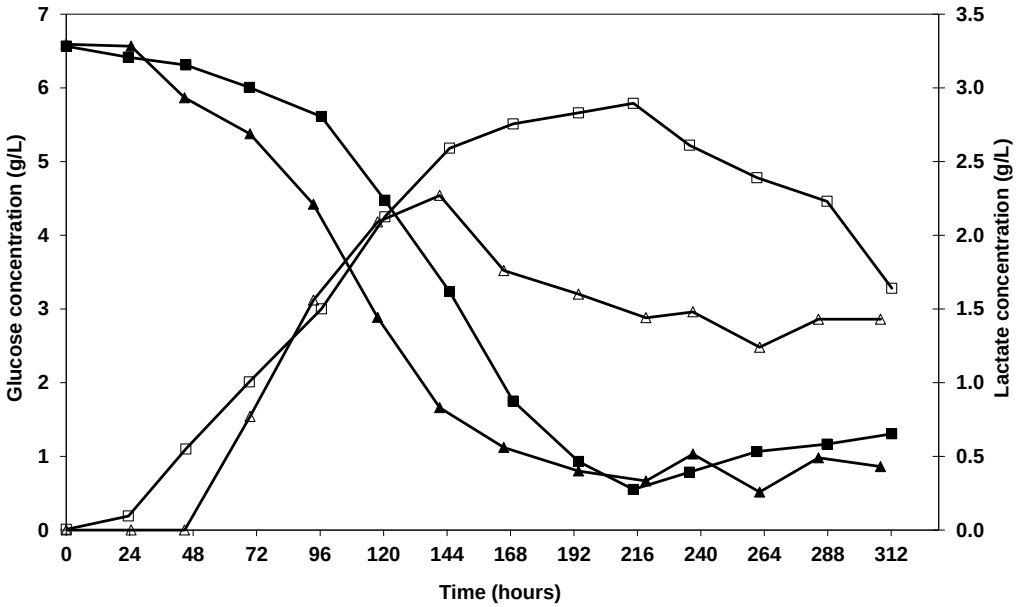

Figure 5.9: **Comparison of the glucose and lactate concentration profiles of the fed-batch 5L STR operated with direct sparging and the MBR operated with surface aeration.** Glucose concentration for the 5L STR (▲) and glucose concentration profile for the MBR (■). Lactate concentration for the 5L STR (Δ) and lactate concentration for the fed-batch MBR (□). Metabolite concentrations were measured using the NOVA Bioprofile as described in Section 2.8.

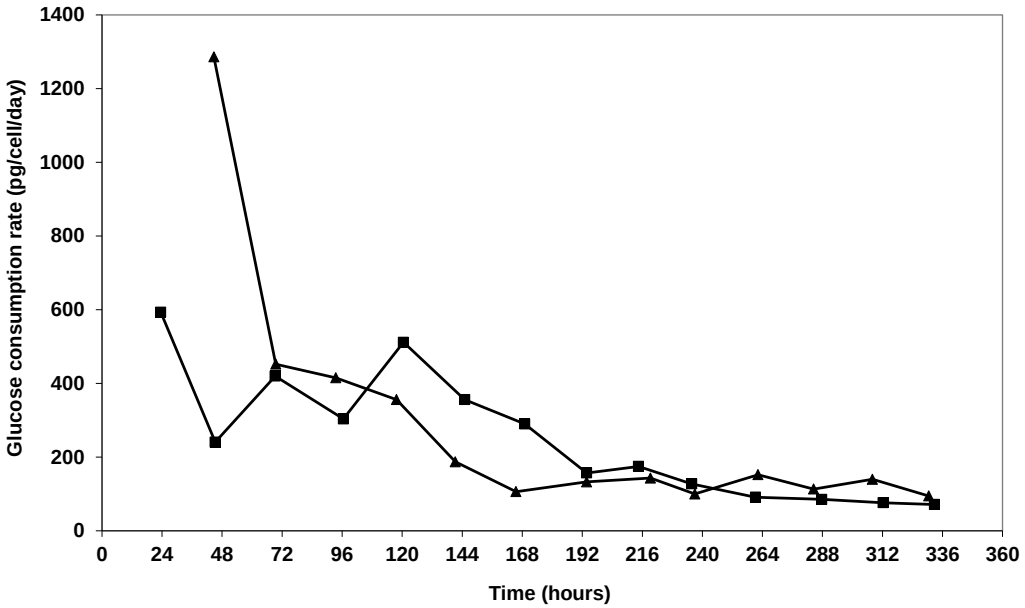

Figure 5.10: **Comparison of the glucose consumption rate profiles for the fed-batch 5L STR operated with direct sparging and the directly driven MBR operated with surface aeration.** The 5L STR (▲) and the MBR (■). These rates were calculated by dividing the glucose consumed per day by the delta IVCC per day. Delta IVCC is the IVCC for a specific day and the IVCC is the sum of the delta IVCC for each day.

Lactate has been widely reported to be toxic to CHO cells in high enough concentrations (Li et al 2012 and Lao and Toth 1997) with the tolerance to lactate varying from cell line to cell line. The toxic effects of lactate are related to their effects on culture pH as it is acidic which drives the addition of base to increase pH. The addition of high quantities of base can have harmful effects on the culture by increasing osmolality (Gorfien et al, 2003). Lao and Toth (1997) also reported that high levels of lactate can inhibit glycolysis which diverts more energy into the maintenance of ion gradients which can result in reduced growth rates. With regards to the MBR cultures, there was a minimal addition of base throughout the culture. On average there was an addition of 5 ml (1.7% culture volume) of base per cultivation in the MBR compared to roughly 200 ml (5.7% culture volume) in the 5L STR. Hence the 5L STR received a greater volume of base addition than the MBR.

It is normal for lactate to accumulate in the early stages of cultivation, however a large amount of lactate production is associated with poor culture performance. Lactate is produced by the metabolism of glucose as can be seen below.

$$C_6H_{12}O_6 \rightarrow 2\ CH_3CHOHCOOH \quad 5.1$$

Even in the presence of sufficient oxygenation CHO cells still metabolise glucose inefficiently to produce lactate. Both the MBR and 5L STR were adequately oxygenated with good control around a DOT setpoint of 30% and hence poor oxygenation would not have led to lactate accumulation. Poor culture performance is often linked to an increased production of lactate and to a certain extent this seems to have happened with regards to the MBR. Figure 5.4 shows that the MBR did produce higher concentration of lactate after 144 hours.

It is normal for lactate production to occur in the growth phase as the cells have a higher Q_{glc}, however there is a decrease in lactate production during the stationary phase which is the most productive phase of the culture (Gagnon et al, 2011). Lactate is produced as a result of a build-up of pyruvate due to its high synthesis rate in the glycolytic pathway and limited consumption in the tricarboxylic acid cycle (TCA) (Wilkens and Gerdtzen, 2011).

There are often high concentrations of glucose in the basal media to ensure that there is a sufficient amount of energy to allow the cells to proliferate and reach high cell densities. Another strategy to reduce the production of lactate is to minimise the concentration of glucose in the media particularly in the transition and stationary phase of growth. This can be achieved by employing a low culture target glucose concentration of around 1-2 g/L. The use of low concentration targets leads to more efficient primary metabolism and hence reduces the production of waste metabolites and can result in the cells being more productive (Butler, 2005). Lactate is often consumed in the stationary phase of the culture even when there is a sufficient amount of glucose in the culture and when lactate is completely consumed there is often an increase in ammonia production possibly due to increased amino acid catabolism (Li, 2012). This phenomenon occurred in both the MBR and 5L STR cultivations as can be seen in figure 5.4. The reason why lactate is consumed is not entirely known but it is clear that rather than being a waste metabolite, lactate can be an important substrate at certain culture phases.

The lactate concentration profiles are very similar for both reactors until around 140 hours (refer to Fig. 5.9). After this point the 5L STR culture begins to consume lactate hence reducing the culture concentration. This time point coincides with the culture reaching a low glucose concentration (under 2 g/L) and the initiation of feeding. After 140 hours the lactate concentration continues to rise in the MBR, probably due to the consistently lower overall glucose consumption rate throughout the culture until that point. The lactate concentration in the MBR begins to fall after around 210 hours with the final concentrations of both reactors being almost equal. The peak lactate concentration in the 5L STR was 2.27 g/L and 2.89 g/L in the MBR. Lao and Toth (1997) found that it took lactate concentrations of around 20 mmol/L (1.8 g/L) to begin to have an adverse effect on cell growth but that the effect is very much cell line dependent.

5.4.2 Glutamine

Overall the glutamine concentration profiles follow the same trends in both reactor systems (refer to Fig. 5.11). Initial glutamine concentrations are minimal because the basal media, CD-CHO, is glutamine free. There are very small amounts of glutamine in the cultures and this is most likely due to the glutamine present in the inoculum. The glutamine concentrations then began to rise as the cells synthesised glutamine and consumed glucose as a primary carbon source. However, at around 70 hours the glutamine concentration in the 5L STR started to level off and then reduced which coincides with the start of the exponential growth phase and also because the glucose levels are being rapidly diminished at this point. Hence, feeding is initiated soon after this point in the culture. Again the MBR is slightly behind with the glutamine concentration starting to reduce at around 140 hours. This is probably due to the MBR having a slightly lower μ_{max} and a lower IVCC until this point.

The glutamine concentration for both cultures began to rise again after 200 hours which coincides with the stationary growth phase. This stage of the culture is characterised by no net increase in growth but with the most productive period of the culture. Hence, the glutamine concentrations rise again because there is a reduced need for energy for growth.

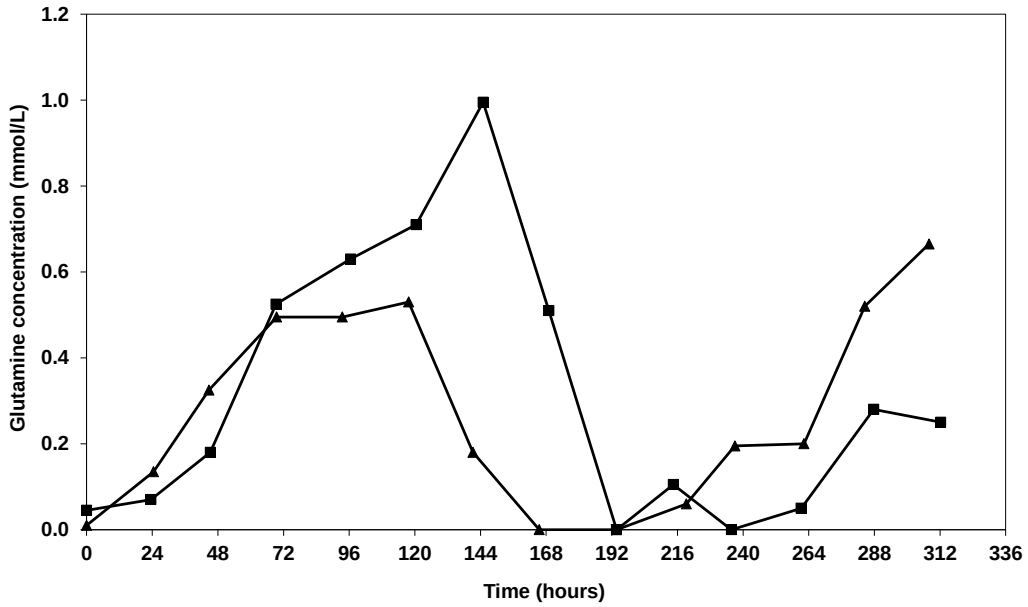

Figure 5.11: **Comparison of the glutamine concentration profiles for the fed-batch 5L STR operated with direct sparging and the directly driven MBR operated with surface aeration.** The 5L STR (▲) and the fed-batch MBR (■). Glutamine concentrations were measured using the NOVA Bioprofile as described in Section 2.8.

5.4.3 Ammonium

Ammonium has been reported to be toxic to mammalian cell culture and can result in reduced growth rates, lower peak cell densities and also reduced productivity. It is produced mainly by amino acid metabolism and in particular glutamine. Hence a strategy that can be taken to reduce ammonium production is to reduce the concentration in the media or use glutamine free media (Schneider et al, 1996). The ammonium levels for both the reactor systems are very similar throughout the cultivations (refer to Fig. 5.12) and reach a peak concentration of 3.84 mmol/L for the 5L STR and 3.91 mmol/L for the MBR. These are not levels that are typically known to be toxic to recombinant CHO cells. Lao and Toth (1997) reported that there was no significant effect on growth of a recombinant CHO cell line with concentrations of ammonium up to 10 mmol/L.

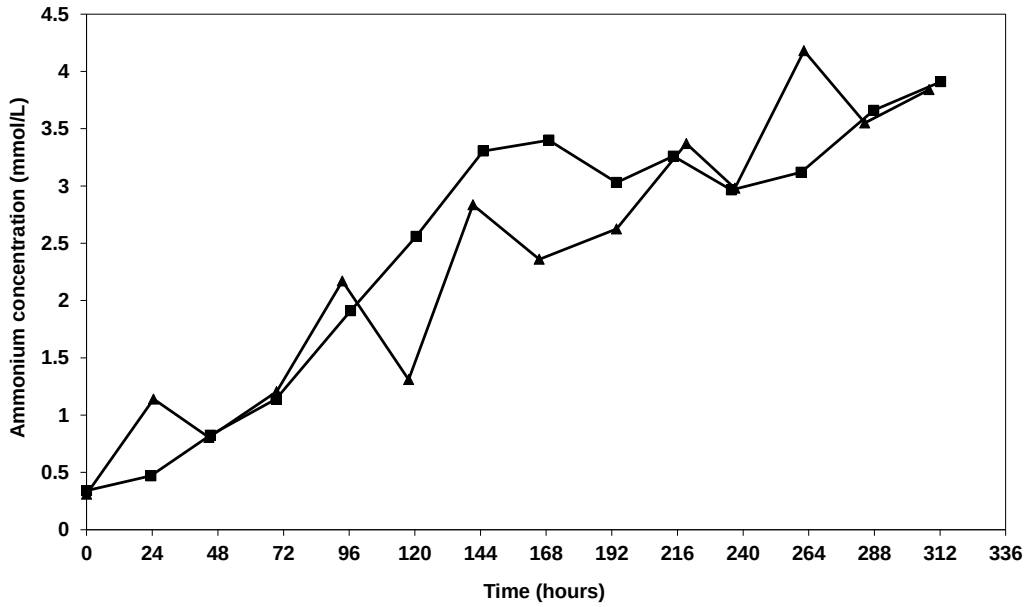

Figure 5.12: **Comparison of the ammonium concentration profiles for the fed-batch 5L STR operated with direct sparging and the directly driven MBR operated with surface aeration.** The 5L STR (▲) and the fed-batch MBR (■). Ammonium concentrations were measured using the NOVA Bioprofile as described in Section 2.8.

5.5 Continuous feeding

5.5.1 Overview and advantages of continuous feeding

Having demonstrated fed-batch operation using bolus additions the next step was to show that the MBR is capable of performing continuous feeding (CF) in order to maintain a constant glucose concentration in cell culture.

CF has 4 main advantages:

1. Significantly reduces the chances of contaminating the cell culture compared to daily bolus injections through a septum. This is because there is only a single intervention as opposed to at least 1 daily when making bolus additions.

2. For cell lines that have a high cell specific glucose metabolism, 2-3 bolus additions will have to be administered every day to each reactor. This will prove to be very labour intensive, particularly if there are many MBRs in operation. It

will also be very inconvenient if additions have to be made at un-sociable hours. CF overcomes both of these issues as the feed is being continuously added at very low flow rates maintaining a minimum constant glucose concentration throughout the culture.

CF can also facilitate automated dynamic feeding which is a mechanism that monitors the culture's glucose and nutrient needs in real time and then responds by altering feed flows to maintain nutrient levels. This would of course require constant culture analysis using online analysis and sophisticated algorithms to calculate the flow rates required to maintain nutrient levels. The advantage of this is instant adjustment to meet the culture's needs but also reducing the labour intensity of sampling and then manually re-adjusting feed flow rates.

3. The feed that is often used in mammalian cell culture is a very concentrated solution of nutrients. These solutions can have a high pH and hence if added in significant amounts, can result in pH spikes. Also if they have been refrigerated they can lower the culture temperature upon addition. If these additions are being made several times a day then the resulting alteration of culture conditions may have an adverse impact on the performance of the cell culture. CF overcomes this issue by making very small, but constant additions of feed and hence will not produce any noticeable effects on the pH and temperature.

4. Controlling the culture glucose concentration by making bolus additions will inevitably lead to the glucose concentration falling well below the target concentration and then rising very suddenly once the addition is made. This sudden addition of glucose could impact on the cells' metabolism.

5.5.2 Feed storage analysis

With bolus fed batch operation the feed is stored in a +4°C fridge as recommended by the manufacturers as refrigeration helps to preserve the vitamins and amino acids in the feed. It is also best practice to protect the feed

from light as some vitamins and amino acids are light sensitive and hence may become denatured if exposed to too much light.

With continuous feeding the feed would have to be kept on the bench at room temperature as it has to remain connected to the reactor from the time feeding is initiated. It has been noted anecdotally that leaving feed on the bench can result in a significant amount of precipitation which could make the feed less effective, especially if the precipitation contains essential elements. Hence a shake flask experiment was conducted to assess the effects that placing the feed on the bench in room temperature could potentially have on cell culture performance. During the experiment it was noticed that there was a noticeable amount of precipitation in both the feeds that were left on the bench, both covered and uncovered.

The following experiment assessed the effects of storing the feed in the fridge which also protected it from light, keeping the feed on the bench and also protected from light and on the bench without protection from light. This experiment used duplicate 250 ml shake flask cultures.

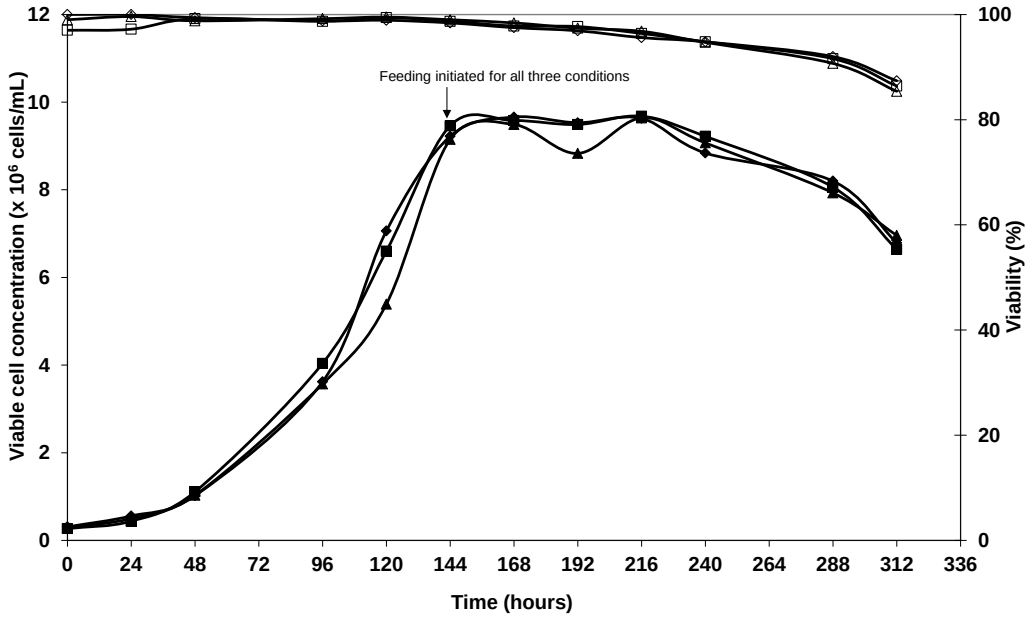

Figure 5.13: **Comparison of the growth and cell culture viability profiles of fed-batch shake flask cultures that received daily bolus feed additions.** VCC for cultures that received feed stored in the fridge (♦); on the bench but covered (■) and on the bench uncovered (▲). Cell culture viability for cultures that received feed stored in the fridge (◊); on the bench but covered (□) and on the bench uncovered (Δ). Feeding was initiated for all cultures at 144 hours. All data points represent the mean of duplicate shake flask cultures.

Figure 5.13 clearly shows that the storage of the feed had no noticeable effect on cell growth. The cultures are all similar post feeding (from 144 hours onwards) except for one data point at 192 hours where the VCC of the culture that was fed from the uncovered feed stored on the bench was slightly lower than the other two cultures. This however does appear to be a slight anomaly as the culture profiles are very similar other than this point. Cell viability in all three cultures was also very similar throughout the cultivations even after the initiation of feeding.

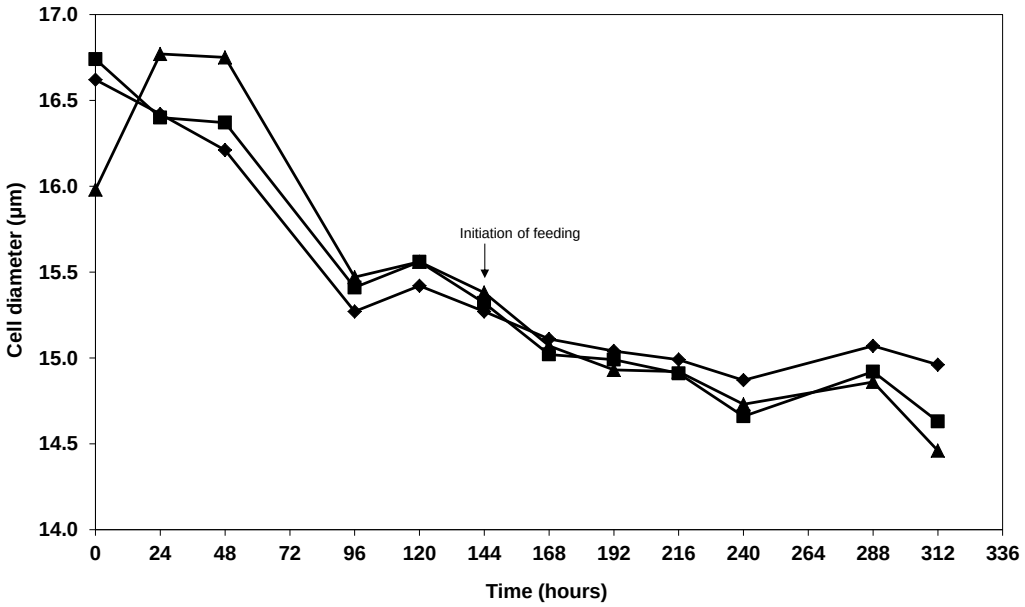

Figure 5.14: **Comparison of cell size profiles of fed-batch shake flask cultures that received daily bolus feed additions.** Comparison of the cell size profiles of cultures that received feed that was stored in the fridge (♦); on the bench but covered (■) and on the bench uncovered (▲). Feeding was initiated at 144 hours. Cell size was measured by using the Vi-CELL as described in Section 2.7.

Figure 5.14 shows that there is no significant difference in cell size throughout the cultivations. There does appear to be a slight difference that emerges after 216 hours where the average cell size in the culture being fed from feed stored in the fridge is slightly higher than that in the cultures being fed from feed stored on the bench. However this difference is not significant particularly as there is no significant difference in growth between the 3 cultures.

5.5.3 Continuous feeding cultivation

Figure 5.15 shows that the MBR can facilitate effective cell culture with continuous feeding. The culture produced good growth by reaching a maximum VCC of 9.3 x 10^6 cells/mL and maintained culture viability above 80% until 288 hours.

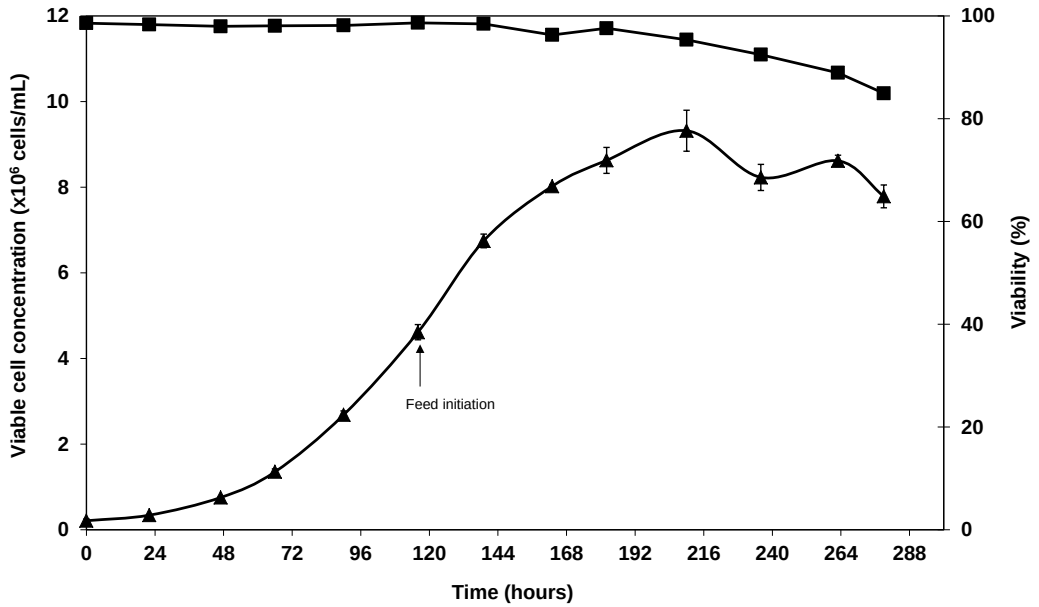

Figure 5.15: **Growth and viability profiles of the continuously fed MBR culture.** Cell culture viability (■) and VCC (▲). Feeding was initiated at 120 hours. Process parameters are detailed in Section 2.6 and 2.10. Error bars represent ± 1 standard deviation from the mean (n=3).

Feeding was initiated at 120 hours which is around 24 hours sooner than is often the case with bolus feeding. This is because feeding is initiated in advance of the glucose concentration falling below the target concentration of 2 g/L. Hence, a feed flow rate is estimated to ensure that the glucose concentration does not fall below 2 g/L (refer to Section 2.10).

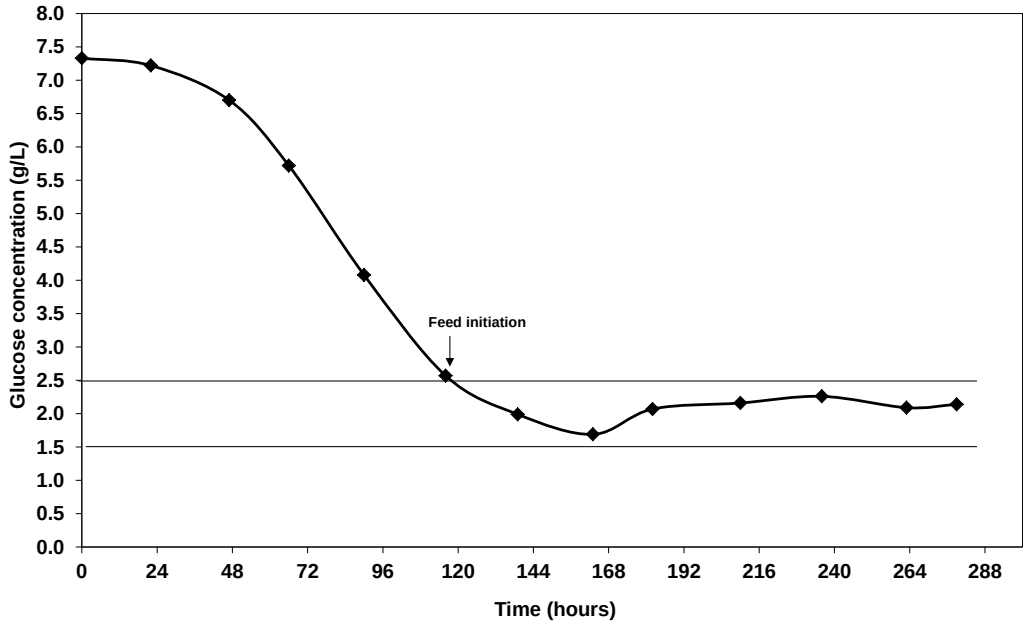

Figure 5.16: **The glucose concentration profile of the continuously fed MBR culture.** The glucose concentration of the feed used was 130 g/L. Feeding was initiated at 120 hours and flow rates were adjusted daily to achieve a constant culture glucose concentration of 2.0 g/L. Flow rates varied from 0.1-0.4 ml/h. Glucose concentration was measured using the NOVA Bioprofile as described in Section 2.8.

Figure 5.16 shows that the MBR is capable of maintaining fairly tight control of the culture glucose concentration after feed initiation, with the lowest concentration being 1.69 g/L and the highest being 2.26 g/L. This means that culture glucose concentration was kept within 2.0 ± 15 % g/L.

The initial feed flow rate (from culture time 116 hours) was calculated based on the amount of glucose consumed at a similar culture time in the fed-batch MBR cultivation reported in Section 5.2. In the fed-batch cultivation, glucose concentration fell from 4.5 to 3.2 g/L in 24 hours; a 1.3 g/L reduction in culture glucose concentration. This culture glucose consumption rate (refer to Table 5.2) was used to calculate the required feed rate (calculation shown below) to achieve a culture glucose concentration of 2 g/L. After the first 24 hours of feeding, feed rates were calculated by measuring the amount of glucose consumed in the previous 24 hours and assuming the same amount would be required over the next 24 hours.

Example calculation:

Predicted glucose consumption rate = 1.3 g/L/24 hours

Glucose concentration at time 116 hours = 2.6 g/L, predicted glucose concentration at time 140 hours = 1.3 g/L

Required glucose addition = 2.0 – 1.3 = 0.7 g/L

The culture volume was estimated to be 0.3 L

Required glucose addition was 0.3 x 0.7 = 0.21 g

Glucose concentration in the feed = 130 g/L

The amount of feed addition required over 24 hours = 0.21/130 =

1.6×10^{-3} L = 1.6 mL.

Feed rate required to deliver 1.6 mL feed over 24 hours = 0.07 mL/hr

The feed pump was capable of a minimum feed rate of 0.10 mL/hr, which is higher than the required feed rate, so the commencement of feeding was delayed until it was estimated that a feed rate of 0.10 mL/hr was required.

Table 5.2 shows the amount of glucose that was fed into the MBR and the average feed rate used to deliver that amount of glucose. Feed rates were reviewed 4-6 hours after the time of daily monitoring and may have been slightly altered if the glucose concentration was not maintaining the expected trajectory to achieve/maintain a concentration of 2 g/L.

Table 5.2: **Daily glucose additions and average feed rates in the continuously fed cultivation.** The glucose concentration of the feed used was 130 g/L.

Culture time (hours)	Required glucose addition to achieve 2 g/L glucose concentration in 24 hours (g)	Average feed rate (mL/hr)
116	0.21	0.10*
139	0.45	0.15
163	0.39	0.13
182	0.42	0.14
210	0.39	0.13
236	0.30	0.10
263	0.30	0.10

* The feed pump was capable of a minimum feed rate of 0.1 mL/hr which is higher than the required feed rate so the commencement of feeding was delayed until it was estimated that a feed rate of 0.1 mL/hr was required.

There are a couple of limitations with regards to this form of feeding and with the setup used. In trial runs, a needle of 0.08 cm bore size was used to try to create minute droplets to try to produce as constant a flow of feed as possible. However, precipitation in the feed blocked the narrow opening in the needle and prevented feed from flowing through the needle and into the vessel. Hence a standard connector tube of 0.31 cm diameter was used to connect the tubing from the bottle to the vessel. This resulted in larger droplets which meant that there was a longer gap between additions to the culture. On average there was a 10 minute gap between additions due to the time taken for a droplet to form and then disassociate from the connector tube compared to 2 minutes when using the smaller needle.

The other limitation was that the feed remained in the tubing for a significant amount of time while it is being pumped into the vessel due to the very slow flow rates. This poses problems if the feed requires refrigeration, although this was not a problem with the cell line and feed used in this experiment. It can take 2-3 days for feed from the bottle to reach the vessel which means that even if the feed bottle was refrigerated, the feed would spend a considerable amount of time at

room temperature as it flows through the tubing to the vessel. This period of time can result in significant precipitation in the tubing as has already been mentioned.

5.6 Conclusions

Scale comparison cultivations were carried out with the MBR and 5L STR at a matched P/V of 20.5 W/m^3 and matched mixing time of 6 seconds. These scale comparison cultivations showed that the directly driven MBR can successfully perform high cell density fed-batch cultivations. The growth profiles for the 5L STR and the MBR showed good similarity. The maximum VCC for the 5L STR and the MBR were very similar and varied by 6%. There was also good similarity in the IVCC and μ_{max} for both the reactors. The IVCC in the 5L STR was 13% higher than in the MBR and the μ_{max} was 17% higher in the 5L STR than in the MBR. Both the reactors produced very similar product titres with only a 2% variation between the two bioreactor systems. Process parameter profiles for DOT, pH and temperature also showed good similarity with both the 5L STR and MBR able to control the parameters within similar ranges.

It should be noted that the directly driven MBR was operated using surface aeration and the 5L STR was operated using gas sparging. Although the cultivations were comparable, the modes of gas delivery represent a significant operational variance. Future work should focus on optimising the performance of the MBR system when operated with gas sparging as this could ensure more comparable hydrodynamic conditions in both the reactor systems.

It was also shown that the MBR is capable of continuous feeding using extremely low flow rates of between 0.1-0.2 ml/h. The MBR was capable of maintaining fairly tight control around the culture target glucose concentration of 2.0 g/L after feed initiation, with the lowest concentration being 1.69 g/L and the highest being 2.26 g/L. This means that culture glucose concentration was kept within 2.0 ± 15 % g/L. The variation in the glucose concentration after the initiation of feeding in the bolus fed cultivations was much higher. At its lowest

the glucose concentration reaches 0.5 g/L which is 75% below the target glucose concentration (refer to Fig. 5.9).

Chapter 6: Summary and conclusions

This study involved the evaluation and optimisation of a 4 x 500 ml MBR system that is capable of parallel mammalian cell culture. This unit also has the capability of operating 16 parallel bioreactors hence providing the potential for an effective, high throughput process development/optimisation tool. The MBR system was mechanically and geometrically similar to a standard 5L STR that was used to carry out scale comparison studies.

Initial design modifications were made to the hardware to make it suitable for mammalian cell culture. This included designing and fitting a sampling mechanism that provided a simple to use solution. Also a variety of sparger designs were produced to replace the 15 µm sintered sparger that was provided with the unit due to its excessive foaming in CD-CHO media.

A comprehensive engineering characterisation of the MBR and 5L STR was conducted to evaluate the MBR system's performance and in order to facilitate scale comparison studies. Characterisation included mechanical power input, k_La, mixing time and hydrodynamics. Power input was measured for the directly and magnetically stirred MBRs by using a small scale air bearing dyanometer. The N_p was calculated for both agitation configurations with the N_p for the direct driven impeller equalling 0.42. The N_p for the magnetically driven impeller was not accurately measured due to limitations with the experimental set up, however at higher impeller speeds the N_p for both impeller types became similar. The N_p of the 5L STR was measured previously as 0.97 (Nick Silk, personal communication). The 5L STR was run at 260 rpm and at this speed it had an estimated P/V of 20.5 W/m^3. At matching P/V the agitation speed of the directly driven MBR was estimated to be 410 rpm and 350 rpm for the magnetically driven MBR.

k_La was measured for the MBR system and the 5L STR as a function of agitation rate using the static gassing out method with CD-CHO media at 37°C, as this mimicked cell culture conditions. k_La measurements were highest for the 90 µm

sintered sparger design for both the directly and magnetically driven impellers (16-24 h^{-1}). On average the k_La measurements obtained for the other sparger designs were similar and varied between 5-14 h^{-1}. k_La was also measured for the MBR using surface aeration and the values obtained were between 1.25-2.25 h^{-1}. The k_La for the 5L STR was measured at different agitation and gas flow rates (100-260 rpm and 0.03-0.06 vvm). The k_La at 0.03 vvm and P/V = 20.5 W/m^3 was 3.8 h^{-1}, doubling the gas flow rate only increased the k_La to 4.6 h^{-1}. It was found that the agitation rate had a more profound effect on k_La than gas flow rate which is consistent with literature data for bench and pilot scale reactors (Van't Riet, 1979).

Mixing times were measured for the MBR system using both a decolourisation method and the pH tracer method as a function of both agitation rate and fill volume. Mixing times reduced significantly at faster agitation rates and with smaller fill volumes. The directly driven impeller produced lower mixing times compared to the magnetically driven impeller. The 5L STR had a mixing time of 6 seconds at P/V = 20.5 W/m^3 which was very similar to the directly driven MBR which produced a mixing time of 6.3 seconds at matched P/V. It was found that the mixing times measured using the decolourisation method with the directly driven impeller were similar to those predicted by a correlation developed by Nienow (1998).

$$T_m = 5.9D_T^{2/3}(\overline{\varepsilon}_T)^{-1/3}(Di/D_T)^{-1/3} \qquad 6.1$$

The hydrodynamic conditions in the MBR and 5L STR were evaluated and their potential impact on the cells was analysed. It was found that at a matched P/V of 20.5 W/m^3 the Kolmogorov eddy sizes in the impeller region of the directly and magnetically driven MBRs and the 5L STR was above the average cell diameter. Hence it was found that the conditions produced by the reactor systems at matched P/V should not have resulted in substantial mechanic shear damage on the cells.

An initial batch scale comparison cultivation was conducted comparing the performance of the directly and magnetically driven MBRs and the 5L STR. Constant P/V was used as a scale down factor which also resulted in a constant mixing time for the 5L STR and the directly driven MBR. There was a significant difference between the maximum VCC of the 5L STR (9.9 x 10^6 cells/ml) and both the magnetic and direct driven MBRs (5.1 and 4.9 x 10^6 cells/ml respectively). The specific productivities obtained in the magnetic and directly driven MBRs were higher than that achieved in the 5L STR (26 pg/cell/day in the magnetically driven MBR; 21 pg/cell/day in the directly driven MBR and 16 pg/cell/day in the 5L STR).

A series of batch cultivations were carried out in the MBR system using the directly driven impeller to optimise its performance. These cultivations focused on optimising the gas delivery mechanism to the system and evaluated surface aeration and gas sparging. These cultivations showed that the design and operation of different gas delivery configurations can have profound effects on cell culture performance. The 90 μm sintered sparger was found to be unsuitable for use with the GS CHO cell line trialled in these cultivations. It was shown to significantly hinder cell growth to the extent that the cell culture did not enter into the exponential growth phase. The configuration that involved gas sparging using the singular opening 0.31 cm diameter sparger design yielded far better culture performance. It produced a maximum VCC of 6.8 x 10^6 cells/mL, a μ_{max} of 0.023 h^{-1} and a product titre of 0.58 g/L. The configuration that involved surface aeration produced better cell growth reaching a maximum VCC of 8.1 x 10^6 cells/mL and a μ_{max} of 0.028 h^{-1}; however it produced a slightly lower titre of 0.52 g/L. The culture that involved direct sparging produced cells that had a significantly higher cell specific productivity of 16 pg/cell/day compared to 10 pg/cell/day in the cultivations that employed surface aeration.

Scale comparison cultivations were carried out with the MBR and 5L STR at a matched P/V of 20.5 W/m^3 and matched mixing time of 6 seconds. Gas was delivered to the culture via surface aeration as this mode of gas delivery resulted in better cell growth compared to direct gas sparging. This scale comparison showed that the directly driven MBR using surface aeration can successfully

perform high cell density fed-batch cultivations. The growth profiles and the antibody productivity for the MBR and 5L STR showed good similarity (refer to Section 5.2.1).

It was also shown that the MBR system can be adapted to enable continuous feeding using extremely low flow rates of between 0.1-0.2 ml/hour. The MBR was capable of maintaining fairly tight control around the culture target glucose concentration of 2.0 g/L after feed initiation, with the lowest concentration being 1.69 g/L and the highest being 2.26 g/L. This means that culture glucose concentration was kept within 2.0 ± 15 % g/L.

In summary, the BioXplorer^{TM} MBR system is capable of producing similar growth kinetics and product titres to lab-scale bioreactors and hence offers an economical and user friendly scale-down process development/optimisation technology. Its working volume of ~ 300 ml provides enough culture volume to facilitate regular sampling for offline analysis. It is also capable of performing bolus and continuous feeding operations both of which are now standard and essential elements of modern industrial mammalian cell culture processes.

Chapter 7: Future work

7.1 Future developments of the 500 ml MBR

This work has shown that the performance in the directly driven MBR system compares well with a 5L STR while performing routine fed-batch processes at matched P/V and mixing time. The scale comparison cultivations compared the performance of duplicate MBR cultivations and 2 x 5L STR cultivations. Increasing the number of scale comparison cultivations would add a greater level of depth to the comparison data and facilitate more extensive statistical analysis. The MBR system should be further tested to operate 4 MBRs in parallel to evaluate its increased throughput potential. It would also be beneficial to further develop the MBR system to explore whether its performance would compare well while operating more complicated processes like implementing temperature shifts.

During the scale comparison cultivations the MBR was operated using surface aeration and not direct sparging which is a significant difference between the operation of the 2 bioreactor systems. The MBR system was able to support high cell density cultivations with a maximum VCC of just under 11 x 10^6 cells/ml, however some modern industrial cell culture processes can reach a maximum VCC of up to 30 x10^6 cells/ml. These high cell densities will require systems that can provide higher k_La values which may not be possible when operating surface aeration. Hence, it would be key to improve the MBR's performance when using direct sparging as this mechanism of gas delivery produces significantly higher k_La values and would potentially support higher cell densities. A possible mechanism of doing this could be to reduce the gas flow rates to a minimum and operate continuous gassing. This mode of operation would also eliminate the bursts of gas which result in cell culture being drawn up the sparger shaft potentially producing shear stress on the cells. At the moment the system can only sparge a single gas into 1 reactor at a time, hence each vessel's needs are addressed periodically. This means that each reactor will have a limited time of gas control and hence gas flow rates are operated at a high level in order to

deliver enough gas to control at the process setpoints. For the MBR system to have the ability of catering for each vessel's gas needs independently, it would require separate gas control for each vessel. In order to have continuous sparging these controllers would need to have gas mixing capability. This would represent a significant upgrade in the systems hardware and would result in increasing the foot print of the unit and also significantly increasing the cost.

The geometry of the bottom of the MBR's vessel is flat which is different to that of the 5L STR which is curved. It could improve cell culture performance if the vessels in the MBR system were designed with curved bottoms. The only potential problem that could occur is with temperature control because the vessel is heated via the bottom of the polyblock holder. However, heating occurs at a very small point and hence as long as there is some contact between the vessel and this heating point, temperature control should not be a limitation.

Automating the system as much as possible would be a worthwhile improvement. There is a great deal of interest in automating sampling and hence cell counting and metabolite analysis or to develop probes that could conduct on-line analysis. There has been some progress in the field with regards to on-line biomass measurements in microbial bioreactor systems (Gill et al 2008), however there has not been the same level of progress in mammalian cell culture systems. In theory, it would be possible to have an automated sampling mechanism (a robotic arm for example) that could take samples aseptically and feed them into an automated cell counter similar to the Vi-CELL or into a metabolite analyser. However, this would be a very expensive setup and would add a considerable amount to the capital investment in the system.

7.2 Development of a smaller 100 ml vessel

A 100 ml vessel was developed and briefly evaluated to assess the potential of the system providing a smaller MBR design and hence further reducing the systems foot print and running costs. This reactor had a diameter of 0.056 m and a height of 0.13 m. It was fitted with the same probes used in the larger 500 ml

reactors, a magnetically stirred impeller and a temperature probe which was placed in the hollow impeller shaft. In this case the combined diameter of the probes occupied nearly 50% of the diameter of the vessel.

7.2.1 Mixing time in the 100 ml vessel

Mixing time experiments were carried out in the 100 ml vessel at various agitation speeds (refer to Fig 7.1). Mixing time reduces with increasing impeller speed which is both logical and consistent with the larger scale bioreactors.

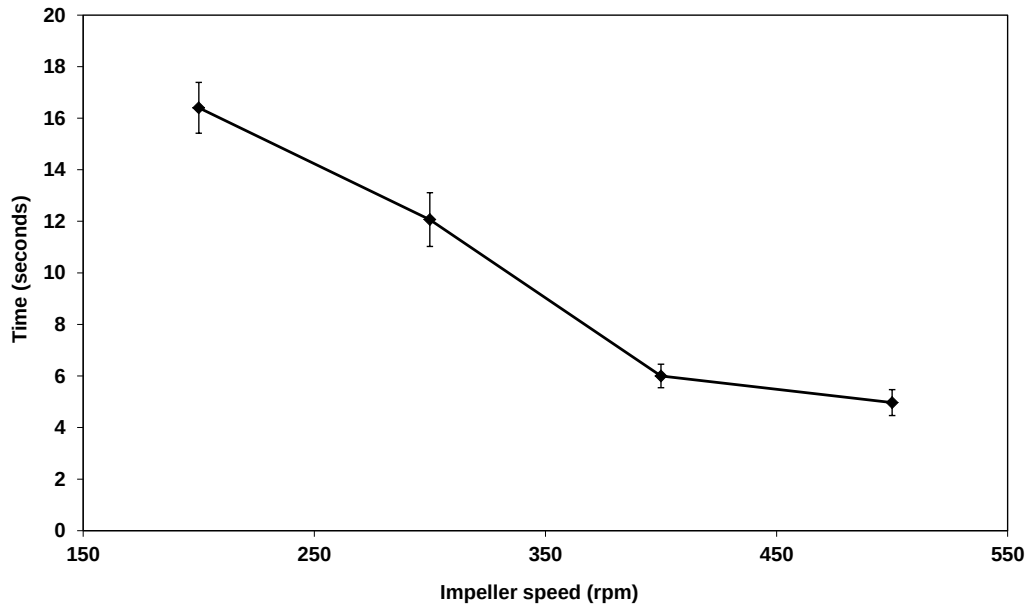

Figure 7.1: **Mixing times for the 100 ml MBR with a working volume of 35 ml**. Mixing time was measured using the decolourisation method and is the same as that mentioned in Section 2.13.1. Error bars represent ± 1 standard deviation about the mean (n=3).

7.2.2 Initial scale comparison cultivation

An initial scale comparison cultivation was carried out using constant mixing time as a scale down constant. The 100 ml vessel produced a mixing time of 6 seconds at an impeller speed of 400 rpm which is the same impeller speed that produced a mixing time of 6 seconds in the 500 ml vessel.

The early stages of a cell culture is often characterised by the lag phase where growth is slow, however in the case of the 100 ml culture the growth profile is

not typical as the majority of the growth occurs over the first 3 days. The culture was terminated at 168 hours as it was clear that the cells were not growing (refer to Fig. 7.2). At this point the culture reached a maximum VCC of 0.78 x 10^6 cells/ml and a viability of 79%.

Poor growth in the vessel could be explained by 3 factors, the aspect ratio, the impeller design and the presence of the DOT and pH probes which provided an amplified baffling effect.

The aspect ratio of the vessel is high for mammalian cell culture where typically it should be below 2:1. Higher aspect ratios can result in compartmentalisation in large reactors and can leave sections of the vessel poorly mixed, which can lead to areas that have poor oxygen and pH control particularly as the DOT and pH probes sensors are at the bottom of the vessel. This affect is amplified due to the magnetic stirrer having no clearance from the bottom of the vessel. Although the vertical rectangle impeller can be doubled in height it is still not tall enough to compensate for the excessive relative height of the liquid surface. The small size of the reactor would certainly reduce the scale of compartmentalisation but may not eliminate it altogether.

Also mammalian cell culture bioreactors are usually not baffled because baffles are designed to create turbulence and shear which breaks up bubbles. Although this improves k_La it can result in harmful effects on shear sensitive mammalian cells (Garcia-Ochoa and Gomez, 2009). The 100 ml vessel has amplified some of the limitations of the 500 ml vessel by employing probes with the same diameter within a smaller vessel.

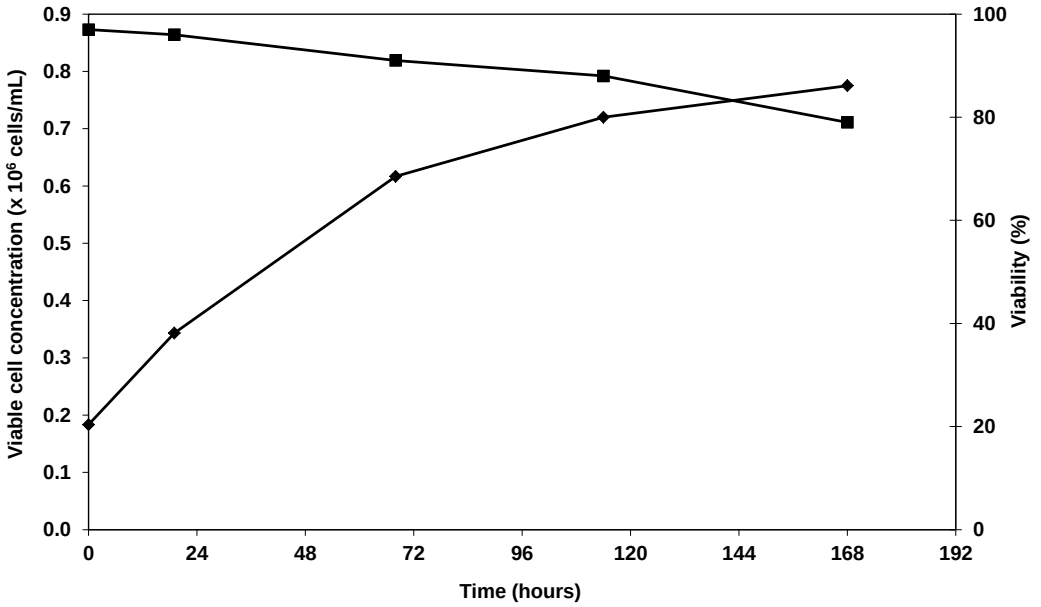

Figure 7.2: **Batch cell culture growth and viability profile of the 100 ml vessel**. VCC (♦) and cell culture viability (■). Process parameters are detailed in Section 2.6 and are the same as those used for the direct driven MBR except that the impeller speed was 400 rpm.

It could be worthwhile further developing this size of bioreactor; however it would only be worthwhile if the reactor was fitted with significantly smaller probes to reduce the baffling effect. Suresh et al (2009) make this same observation with regards to the baffling effect of large probes in MBRs and also mention that there are as of 2009 no suitable miniaturised probes.

Alternatively, non-invasive oxygen sensors could be used with glass vessels, shake flasks and microtitre plates. These are generally autoclaveable patches that can be glued onto the inner surface of the vessel, however the measurement requires a fibre optic probe that is firmly placed against the side of the vessel wall. This is a potential problem for the MBR because it is housed in a polyblock which prohibits the use of optical systems that can measure the extent of dynamic luminescence quenching (online reference four). Hence, the polyblock would have to be re-designed to accommodate optical systems. Non-invasive pH sensors are also available, however they are not autoclavable. Gill et al (2008) reported the use of miniature pH and DOT probes with diameters of 6mm which

would reduce the space occupied by the current probes by 50% and provide a more cost effective alternative.

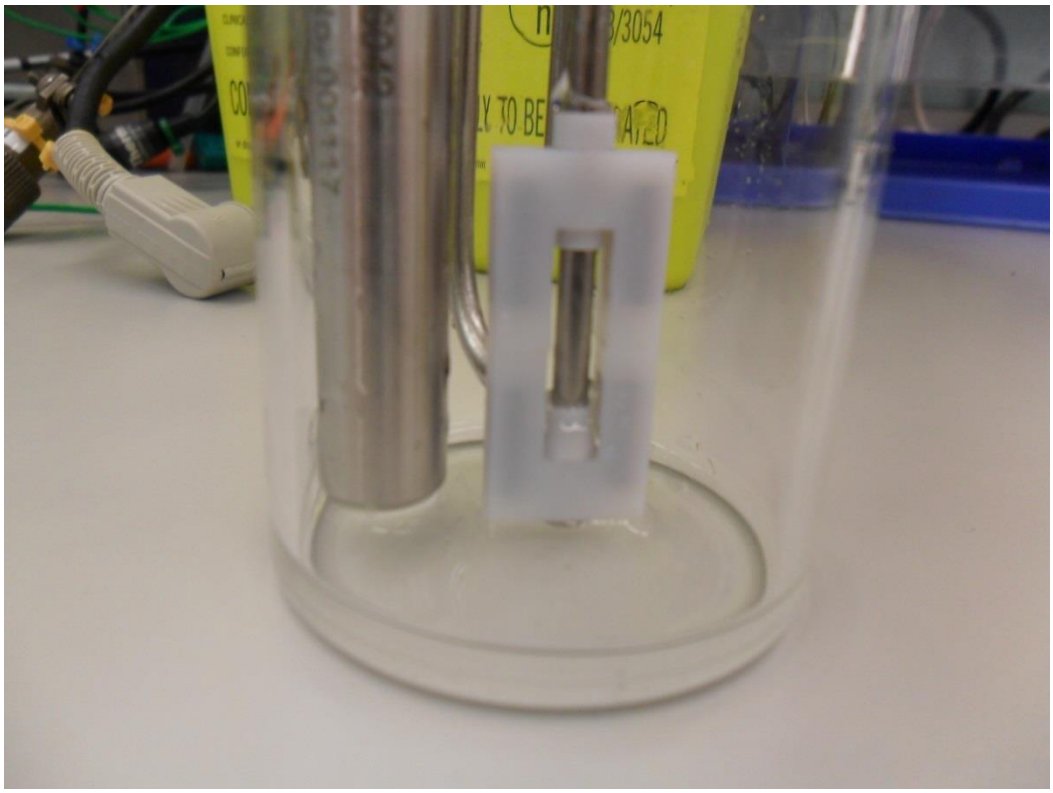

Figure 7.3: **Photo of the 100 ml vessel with the fully extended rectangle impeller and DOT probe.**

Chapter 8: Bioprocess validation

8.1 Introduction

As has been described in this study, a MBR system that is capable of parallel mammalian cell culture has been characterised and shown to closely replicate culture performance at larger scale under one set of conditions. Hence, the MBR could be a suitable system to utilise in process development and process optimisation and could be a potential substitute for larger lab-scale bioreactors. This chapter will explore the regulatory requirements that must be met to ensure compliant and effective use of the system in industry.

The Food and Drugs Association (FDA) define process validation as 'establishing by objective evidence that a process consistently produces a result or product meeting its predetermined specifications'. Validation should not simply be viewed as a tick box exercise but be recognised for the value it adds to the successful planning and operation of bioprocesses.

It is not envisaged that this system will be used to manufacture product that will be commercialised or used for clinical trials due to the small scale of operation. Hence, this system and its operation would not have to undergo the more thorough validation that is required for manufacturing equipment and processes. However, it is always best practice to adhere to cGMP standards while conducting research and development.

8.2 Reproducibility and control

Scale-down process development systems must exhibit consistent and reproducible culture performance in which the process limits are defined and can be closely controlled throughout the culture. Hence, detailed and comprehensive standard operating procedures (SOPs) should be formulated. The system must be able to show consistent reproducibility of culture growth, productivity and

product quality (Corrigan et al, 1995). The fact that a serum free cell culture media is used helps in making the process more reliable and predictable, especially if it is chemically defined and animal component free and this will help in the overall validation.

8.3 Installation qualification

Installation qualification (IQ) is a documented verification that all aspects of the installation of the equipment meet manufacturer's specifications, appropriate safety requirements, company specifications and design intentions. When installing new equipment it is very important to refer to the manufacturer's protocol and installation manual. This is because the equipment has been designed to be installed in a specific manner.

Good installation qualification involves:

1. Ensuring that all equipment and ancillaries are received in good condition.

2. Checking documentation for completeness (operating manuals, maintenance instructions, standard operating procedures for testing, safety and validation certificates).

3. Installing hardware (ancillaries and any monitoring equipment).

4. Verifying that the installation site satisfactorily meets vendor-specified environmental requirements.

5. Performing any initial diagnostics and testing. Assembly and installation of a complex instrument is best done by the vendor or specialized engineers. In the case of this MBR system it would be better for the system to be installed by trained personnel.

6. All filters that are used whether they are air inlet filters or stericup filters should be used according to the manufacturer's guidelines. If filters are single

use then they should be replaced after each run, if filters are re-usable then a record should be kept recording each filters usage ensuring they are not over utilised as this can compromise their performance.

8.4 Operation qualification

It is important that the IQ step is completed to a satisfactory level before progressing to operation qualification (OP) and if problems have been encountered at the IQ stage that they are resolved. OQ is the documented verification that the equipment, when assembled and used according to the standard operating procedures, does in fact perform as defined by the manufacturer's specifications. It should be highlighted here that there is a distinction between the stated range by the manufacturer and the required range of operation, which does offer some flexibility in future operations, if need be.

In general, OQ tests should verify the system's operation according to specifications in the user's environment. Some OQ tests may not be required to be repeated at a regular interval. Rather, when the instrument undergoes major repairs or modifications, relevant OQ tests should be repeated to verify whether the instrument continues to operate satisfactorily.

The MBR system comes equipped with DOT and pH probes which are manufactured by Hamilton. It is important to test these regularly and ensure that they meet the manufacturer's specification with regards to accuracy and response time. All probes should be tested and calibrated before each fermentation and in the case of the DOT probe, replacing the membrane according to the manufacturer's guidelines is essential. DOT and pH probe calibration has been discussed in the materials and methods section.

A temperature mapping exercise like that conducted in Appendix A can confirm that the system's temperature control is working effectively. In general good performance qualification for temperature control would be to raise the temperature setpoint to a certain point and test whether the system could hold the temperature at that setpoint and then to lower the setpoint and test whether the

system can hold at a lower temperature. All this must of course be carried out with a reference thermocouple.

The agitator must be shown to operate accurately at different impeller speed setpoints and can be verified by a digital tachometer.

The system comes with in-built pumps; these should be tested to ensure that they are capable of performing across the range that the manufacturer has identified. This is particularly important for the lowest flow rates that will be used for continuous feeding.

The system comes with alarms that shutdown the system when certain events occur like contamination. These should be tested to ensure that they operate at the criteria that have been specified. There are also two sensors in each vessel that can monitor antifoam levels and when excessive foaming occurs these sensors can initiate the system to make antifoam additions. This mechanism should also be tested

8.5 Performance qualification

Performance qualification (PQ) is the process of demonstrating that an instrument or equipment consistently performs according to the specification appropriate for its routine use.

PQ can mean system suitability testing, where critical key system performance characteristics are measured and compared with documented, pre-set limits. Many of the tests that occur here are similar to those for OQ except that the most desirable parameters that would be used in the process are tested rather than just the specified performance parameters that the manufacturer has stipulated.

8.6 Continuous validation and risks

Validation is an on-going process and therefore the process aspects that were tested and assessed in the validation protocol should be continuously monitored.

There are generic and specific risks that engineers must pay attention to and these are described below.

There are generic risks that must always be considered and contingency plans drawn up. A risk that is always present is that any of the equipment may malfunction or break down at any time. It is best practice to have spare parts that can directly replace any that have malfunctioned to minimise any disruption to the process while new parts are being ordered.

Another generic risk that faces any biological process is that of contamination and this is particularly the case with mammalian cell culture processes. An effective and robust cleaning and preparation protocol must be followed when preparing the system for fermentation and after a fermentation has been completed. The continuous practice of aseptic technique is also essential to ensure that contamination does not occur. The connections and o-rings must be replaced if they are damaged or worn. Appropriate checks must be made to ensure that the autoclaving process is adequately sterilising the vessels. Unlike large scale stainless steel bioreactors, lab scale and MBR systems do not have built-in Clean in Place (CIP) capability and hence a protocol must be developed to clean the vessels and then sterilise to ensure that all previous cell culture material has been removed from the vessels and that a satisfactory level of sterility has been achieved. As mentioned before the system is equipped with alarms that can shut down the system if the vessels become contaminated. The alarm recognises a contamination as an extreme loss of control capability in DOT and pH control due to the respiratory and metabolic needs of contaminants. Unfortunately the system can struggle to control DOT and pH due to other mechanical failures and hence the system may incorrectly shut down incorrectly recognising a contamination.

As scale-down studies are being conducted there is always the risk that upon scale-up the process does not operate in an identical manner. One of the biggest challenges regarding biological processes is consistency and reliability and this is because biological systems can be unpredictable and to a certain extent unstable. Therefore, measures should always be taken to keep the process as generic as

possible and to use well established, robust and reliable technology. Any event that could affect the process time or scheduling and hence throughput would be a risk and contingency for this must be put in place as time is a critical parameter in the pharmaceutical industry and longer process times and lower throughput, results in higher cost of goods (online reference five).

Chapter 9: Management of bioprocesses

The MBR system that has been developed and optimised in this study is a product that has commercial potential. The work in this thesis gives an overview of the system and its ability to perform accurate scale-down cultivations. This could make it a viable option for industry and academia that are looking to invest in new process development/optimisation equipment. Its ability to perform continuous feeding will further strengthen its appeal for companies who run continuously fed manufacturing processes.

There are aspects of the system that are sourced from a variety of companies like the DOT and pH probes, the pumps and the PC. As the probes are sourced it is always a concern that they may become dis-continued and hence no longer available. This is very unlikely with regards to the DOT and pH probes supplied with the MBR because they are standard probes that are used by many different reactor systems. Also the company that manufacturers them, Hamilton, are a well established company which again reduces the risk of these probes becoming unavailable. The in-built pumps are again standard pumps that are widely available.

The company which sells this product could profit from service agreements. The platform technology is relatively easy to use; however user training would be required and potentially on-going technical support and advice. On-going maintenance is mainly around the DOT and pH probes and the impeller motors, however software updates could be issued periodically making an on-going service agreement more attractive.

To market this product effectively and make it an attractive investment for academia and industry it is essential that the system's strengths are highlighted and quantified. Currently, industry utilises lab-scale bioreactors of at least 5L scale to conduct process optimisation and hence the operating volume of the BioXplorer^{TM} system is at least 10 times less than that of standard lab-scale bioreactors.

Generally, there are significant cost savings that can be made for industry by scaling down the size of their research and development bioreactor systems to a miniature scale. Cost savings can be realised by significantly reduced capital investments as well as lower recurring costs associated with purchasing lower volumes of consumables. Significant cost savings can also be realised due to the smaller footprint of MBR systems compared to larger lab-scale bioreactor systems. Also cost savings can be realised by reducing the size of the autoclave used for sterilisation. The development of MBR systems that offer automated operation could also reduce labour costs associated with process operation and help companies focus their resources more on expanding their research portfolios. Until that point however, the MBR systems currently on the market, including the BioXplorer^{TM} system will not result in a significant reduction in operator man hours. There may be time savings in the preparation and cleaning of the reactors due to their ease in handling, however these will not be significant enough to result in noticeable cost savings.

Table 9.1 illustrates the potential cost savings that can be made by opting for the MBR system over a conventional 5L STR system. This table compares the non-recurring and recurring costs of purchasing and operating 16 5L STRs and 16 HEL MBRs for 17 fed-batch fermentations (14 day cultivations and 7 days turnaround) per year each.

Table 9.1: A summary of the significant non-recurring and recurring costs.

Non-recurring costs	**5L STR**	**MBR**
Purchase and installation of 16 x 5L STR (£k)	16 x £17.5k* (only the reactors) = 280	4 x £60k* (includes controller, polyblock and 4 reactors) = 240
Control units (£k)	16 x 2.5 = 40	NA
Total £k	320**	240**
Recurring costs		
Media (£k)	47.5	4
Feed (£k)	27.5	3
Total (£k)	75	7

*Quotes were obtained from Applikon and HEL for the respective systems. In the case of Applikon this was a verbal quote and in the case of HEL this was the cost of the unit to University College London.
**Includes installation cost.

Media cost calculation:

The cost of media per annum is calculated by multiplying the cost of 1L of CD-CHO media (~£50) multiplied by the volume of feed per fermentation (3.5L for the 5L STR and 0.3L for the MBR) multiplied by the number of bioreactors (16) multiplied by the number of fermentations a year (17). Cost of CD-CHO media was obtained from Gibco™.

Feed cost calculation:

Feed cost was calculated in the same way as the media cost, however the volume of feed used per 5L STR run is roughly 200 ml which costs the equivalent of 2 L of CD-CHO due to the feed being 10 x concentration CD-CHO media. The MBR would use roughly 20 ml feed per run.

The 5L STRs cost £80k more to buy and install and costs a further £68k per annum to run compared to the MBRs. Over 5 years the 5L STRs cost £695k including the capital investment and recurring costs compared to £275k for the MBR. This means the MBR could save a company at least £420k to purchase and run for 5 years compared to the 5L STRs.

This appraisal does not consider savings that could be made as a result of the smaller footprint of the MBR occupying a smaller area in R&D labs, which could be considerable. The MBR system could occupy 5-10 times less space than the 5L STRs which would make a significant impact on building costs if a new lab was to be constructed.

References

Agrawal V and Bal M: **Strategies for rapid production of therapeutic proteins in mammalian cells.** BioProcess International. (2012), 10(4): 32-48

Al-Rubeai M, Emery A N, Chalder S: **Flow cytometric study of cultured mammalian cells.** Journal of Biotechnology. (1991), 19: 67-82.

Al-Rubeai M, Emery A N, Chalder S and Jan D C: **Specific monoclonal antibody productivity and the cell cycle comparisons of batch, continuous and perfusion cultures.** Cytotechnology. (1992), 9: 85-97.

Anderlei T and Buchs J: **Device for sterile online measurement of the oxygen transfer rate in shaking flasks. Biochemical Engineering Journal.** (2001), 7: 157-162.

Anderlei T, Zang W, Papaspyrou M and Büchs J: **Online respiration activity measurement (OTR, CTR, RQ) in shake flasks.** Biochemical Engineering Journal. (2004), 17: 187-194.

Arden N and Betenbaugh M J: **Life and death in mammalian cell culture: strategies for apoptosis inhibition.** Trends in Biotechnology. (2004), 22(4): 174-180

Asenjo J A and Merchuk J C: **Bioreactor system design.** New York: Mercel Dekker, inc. (1994), Page 529.

Barrett S L, Boniface R, Dhulipala P, Slade P, Tennico Y, Stramaglia M, Lio P, and Gorfien S: **Attaining next-level titers in CHO fed-batch cultures.** BioProcess International, (2012), 10(10).

Bates R L, Fondy P L and Corpstein R R: **An examination of some geometric parameters of impeller power.** Industrial & Engineering Chemistry Process Design and Development, (1963), 2(4): 310-314.

Betts J I and Baganz F: **Miniature bioreactors: current practices and future opportunities.** Microbial Cell Factories. (2006), 5(21). Page numbers not available

Bibila T A and Robinson D K**: In pursuit of the optimal fed-batch process for monoclonal antibody production.** Biotechnology Progress. (1995), 11: 1-13.

Birch J R, Mainwaring D O and Racher A J: **Modern biopharmaceuticals: design, development and optimization. Use of the glutamine synthetase (GS) expression system for the rapid development of highly productive mammalian cell processes.** Edited by Jorg Knablein, Wiley-VCH, (2005) Chapter 4: 817-818.

Browne S M and Al-Rubeai M: **Selection methods for high-producing mammalian cell lines.** Trends in Biotechnology. (2007), 25: 425-432.

Buchs J, Maier U, Milbradt C and Zoels B: **Power consumption in shaking flasks on rotary shaking machines: II. Nondimensional description of specific power consumption and flow regimes in unbaffled flasks at elevated liquid viscosity.** Biotechnology Bioengineering. (2000), 68: 594-601.

Bujalski W, Takenaka K, Paolini S, Jahoda M, Paglianti A, Takahashi K, Nienow A W and Etchells A W: **Suspension and liquid homogenization in high solids concentration stirred chemical reactors.** Institution of Chemical Engineers Trans IChemE. (1999), 77: Part A: 241-247.

Butler M: **Animal cell cultures: recent achievements and perspectives in the production of biopharmaceuticals.** Applied Microbiol Biotechnology (2005), 68: 283–291.

Cacciuttolo M A, Trinh L, Lumpkin J A and Rao G**: Hyperoxia induces DNA damage in mammalian cells.** Free Radical Biology & Medicine. (1993), 14: 267-276.

Carter P J: **Potent antibody therapeutics by design.** Nature Reviews Immunology (2006) 6: 343–357.

Castilho L, Moraes A, Augusto E and Butler M: **Animal cell technology: from biopharmaceuticals to gene therapy.** Taylor and Francis Group. (2008), 25-27.

Chalmers J J: **Cells and bubbles in sparged bioreactors.** Cytotechnology. (1994), 15: 311-320.

Chen A, Chitta R, Chang D and Amanullah A: **Twenty-four well plate miniature bioreactor system as a scale-down model for cell culture process development.** Biotechnology and Bioengineering. (2008), 102 (1): 148-160.

Chisti Y and Moo-Young M: **On bioreactors in Encyclopedia of Physical Science and Technology.** Meyers, R.A., ed., Academic Press, San Diego, (2002), 2: 247-271.

Chisti Y: **Animal cell culture in stirred bioreactors: observations on scale-up.** Process Biochemistry. (1993), 28: 511-517.

Cutter L A: **Flow and turbulence in a stirred tank.** American Institute of Chemical Engineers. (1966), 12: 35-45.

Czermak P, Pörtner R, Beix A: **Special Engineering Aspects**. Cell and Tissue Reaction Engineering Principles and Practice. (2009), 83-172.

Davies J T: **A physical interpretation of drop sizes in homogenisers and agitated tanks, including the dispersion of viscous oils.** Chemical Engineering Science (1987) 42: 1671-1676.

De Jesus M and Wurm F M: **Manufacturing recombinant proteins in kg-ton quantities using animal cells in bioreactors.** European Journal of Pharmaceutics and Biopharmaceutics (2011), 78: 184–188

Diao J, Young L, Zhou P and Shuler M L: **An actively mixed mini-bioreactor for protein production from suspended animal cells.** Biotechnology and Bioengineering. (2007), 100(1): 72-81

Dickey D S: 2010. **Mixing and Blending.** Kirk-Othmer Encyclopedia of Chemical Technology. (2010), 1–71.

Doran. P: **Bioprocess engineering principles.** Elsevier Academic press, (1995), p150.

Elmahdi I, Baganz F, Dixon K, Harrop T, Sugden D and Lye G J**: pH control in microwell fermentations of S-erythraea CA340: influence on biomass growth kinetics and erythromycin biosynthesis.** Biochemical Engineering journal. (2003), 16(3): 299 - 310.

Farid S S: **Process economics of industrial monoclonal antibody manufacture.** Journal of Chromatography B. (2006), 848: 8-18.

Frahm B, Blank H, Cornand P, Oelßner W, Guth U, Lane P, Munack A, Johannsen K and Portner R: **Determination of dissolved CO2 concentration and CO2 production rate of mammalian cell suspension culture based on off-gas measurement.** Journal of Biotechnology. (2002), 99: 133-148.

Gagnon M, Hiller G, Luan Y, Kittredge A, DeFelice J and Drapeau D: **High-end pH-controlled delivery of glucose effectively suppresses lactate accumulation in CHO fed-batch cultures.** Biotechnology and Bioengineering. (2011), 108(6): 1328-1337.

Garcia-Ochoa F, Gomez E: **Bioreactor scale-up and oxygen transfer rate in microbial processes: An overview.** Biotechnology Advances (2009) 27: 153–176.

Ge X, Hanson M, Shen H, Kostov Y, Brorson K A, Douglas D F, Antonio R M and Rao G: **Validation of an optimal sensor-based high-throughput bioreactor system for mammalian cell culture.** Journal of Biotechnology. (2006), 122: 293-306.

Ghebeh H, Gillis J and Butler M: **Measurement of hydrophobic interactions of mammalian cells grown in culture.** Journal of Biotechnology. (2002), 95: 39–48.

Gill N K, Appleton M, Baganz F and Lye G J: **Design and characterisation of a miniature stirred bioreactor system for parallel microbial fermentations.** Biochemical Engineering Journal, (2008), 39: 164–176.

Gimenez L, Simonet C, Malphettes L: **Scale-up considerations for monoclonal antibody production process: an oxygen transfer flux approach.** BioMed Central, (2013), 7(6): 49

Gorfien S F, Paul W, Judd D, Tescione L and Jayme D W: **Optimized nutrient additives for fed-batch cultures.** BioPharm International. (2003), April: 34-40.

Hacker D L, De Jesus M and Wurm F M: **25 years of recombinant proteins from reactor-grown cells — Where do we go from here?** Biotechnology Advances. (2009), 27: 1023–1027.

Handa-Corrigan A, Nikolay S, Fletcher D, Mistry S, Young A and Ferguson C: **Monoclonal antibody production in hollow-fiber bioreactors: Process control and validation strategies for manufacturing industry.** Enzyme and Microbial Technology (1995), 17: 225-230.

Harnby N, Nienow A W and Edwards M F: **Mixing of liquids in stirred tanks.** Butterworth-Heinemann (1992), p137-158.

Hirata Y, Dote T, Yoshioka T, Komoda Y and Inoue Y: **Performance of chaotic mixing caused by reciprocating a disk in a cylindrical vessel.** Institute of Chemical Engineers. (2007), 85(A5): 576–582

Hockey R M and Nouri J M: **Turbulent flow in a baffled vessel stirred by a 60° pitched blade impeller.** Chemical Engineering Science. (1996), 51: 4405-4421.

Hooks M A, Wade C S, Millikan W J (1991**): Muromonab CD-3: a review of its pharmacology, pharmacokinetics, and clinical use in transplantation.** Pharmacotherapy. (1991), 11(1): 26–37.

Hsu W, Aulakh R P S, Traul D L and Yuk I H**: Advanced microscale bioreactor system: a representative scale-down model for bench-top bioreactors.** Cytotechnology (2012), 64(6): 667-678

Jenkins, R.O., Leach, C.K. and Mijnbeek, G. (Eds). **Bioreactor Design and Product Yield**. Oxford: Butterworth Heinemann (1992), Pages 9-12 and 52.

Kamen A A, Garnier A, Andre G, Archambault J and Chavarie C: **Determination of mass transfer parameters in surface aerated bioreactors with bubble entrainment.** The Chemical Engineering Journal. (1995), 59: 187-193.

Kensy F, Engelbrecht C and Buchs J: **Scale-up from microtiter plate to laboratory fermenter: evaluation by online monitoring techniques of growth**

and protein expression in Escherichia coli and Hansenula polymorpha fermentations. Microbial Cell Factories. (2009), 8: 68

Kilonzo P M, Margaritis A: **The effects of non-Newtonian fermentation broth viscosity and small bubble segregation on oxygen mass transfer in gas-lift bioreactors: a critical review.** Biochemical Engineering Journal (2004), 17: 27–40.

Kretzmer G: **Industrial processes with animal cells.** Applied Microbiol Biotechnology. (2002), 59: 135-142.

Kumar N and Borth N: **Flow-cytometry and cell sorting: An efficient approach to investigate productivity and cell physiology in mammalian cell factories.** Methods. (2012), 56: 366-374.

Kumar S, Wittmann C and Heinzle E: **Minibioreactors.** Biotechnology Letters (2004), 26: 1-10.

Kuystermans D, Mohd A, Rubeai M: **Automated flow cytometry for monitoring CHO cell cultures.** Methods. (2012), 56: 358-365.

Lai T, Yang Y, Kong S Ng: **Advances in Mammalian Cell Line Development Technologies for Recombinant Protein Production.** Pharmaceuticals (2013), 6: 579-603.

Lamping S R, Zhanga H, Allen B, Shamloua P A: **Design of a prototype miniature bioreactor for high throughput automated bioprocessing.** Chemical Engineering Science (2003), 58: 747-758

Lao M and Toth D: **Effects of ammonium and lactate on growth and metabolism of a recombinant chinese hamster ovary cell culture.** Biotechnology Progress (1997), 13: 688-691.

Lara A R, Galindo E, Ramirez O T and Palomares L A: **Living with heterogeneities in bioreactors.** Molecular Biotechnology. (2006), 34: 355-381.

Lavery M and Nienow A W: **Oxygen transfer in animal cell culture medium.** Biotechnology and Bioengineering. (1987), 30(3): 368-373.

Levich V: **Physico-Chemical Hydrodynamics.** Prentice-Hall, New Jersey. (1962), p459

Li J, Wong C L, Vijayasankaran N, Hudson T, Amanullah A: **Feeding lactate for CHO cell culture processes: Impact on culture metabolism and performance.** Biotechnology and Bioengineering. (2012), 109(5): 1173-1186

Lim Y, Wong N S C, Lee Y Y, Ku S C Y, Wong D C F and Yap M G S: **Engineering mammalian cells in bioprocessing – current achievements and future perspectives.** Biotechnology Applied Biochemistry. (2010), 55: 175–189.

Maharbiz M M, Holtz W J, Howe R T and Keasling J D: **Microbioreactor arrays with parametric control for high-throughput experimentation.** Biotechnology Bioengineering. (2004), 85: 376-381

Marks D M: **Equipment design considerations for large scale cell culture.** Cytotechnology. (2003), 42: 21–33.

Markusen J F and Robinson D K: **Monoclonal antibody production, cell lines.** Encyclopedia of Industrial Biotechnology: Bioprocess, Bioseparation, and Cell Technology, edited by Michael C. Flickinger (2010) John Wiley & Sons, Inc. p 2-4.

Matsunuaga N, Kano K, Maki Y and Dobashi T: **Culture scale-up studies as seen from the viewpoint of oxygen supply and dissolved carbon dioxide stripping.** Journal of Bioscience and Bioengineering. (2009), 107(4): 412–418.

Moreira J L, Cruz P E, Santana P C and Feliciano A S**: Influence of power input and aeration method on mass transfer in a laboratory animal cell culture vessel.** Journal Chemical Technology and Biotechnology. (1995), 62: 118-131

Motobu M, Wang P C and Matsumura M**: Effect of shear stress on recombinant Chinese hamster ovary cells.** Journal of Fermentation and Bioengineering. (1998), 85: 190-195.

Nienow A W, Miles D: **A dynamometer for the accurate measurement of mixing torque.** Journal of Scientific Instruments (1969), 2: 994–995.

Nienow A W, Miles D: **Impeller power numbers in closed vessels.** Industrial and Engineering Chemistry Process Design and Development (1971), 10:1.

Nienow A W: **Hydrodynamics of stirred bioreactors.** Applied Mechanics Reviews (1998), 51: 3–32.

Nienow A W: **Reactor engineering in large scale animal cell culture.** Cytotechnology. (2006), 50: 9–33.

Ozturk S S: **Equipment for Large-Scale Mammalian Cell Culture**. Advanced Biochemical Engineering Biotechnology. (2014), 139: 69–92.

Pavlou A K and Belsey M J: **The therapeutic antibodies market to 2008.** European Journal of Pharmaceutics and Biopharmaceutics. (2005), 59: 389-396.

Pelton R: **A model of foam growth in the presence of antifoam emulsion.** Chemical Engineering Science. (1996), 51 (19) :4437-4442.

Reis N, Gonclaves C N, Vicente A A and Teixeira J A: **Proof-of-concept of a novel micro-bioreactor for fast development of industrial bioprocesses.** Biotechnology and Bioengineering. (2006), 95: 744-753.

Rushton J H, Costich E W and Everett H J**: Power characteristics of mixing impellers.** Chemical Engineering Progress. (1950), 46: 467-476.

Sandadi S, Pedersen H, Bowers J S and Rendeiro D: **A comprehensive comparison of mixing, mass transfer, Chinese hamster ovary cell growth, and antibody production using Rushton turbine and marine impellers.** Bioprocess and Biosystems Engineering. (2011), 34: 819–832.

Schneider M, Marison I W and Von Stockar U: **The importance of ammonia in mammalian cell culture.** Journal of Biotechnology. (1996), 46: 161-185.

Silk N J, Denby S, Lewis G, Kuiper M, Hatton D, Field R, Baganz F and Lye G J**: Fed-batch operation of an industrial cell culture process in shaken microwells.** Biotechnology Letters. (2010), 32: 73–78.

Singh V: **Disposable bioreactor for cell culture using wave-induced agitation.** Cytotechnology. (1999), 30: 149–158.

Soley A, Fontovab A, Gálveza J, Sarróa E, Lecinaa M, Bragósb R, Cairóa J J and Gòdiaa F: **Development of a simple disposable six minibioreactor system for suspension mammalian cell culture.** Process Biochemistry. (2012), 47: 597–605.

Stoll T S, Muhlethaler K, Von Stockar U and Marison I W**: Systematic improvement of a chemically-defined protein-free medium for hybridoma growth and monoclonal antibody production.** Journal of Biotechnology. (1992), 45: 111 – 123.

Sunley K, Tharmalingam T, and Butler M: **CHO cells adapted to hypothermic growth produce high yields of recombinant b-interferon.** Biotechnology Progress. (2008), 24: 898-906.

Tribe L A, Briens C L and Margaritis A: **Determination of the volumetric mass transfer coefficient (k_La) using the dynamic "Gas Out-Gas In" method: Analysis of errors caused by dissolved oxygen probes.** Biotechnology and Bioengineering. (1995), 46: 388-392.

Vernon A: **The GS Gene Expression System.** Business briefing: Pharmatech. (2004).

Van Blokland H J M., Kwaks T H J, Sewalt R G A B, Verhees J A, Klaren V N A, Siersma T K, Korse J W M, Teunissen N C, Botschuijver S, Van Mer C, Man S Y and Otte A P: **A novel, high stringency selection system allows screening of few clones for high protein expression.** Journal of Biotechnology. (2007), 128: 237-245.

Van der Valk J, Brunner D, De Smet K, Fex Svenningsen Å , Honegger P, Knudsen L E, Lindl T, Noraberg J, Price A, Scarino M L and Gstraunthaler G: **Optimization of chemically defined cell culture media – Replacing fetal bovine serum in mammalian in vitro methods.** Toxicology in Vitro. (2010), 24: 1053–1063.

Van't Riet K: **Review of measuring methods and nonviscous gas–liquid mass transfer in stirred vessels.** Industrial & Engineering Chemistry Process Design and Development. (1979), 18: 357–364.

Varley J and Birch J: **Reactor design for large scale suspension animal cell culture.** Cytotechnology. (1999), 29: 177–205.

Wen Y, Zang R, Zhang X and Yang S: **A 24-microwell plate with improved mixing and scalable performance for high throughput cell cultures.** Process Biochemistry. (2012), 47: 612–618.

Weuster-Botz D, Puskeiler R, Kusterer A, Kaufmann K, John G T and Arnold M: **Methods and milliliter scale devices for high-throughput bioprocess design.** Bioprocess and Biosystems Engineering. (2005), 28: 109-119.

Wilkens C A and Gerdtzen Z P: **Engineering CHO cells for improved central carbon and energy metabolism.** Wilkens and Gerdtzen BMC Proceedings. (2011), 5 (8): 120

Wu J**: Mechanisms of animal cell damage associated with gas bubbles and cell protection by medium additives.** Journal of Biotechnology. (1995), 43: 81-94.

Yanga Y, Chusainowb M J and Yap M G S: **DNA methylation contributes to loss in productivity of monoclonal antibody-producing CHO cell lines**. Journal of Biotechnology. (2010), 147: 180-185.

Yoshinari K, Arai K, Kimura H, Matsumoto K and Yamaguchi Y: **Long-term production of human monoclonal antibodies by human-mouse heterohybridomas.** Journal of Immunological Methods. (1995), 186: 17-25

Zhang S, Handa-Corrigan A and Spier R E**: Foaming and media surfactant effects on the cultivation of animal cells in stirred and sparged bioreactors.** Journal of Biotechnology. (1992), 25: 289-306.

Zhu J: **Mammalian cell protein expression for biopharmaceutical production.** Biotechnology Advances. (2012), 30 (5): 1158–1170

Zuniga L and Calvo B: **Biosimilars approval process.** Regulatory Toxicology and Pharmacology. (2010). 56: 374-377.

Online references:

Online reference one

http://www.businesswire.com/news/home/20111205005889/en/Research-Markets-Monoclonal-Antibodies-Market-2017--

Online reference two

http://www.gelifesciences.com/webapp/wcs/stores/servlet/catalog/en/GELifeSciences-UK/brands/wave/

Online reference three

http://www.tapbiosystems.com/tap/cell_culture/ambr.htm#

Online reference four

http://www.presens.de/support/faqs/question/how-does-an-oxygen-sensor-work.html

Online reference five

(http://www.usvalidation.com/kb/knowledge_base.aspx)

Appendix A: Temperature mapping in the MBR

A temperature mapping exercise was conducted to ensure that the system's temperature control was effective. All four vessels were filled with water and the temperature set at 37°C at point A shown below in figure A.1. Point A is where the thermocouple was placed and is the only point in which the thermocouple could be placed in the vessel. Agitation was provided by the magnetic and directly driven impellers at an impeller speed of 350 and 410 rpm respectively. Both the magnetically stirred and directly driven impellers produced a temperature map presented in figure A.1.

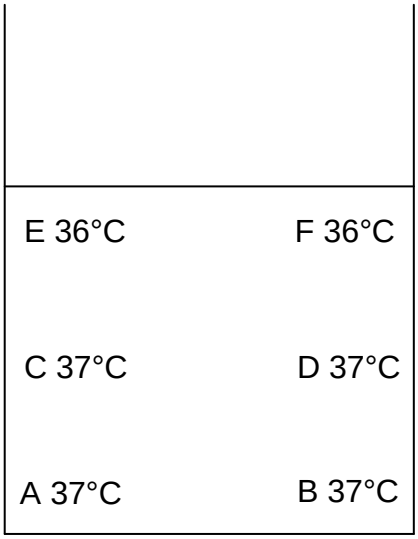

Figure A.1: **A schematic illustrating the temperatures at different points in the MBR vessel.**

The temperature control in the MBR vessel is fairly tight with a variation of 36.5°C $\pm$0.5°C. There is a single point of heating that takes place which is close to point A and the temperature profile does reflect this with the lower temperatures being at the most extreme points at the top of the vessel. This may not have occurred had the MBR vessels been closely enveloped by a heating jacket like lab-scale STRs.

Appendix B: Autoclave validation

In the early part of this research an old and now de-commissioned autoclave was in operation in the Advanced Centre of Biochemical Engineering. This autoclave had a lot of residue in its chamber and on occasion this residue would enter and deposit into the bioreactor vessels. Before the vessels are filled with media before fermentation, this residual liquid in the vessels is removed to ensure there is no water or deposits that have come from the autoclave.

However, a simple shake flask experiment was conducted to evaluate whether these deposits were having an adverse effect on cell culture performance. This experiment included a control shake flask that was filled with media straight from the bottle and an experimental shake flask which was filled with media that came from an autoclaved vessel.

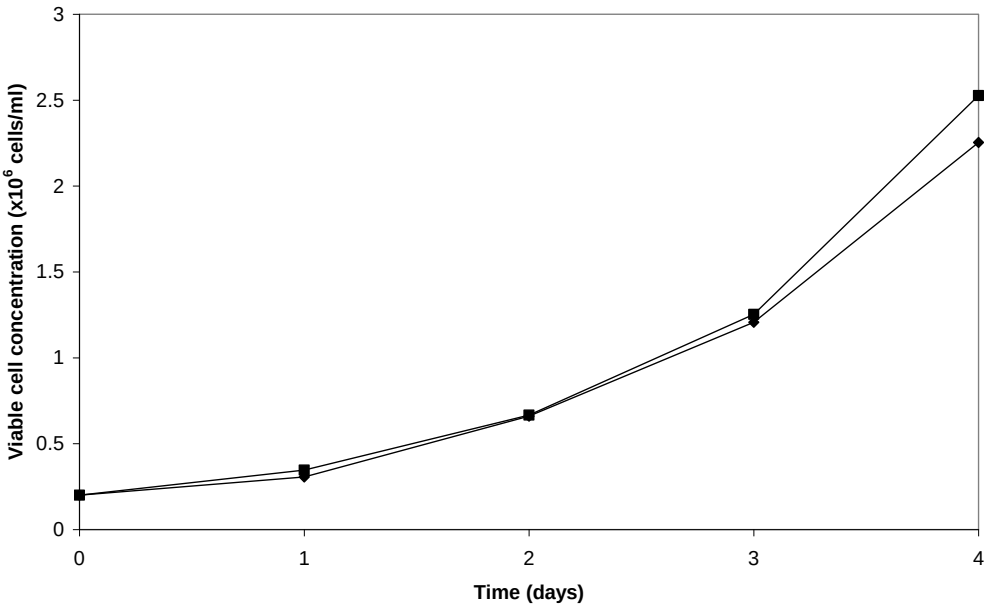

Figure B.1: **Growth profiles for the autoclave validation cultures.** Control shake flask (■) and the experimental shake flask (♦).

Figure B.1 clearly shows that there is no significant difference in growth produced by the control shake flask and the shake flask that was filled with media from an autoclaved vessel.